Synthesis of hydrophobically modified polyacrylamide and investigation of its behaviour in porous media

By

Hassan Zabihi

(Student ID: 3030656)

A Doctoral Thesis submitted in partial fulfilment of
the requirements for the award of the degree of
Doctor of Philosophy in Chemical Engineering

Supervisors

Dr. Pedro Diaz

Dr. John Orrin

School of Engineering

London South Bank University

Sep 2017

Acknowledgement

Thanks to the almighty God for giving me the opportunity, strength and patience to complete my PhD thesis. Special thanks to my supervisors for their continuous support and guidance.

I would like to express my appreciation to technicians in Applied Science and School of Engineering for their assistance towards my research. Without their guidance, the task would have been more difficult for me.

The completion of this research would not have been possible without the support of my precious family. They provided all the moral support and given me the strength to strive in order to achieve all this.

Abstract

Approximately half of the world oil production is a result of water flooding. A major concern in this process is the mobility control of the injected phase with unfavourable fluid mobility ratio, channelling through permeable zones and, fingering effects can occur leading to an early water breakthrough and an inefficient flooding.

Technically, it is possible to improve the flooding efficiency by applying enhanced oil recovery (EOR) processes (e.g. polymer flooding, steam injection and surfactant flooding). EOR processes intend to improve the sweep efficiency by reducing the mobility ratio between injected and in-situ fluids and/or to improve the displacement efficiency by reducing the capillary and interfacial forces. Polymer flooding is an enhanced water flooding process in which the water/oil mobility ratio is lowered by adding water-soluble polymers to water to increase its viscosity.

The most applied polymer for EOR processes is the synthetic partially hydrolyzed polyacrylamide (HPAM). Several field projects have been carried out utilising HPAM, and the observed trend is that these polymers show low shear stress stability, and low salt tolerance. They are also sensitive to elevated reservoir temperature. Additionally, polymer retention and adsorption affect the rheological properties of the polymer solution significantly and reduce permeability. Therefore, polymers with greater salinity resilient and temperature resistance are needed.

Hydrophobically modified polyacrylamide is a type of associative polymers that has been introduced to oil field applications as an alternative to HPAM for the past two decades. The main characteristics of these polymers are their significant enhancement of water viscosity compared with the conventional polymers such as HPAM, and their salinity tolerance and temperature resistance that would be more important in the real application.

In this project, phenyl-polyacrylamide (PPAM), a hydrophobically modified polyacrylamide is studied as a potential viscosifier in waterflooding process. PPAM is synthesised by free radical micellar copolymerisation. The

synthesised copolymer was characterised and the polymer composition was determined. Viscosity average molecular weight of copolymer was measured, and the rheological behaviour of the polymer was investigated in both, distilled water and NaCl solution and the results were compared with those obtained for HPAM. Greater viscosity values were observed for PPAM in distilled water and saline brine than HPAM.

Comparative flow experiments for polymer solutions were carried out in sand packs to investigate the interaction of polymer, sand, and brine, and also to study the effect of the shear rate on viscosity of the polymer in-situ. The polymer solutions exhibited a shear thinning, shear thickening and degradation behaviour at different shear rates. The experiments were further carried out to investigate the polymer retention at different polymer concentrations, and brine salinity, and the results were compared with those from conventional hydrolysed polyacrylamide. Greater polymer adsorption was observed at higher brine salinity for HPAM than PPAM, however, polymer adsorption for PPAM is slightly greater than HPAM in distilled water.

Oil displacement tests were further conducted through consolidated core samples (Benthemier sandstone). The reduction of permeability to water was estimated, and oil recovery was measured. A greater permeability reduction to water was observed for PPAM than HPAM solution at low salinity which is not desirable, however, oil recovery at higher concentration of PPAM was greater than HPAM.

In summary, PPAM can be used as a good alternative to conventional HPAM due to strong viscosity behaviour in high salinity and temperature. Inter-molecular association of hydrophobic monomers in copolymers of PPAM form a bulky structure which causes great viscosity enhancement of polymer solution in distilled water. PPAM solubility in high salinity water is proven to be greater than HPAM and the results from polymer precipitation tests showed much less polymer precipitation for PPAM than HPAM in high saline brine. Moreover, the results for temperature effect on polymer viscosity demonstrated stronger temperature resistance for PPAM than HPAM.

List of Abbreviations

AM	Acrylamide monomer
API	American petroleum Institute
BPR	Back Pressure Regulator
C*	Critical Aggregation concentration
C_3H_5NO	Acrylamide monomer Chemical formula
C_9H_9NO	Phenyl-acrylamide monomer
$CaCl_2$	Calcium Chloride
$CaCo_3$	Calcium Carbonate
C-H	Methyl group
CMC	Critical Micelle concentration
$-CONH_2-$	Amide group
COO^-	Carboxylate group
cp	Centi-poise
E	Overal sweep efficiency
E_d	Microscopic sweep efficiency
Ei	Vertical sweep efficiency
EOR	Enhanced Oil Recovery
Es	Aerial sweep efficiency
E_V	Volumetric sweep efficiency
f_o	Oil fractional flow
f_w	Water fractional flow
FT-IR	Fourier Transform Infra-red Spectroscopy
HMPAM	Hydrophobically modified polyacrylamide
HMPs	Hydrophobically modified polymers
H-NMR	Nuclear magnetic resonance
HPAM	Hydrolyzed poly-acrylamide
IPV	Inaccessible pore volume
$K_2S_2O_8$	Potassium persulphate
KCl	Potassium Chloride
K_H	Huggins constant
KNO_3	Potassium Nitrate

K_O	Oil permeability
KPS	Potassium persulphate
Kr_o	Oil relative permeability
Kr_w	Water relative permeability
K_W	Water permeability
L	Length
M	Mobility
mD	Milli-darcy
$MgCl_2$	Magnesium chloride
mPa.s	milli pascal.second
M_w	Average molecular weight
$NaC_{12}H_{25}SO_4$	Sodium dodecyl sulphate
NaOH	Sodium hydroxide
N_H	Number of hydophobe per micelle
N-H	Amide group
η_I	Inherent viscosity
η_R	Reduced viscosity
η_r	Relative viscosity
η_s	Solvent viscosity
η_{sp}	Specific viscosity
-O-	Oxygen
PA	Poly-acrylamide
PPAM	Poly-Phenylacrylamide
ppm	Part-per-million
PV	pore volume
q	Fluid flow rate
RF	Resistance factor
RRF	Residual resistance factor
SDS	Sodium dodecyl sulphate
So_r	Residual oil saturation
Sw_f	Water flooding
Sw_i	Irreducible water saturation

T	Temperature
UV	Ultra-violet spectroscopy

List of Nomenclature

V_b	Bulk volume
λ_O	Oil mobility
λ_W	Water mobility
μ_o	Oil viscosity
μ_w	Water viscosity
γ	Shear rate
ε	Molar adsorption coefficient
$[I_0]$	Initial concentration of initiator
[M]	Initial concentration of monomers at time t
$[M_0]$	Initial concentration of monomers
[η]	Intrinsic viscosity
∅	Porosity
∆P	Pressure drop

List of Figures

List of Tables

Table of contents

Chapter 1

Introduction

1. Introduction

1.1 Overview and background

Fast depleting oil reserves coupled with ever increasing demand for energy is pushing companies to develop techniques to make energy recovery and consumption more efficient. As it is witnessed today, the rate of replacement of produced reserves by new discoveries has been declining steadily (IEA 2015). This scenario leads to the conclusion that the demand for oil may not only be met by putting more efforts in exploration alone but also by improving the production techniques from known and existing reservoirs.

Oil covers approximately 35% of the primary energy supply (IEA 2015). New sources, such as renewables, have not been demonstrated to be reliable yet as it accounts for only 12 % (projected to reach 15% by 2035) of the total world energy consumption (IEA 2015). Therefore, to guarantee the supply of energy and provide a transition period between current sources and the renewables ones, current sources have to be exploited in a more efficient manner.

Implementation of enhanced oil recovery (EOR) techniques is a crucial contribution to address the global need for energy. Today, the oil recovery around the world lies between 30-40%, and considering the increasing world population and the global energy demand, this recovery efficiency is not satisfying. An increase in efficiency of the recovery process above 60% will be more adequate (Kasimbazi, 2014).

Enhanced oil recovery comes into picture when primary and secondary recovery techniques have been applied and a considerable portion of original oil in place (OOIP) still resides in the reservoir.

Primary recovery process involves displacing oil from porous rocks in the reservoir towards the production well using its own reservoir energy, such as natural water drive, gas-cap drive, or reservoir pressure. In secondary recovery, a fluid (water or gas) is injected into the reservoir in order to

maintain reservoir pressure, and to continue oil displacement into the wellbore.

Water flooding is a standard practice due to its low cost, to maintain reservoir pressure, and also to sweep out oil in most reservoirs (Alexis 2016). Water flooding has been studied and applied to numerous fields worldwide with variable degree of success. After waterflooding, still a significant proportion (30-60%) of oil is left in the reservoir due to unfavourable mobility ratio of water to oil (Alexis 2016). EOR methods are then aimed at recovering this residual oil. Conventional oil production strategies have followed the order of primary depletion, secondary recovery and tertiary recovery processes (Wassmuth 2012). Transition from one recovery method to another occurs when the current method becomes uneconomical or the oil production rate drops to very low values. However, in many cases, applying tertiary recovery methods directly after the primary depletion have proved to be more efficient (Alvarado 2010). EOR aims at extracting as much recoverable oil from the reservoir as possible. Main categories of EOR methods include gas injection, chemical flooding and thermal processes. A summary of different stages involved in EOR methods is given in Figure 1.1.

A large percentage (40-70%) of oil produced nowadays worldwide is through water flooding (Maugeri 2012), and one of the major concerns associated with water flooding is its poor sweep efficiency. Water-oil mobility ratio causes water to channel through oil regions leaving oil behind in the reservoir resulting in lower oil recoveries. Operators of mature oil fields are faced with a high water production coming from an underlying natural water source, or from previous stimulation attempts involving water injection. For example, Shell's water production has increased steadily from about 350,000 m^3/day in 1994 to more than 1,000,000 m^3/day in 2014, nearly matching Shell's oil production (IEA 2015).

Water production decreases oil production, and it results in large amounts of water that need to be disposed or treated which gives extra costs related to oil/water separation, handling and lifting.

Therefore the oil industry is putting a lot of efforts and money in developing techniques to decrease water handling costs and to reduce water production.

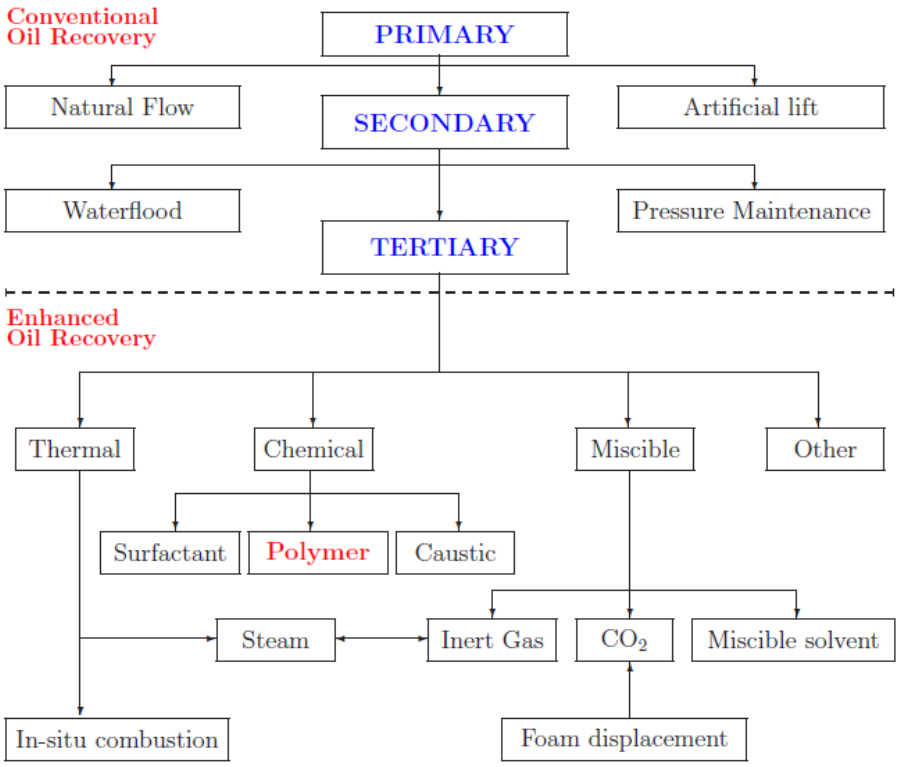

Figure 1. 1: Different stages of oil recovery (Lopez 2004).

Efficiency of a water flood operation can be greatly improved by adding a water-soluble polymer to the injecting water to increase its viscosity and as a result, to lower the water-oil mobility ratio in the system and increase the sweep efficiency. Five field cases (Bohai Bay, Offshore China; East Bodo and Pelican Lake, Canada; Tambaredjo, Suriname; Bati Raman, Turkey; Marmul, Oman) where polymer flooding in heavy oil has been tested, show results of recovery up to 59% of heavy oil (Alexis 2016; BASF 2016). Importance of polymer flooding is evident from the fact that, currently, more oil is produced by polymer flooding than all of the other chemical EOR processes combined (Pope, 2014). Polymer flow and retention behaviour upon injection in the porous rock which reduce permeability beside viscosity

reduction of polymer in reservoir are important issues for a successful polymer flooding process.

1.2 Problem statement

The use of water-soluble polymers improves the water-oil mobility ratio, and leads to enhanced oil recovery. As discussed in background, the most applied and studied polymer for EOR purposes around the world is the conventional partially hydrolysed polyacrylamide (HPAM). This synthetic polymer is largely industrially available and has a lower price compared to other polymers, like the biopolymer Xanthan (Morel et al., 2008). However, the harsh conditions present in most oil reservoirs, such as high salt concentration, high temperature, and high injection rate, reduce functionality of these conventional water-soluble polymers.

Hydrophobically modified polymers (HMPs) have been introduced to oil field to replace conventional polymers and obtain better properties such as higher viscosity at different shear rates, higher salinity tolerance, higher temperature resistance, and lesser sensitivity to mechanical degradation (Dupius 2010).

There has been a considerable amount of academic work published on the synthesis and characterisation of HMPs such as Wever et al (2011); Gouveia et al (2009); Fei-peng et al (2008); Peng zhang et al (2011); Blagodatskikh et al (2004), for different applications such as painting, cosmetic and pharmaceutical.

Some hydrophobic monomers such as acrylate and methacrylate-derivatives, (Wever et al, 2011; Mansri et al 2006; Baojiao et al, 2008) have been used to synthesise different copolymers of acrylamide with different chemical structure to be applied for EOR; however, phenyl-acrylamide has not been published yet.

In this study, polymerisation of acrylamide was carried out with a hydrophobic monomer (phenyl-acrylamide) to prepare phenyl-polyacrylamide (PPAM) which is a hydrophobically modified polyacrylamide (HMPAM). Phenyl-acrylamide monomer is more economical compared to

other monomers and easily accessible in the market. Association of phenyl-acrylamide hydrophobic molecule in molecular structure of HMPs form a bulky structure which causes an increase in viscosity of polymer solution and make these polymers a better alternative for EOR (Stavland 2013).

1.3 Research aim and objectives

The aim of this research is to synthesise poly-phenylacrylamide (PPAM) and investigate its solution behaviour in porous media. To achieve this, following objectives need to be addressed.

• To investigate micellar copolymerisation method to synthesise phenyl-polyacrylamide (PPAM) and to study the effect of the hydrophobe monomer, surfactant and initiator concentration on total monomer conversion rate.

• Investigation of the effect of the hydrophobe monomer concentration on the copolymer viscosity to determine the optimum polymer composition for synthesis of PPAM.

• To study comparatively the rheological behaviour of PPAM and HPAM solutions of polymers in high salinity and temperature conditions.

• Investigate PPAM flow behaviour in porous media and its interactions with rock and brine.

• To study PPAM and HPAM adsorption in porous media, and investigate parameters such as permeability reduction and mobility reduction.

• To investigate comparatively the oil recovery performance, using injection of PPAM and HPAM solutions in a sandstone rock.

1.4 Structure of the Thesis

Chapter 1: Introduction, gives a brief overview and background of enhanced oil recovery processes. Challenges and barriers in application of polymers in EOR followed by the aim and objectives of the research work are highlighted and organisation of the thesis was introduced.

Chapter 2: Literature Review, outlines a detailed literature review of four main areas of research: Synthesis, structure and properties of associative polymers, type of polymers used in enhanced oil recovery, polymer flooding

mechanism and terminologies, polymer screening criteria with several case studies and examples.

Chapter 3: Methodology, provides detailed procedure for the preparation and synthesising of PPAM, materials and equipment used, formulae involved and polymer solution preparation. It also presents the method used to study the rheological behaviour of polymer bulk solution, and their flow behaviour in porous media are presented in this chapter. The detailed description of the set-up and procedure developed for the oil recovery experiments are also explained.

Chapter 4: Results and Discussions, the results drawn from PPAM synthesis and characterisation experiments are discussed. The effect of parameters such as, initiator concentration, hydrophobe monomer concentration and surfactant concentration on the rate of monomer conversion are extensively evaluated. The results of the effect of the monomers ratio in polymer structure are discussed. Discussion of the results from rheological behaviour of bulk polymer solutions and the effect of salinity, temperature and polymer concentration on polymer viscosity are presented. This is followed by a detailed discussion of polymer flow behaviour in porous media, and the interaction of polymer, brine and rock and comparing the results with conventional HPAM. Moreover, detailed discussions on all the outcomes of core flooding experiments and oil recovery are presented.

Chapter 5: Conclusions and Recommendations for future work, the general conclusions relating to the overall research findings and suggestions for future work in the field are presented in this chapter.

Chapter 6: References, this chapter lists all the references to the literature materials used and cited in this research work.

Chapter 7: Appendix, some helpful explanations and supporting materials that are relevant to the research work are provided in this chapter.

Chapter 2

Literature Review

2. Literature Review

This chapter provides an overview of the conventional polymers used in enhance oil recovery followed by introducing hydrophobically modified polyacrylamide (HMPAM). Method of synthesis of the novel phenyl-polyacrylamide (PPAM), its structure and properties are discussed. Mechanism of polymer flooding in reservoir is explained with several case studies. Also, polymer flow behaviour in porous media and interaction of polymer solution with brine, oil and rock are thoroughly explained.

2.1 Types of polymers for EOR

The two most general polymer types used in the EOR process are a synthetic material, polyacrylamide in its partially hydrolysed form (HPAM), and the biopolymer xanthan (Shaohua 2015). These kinds of polymers are also extensively used in several industries as thickening agents due to great viscosity enhancement of water.

2.1.1 Hydrolyzed polyacrylamide (HPAM)

The polyacrylamide used in polymer flood application is in its hydrolysed form (HPAM). HPAM is a straight-chain polymer that has the amide group ($CONH_2$) as the monomer and carboxylic group (COO^-) in their structure as shown in Figure 2.1. Acrylamide monomer is reacted with sodium hydroxide (NaOH) and partial hydrolysis can occur in some of these monomers. The carboxyl groups dissociate and leave negatively charged ions leading to polyelectrolyte properties in aqueous solution. Typical degrees of hydrolysis are 25% - 35% that are chosen to optimize the specific properties of the polymer solutions. If the degree of hydrolysis is too low, the polymer will not be water soluble. If it is too high, its properties are overly sensitive to salinity and hardness (Sorbie, 1991).

The typical molecular weight of HPAM used in polymer flood is within the range of 2-20 $\times 10^6$g/mol. The viscosity-increasing feature is derived from the repulsion between polymer molecules and between the segments of the same molecule

As a result of these molecular arrays, the viscosity of polymer increases and causes the lower mobility of the polymer solution (Shaohua 2015).

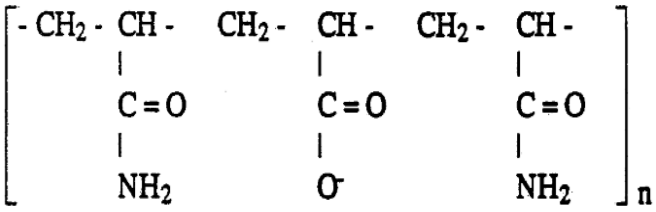

Figure 2. 1: HPAM molecule structure (Shaohua 2015).

Advantages and disadvantages of HPAM polymers

HPAM polymers are inexpensive, excellent viscosifier and more bacteria resistant than biopolymers, but they cannot be used in water with high salinity (> 30000 ppm), especially at raised temperature (> 80°C). Other disadvantages associated with HPAM are low thermal and shear stability, and injectivity problems of high molecular weight and high concentration solutions used for flooding (Nodar 2009; Sochi 2010).

2.1.2 Xanthan Gum (corn sugar gum)

This is another widely used EOR polymer with average molecular weight of 1 x 10^6 to 15 x 10^6 g/mole used in EOR process (Zaitoun 2011). It is the biopolymer produced during fermentation of glucose. As a result, this polymer becomes very sensitive to bacterial attack on surface, even after it has been injected into the reservoir.

The main advantage of Xanthan polymer in EOR is that it is less sensitive to brine salinity and water hardness in comparison to HPAM (Nodar 2009).

On the other hand Xanthan polymer molecules act like a semi rigid rods and are quite resistant to mechanical degradation. However, Xanthan has the disadvantage of having low thermal stability because of the presence of oxygen molecule (-O-) in the backbone of its structure. Once it is subjected to temperatures higher than 80^{O}C, the chemical bonds in the chain are weakened and multiple free radicals are formed. This causes the functional groups in the

polymer chain to change location as the results new compound is formed and the polymer structure is destroyed (Sochi 2010). Chemical structure of Xanthan gum polymer is shown in Figure 2.2.

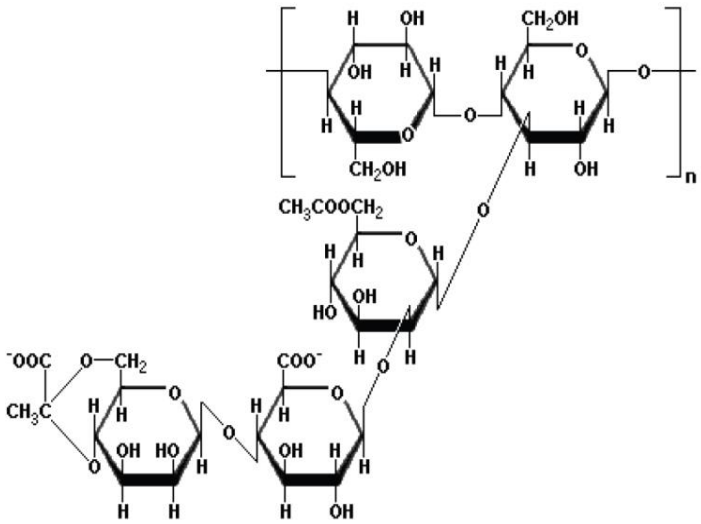

Figure 2.2: Xanthan gum polymer structure (Zaitoun, Makakou et al 2011).

Associative polymers have been introduced two decades ago (Wever 2011) as an alternative to oilfield applications to minimize problems associated with conventional polymers (HPAM and xanthan). Presence of hydrophobic monomers in the molecular structure of associative polymers causes a large aggregation in polymer molecules which make these polymers exceptional for EOR. These polymers offer improved properties such as better viscosity enhancement, greater temperature tolerance, and higher salinity resilience.

2.1.3 Associative polymers

Associative polymers contain a small number of hydrophobic groups attached to the polymer backbone. These polymers are a relatively new class of polymers, which has recently been introduced to oil field applications (Guillaume, 2010; Li et al 2014; Alexis, 2016). They are divided into two groups:

• Water-soluble associative polymers containing hydrophilic group with a small percentage of hydrophobic groups, for example polyacrylamide modified with small amount of hydrophobic monomer (HMPAM).

• Oil soluble associative polymers containing hydrophobic group with a small percentage of hydrophilic groups, for example methacrylate modified with alkyl acrylate (Jimenez 2004).

Essentially, hydrophobically modified polymers (HMPs) consist of a hydrophilic long-chain backbone, with a small number of hydrophobic groups localized either randomly along the chain or at the chain ends (Lara-Ceniceros et al., 2007). When these polymers are dissolved in water, hydrophobic groups aggregate to minimize their water exposure. In aqueous solutions at a basic pH, hydrophobic groups form intramolecular and intermolecular associations that give rise to a three-dimensional network (Caram et al., 2006). These networks significantly increase the viscosity of the polymer solution. The three-dimensional network structure of associative polymers is illustrated in Figure 2.3.

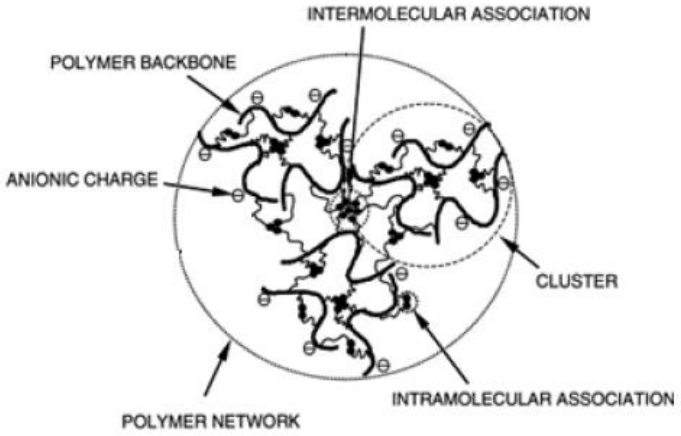

Figure 2. 3: Associative polymer network (Caram 2006).

Another important factor is that the functional groups on these kind of polymers are less sensitive to brine salinity compared to a conventional polymer, as polyacrylamide, whose viscosity dramatically decreases with increasing salinity. Figure 2.4 shows a viscosity reduction comparison between a hydrolysed polyacrylamide (HPAM) and an associative copolymer poly-acrylic acid (PAAC) at different salt ions concentration.

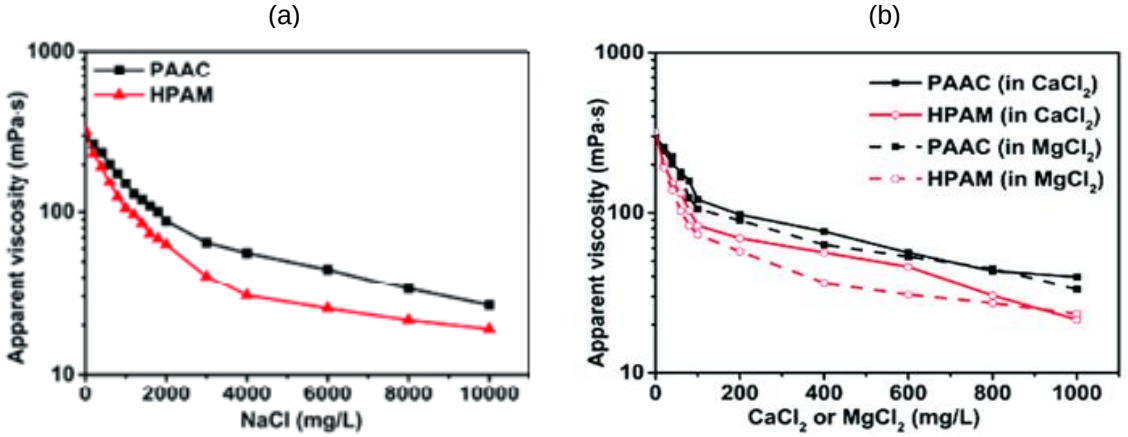

Figure 2. 4: a) Effect of NaCl concentration, b) $CaCl_2$ or $MgCl_2$ concentration on polymer solution viscosity, T= 25° C, shear rate 10 s^{-1} (Shaohua 2015).

A clear greater reduction of viscosity for HPAM is observed compared to PAAC in presence of different monovalent (Na^+) and divalent (Ca^{2+},Mg^{2+}) ion concentration. HPAM copolymer is negatively charged due to presence of carboxylate groups (-COO-) in their molecular structure. This causes a strong binding between carboxylate groups and salt ions which reduce the expansion of HPAM molecules in water and cause a viscosity reduction. However, the presence of hydrophobic monomers in molecular structure of PAAC form a strong aggregation which make the polymer larger dimensionally and less susceptible to viscosity reduction in presence of salts (Buchgraber 2009).

2.2 Methods of synthesis of hydrophobically modified polyacrylamides (HMPAM)

There are three main methods of synthesis of HMPAM: micellar polymerisation, microemulsion polymerisation, and inverse emulsion polymerisation (Wang et al 2003, Sun 2007). The main difficulty in the preparation process of HMPAM solution in all methods is the insolubility of the hydrophobic monomer in the aqueous phase. This problem has been overcome by the following two methods:

a. Microemulsion and inverse emulsion polymerisation can take place in either an organic solvent or water- based solvent mixture, as monomers are soluble in both these mixtures.

b. Polymerisation with micelles, where a surfactant solution is used to ensure the complete solubilisation of the hydrophobic monomer contained in the micelle. In micellar processes, micelle-forming polymerizable surfactants are able to be used as an alternative of the hydrophobic monomer (Biggs 1991). In this study, micellar polymerisation is used to synthesise phenyl-polylacrylamide (PPAM) which is explained further in following section. The micellar polymerisation method so far is the most common method to synthesise the polymer for oilfield applications as it is more cost effective (Karlson 2002).This copolymer (PPAM) is a hydrophobically modified polyacrylamide composes of acrylamide (AM) as a hydrophile monomer and phenyl-acrylamide (PA) as a hydrophobe monomer.

2.2.1 Micellar polymerisation

In micellar polymerisation, surfactant plays an important role to form micelles. Presence of both hydrophilic group (head) and hydrophobic group (tail) in chemical structure of surfactants make them soluble in both, water and organic solvents (Figure 2.5). The presence of surfactant in water causes the hydrophobic tails aggregate and reduce their exposure to water and form a micelle. However, in an oleic solution the hydrophilic heads aggregate and form a micelle (Hill 1993). In order to form these micelles, certain number of molecules must be in solution at a given surfactant concentration. The concentration at which the micelle appears is called critical micelle concentration (CMC) (Candau 1994).

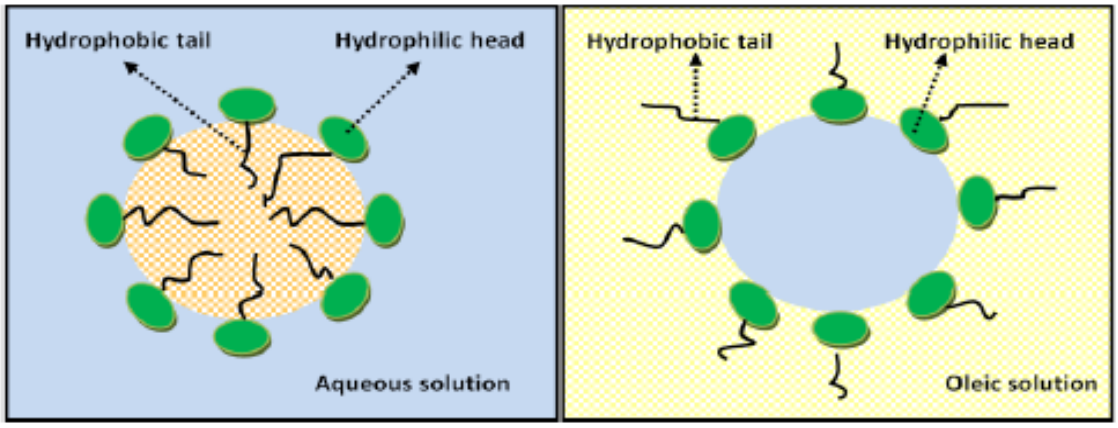

Figure 2. 5: The figure on the left represents micelle in water and on the right illustrates micelles form in oil (Hill 1993).

Figure 2.6 shows the surface tension of a surfactant solution at different surfactant concentration and formation of micelles. As it can be seen from Figure 2.6, surface tension reduces by increasing surfactant concentration until surfactant molecules saturate the surface of solution at which no more reduction in surface tension is observed. When the formation of micelles is desirable, the CMC is a measure of the efficiency of a surfactant.

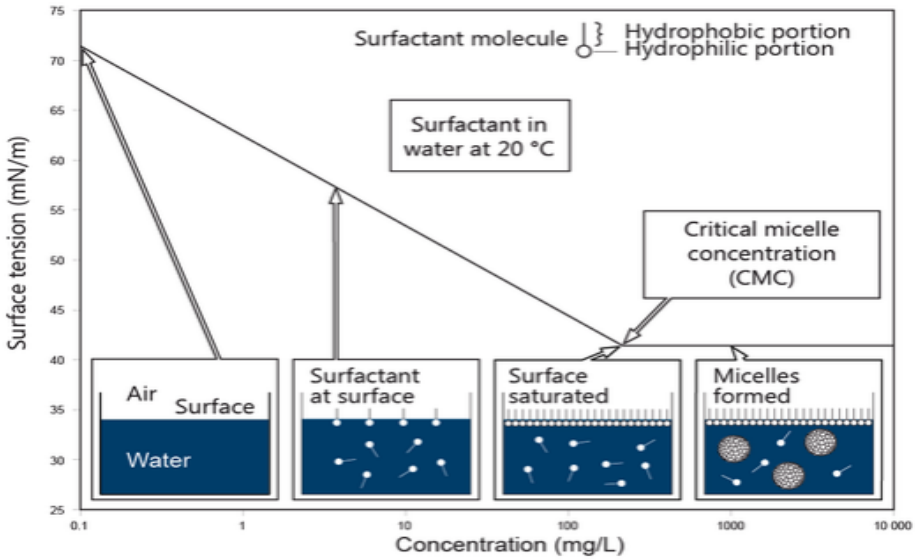

Figure 2. 6: Formation of micelles at different concentration of surfactant (Almgren 2000).

Direct polymerization of hydrophilic monomer with hydrophobic monomer requires a common solvent for both the monomers for the reaction to proceed.

Furthermore, the limited solubility of monomers often leads to heterogeneous copolymer composition and low hydrophobic modification (Vijay 2008).

In order to overcome these problems, a micellar polymerisation/ copolymerisation technique is routinely used. For example, in the micellar copolymerisation, the hydrophobic monomer is solubilized within surfactant micelles, whereas acrylamide is solubilized in water. For neutral or anionically charged hydrophobic polymer, sodium dodecyl sulfate/ethylene glycol is used as surfactant; and for cationically charged polymers, either cationic or nonionic surfactants are used (Nodar 2009). The heterogeneity in the copolymer, i.e. the length of the block of the copolymer can be controlled by the reactivity ratios (ratio of reactivity of a hydrophobic to hydrophilic monomer). This is achieved by the micellar effect, i. e. by varying the concentration of surfactant or number of hydrophobic monomer per surfactant micelle (N_H) during the synthesis. It was observed that a low value of N_H produces more heterogenous copolymer. The generalized chemical structure of HMPAM is shown in Figure 2.7.

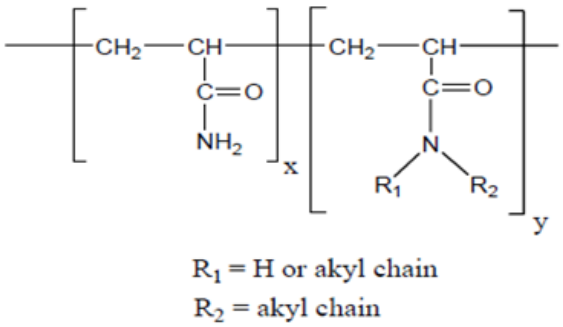

Figure 2. 7: HMPAM chemical structure (Nodar 2009).

2.2.2 Phenyl-polyacrylamide (PPAM) polymerisation

Figure 2.8 shows a schematic diagram for micellar polymerisation that has been modified to illustrate the PPAM. In this process, surfactant is added to water above CMC point to provide enough micelles to solubilise phenyl-acrylamide (hydrophobe monomer). Then, phenyl-acrylamide monomer is dissolved within the surfactant micelles while at the same time acrylamide monomer is dissolved in the aqueous solution. After ensuring the complete solubilisation of hydrophobic and hydrophilic monomers, potassium per sulphate (KPS) as

initiator is added to aqueous solution to start the polymerisation reaction. By dissociation of initiator (*), a free radical is produced, and by addition of the free radical to free orbital of acrylamide monomer (O) in solution, an active acrylamide monomer (O*) is produced. The new radical monomer is added to a new monomer and makes it an active radical and this chain propagates by hundreds or probably thousands of monomers. At some point, an acrylamide active monomer is added to a phenyl-acrylamide free orbital (●) inside a micelle, and adds the phenyl-acrylamide monomers to the propagated chain. This process terminates where two active monomers react with each other and chain stop growing (Wever 2011).

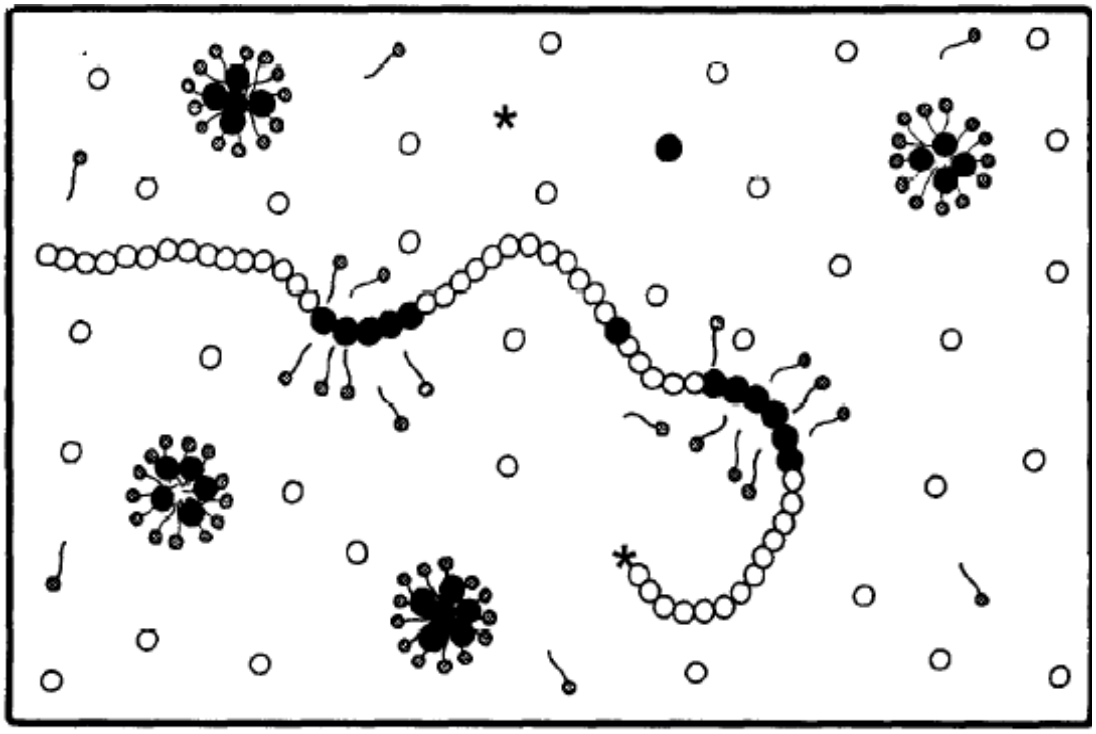

Figure 2. 8: Schematic representation of the micellar polymerization medium ● phenyl-acrylamide monomer; ○ acrylamide; * initiator; ● surfactant (modified from Wever 2011).

Figure 2.9 shows a segment of polymer PPAM. The new synthesised polymer made up of two monomers, acrylamide and phenyl-acrylamide.

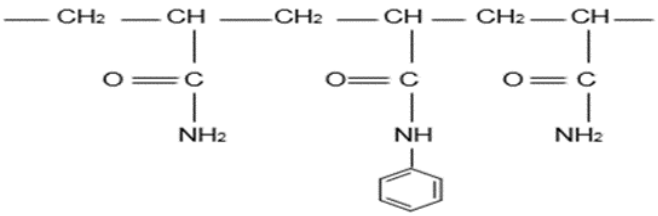

Figure 2. 9: Segment of copolymer structure of acrylamide with phenyl-acrylamide.

● Monomer conversion

Shawki-Hamielec (1991) derived an equation to describe acrylamide monomer conversion to polyacrylamide. The equation presents the conversion-time behaviour of acrylamide monomers polymerised in water with an initiator (KPS).

$$\frac{[\boldsymbol{Mo}]-[\boldsymbol{M}]}{[\boldsymbol{Mo}]} = \mathbf{1} - \left[\frac{\boldsymbol{K_{125}}\,[\boldsymbol{Io}]^{\mathbf{0.5}}[\boldsymbol{Mo}]^{\mathbf{0.25}}\boldsymbol{t}}{\mathbf{4}} + \mathbf{1}\right]^{-\mathbf{4}} \qquad (2.1)$$

[Io] = Initial concentration of initiator (mole/litre)

[M_0] = Initial concentration of monomer (mole/litre)

[M] = monomer concentration at time t (mole/litre)

K_{125}= $1.7\times10^{11}\exp(-16900/1.99T)$

T= Temperature (K)

Several authors such as Biggs and Candau (1991), Hill and Selb (1996) have reported incorporation of small amount (1-3 % mole) of hydrophobe monomer does not affect the rate of acrylamide monomer conversion to polyacrylamide. In this research, Equation 2.1 is used for total monomer conversion of acrylamide and phenyl-acrylamide to phenyl-polyacrylamide (PPAM). According to equation 2.1, conversion is a function of initial concentration of monomers (acrylamide and phenyl-acrylamide), initiator (potassium persulphate), temperature, and time of the reaction. Monomer conversion equation is used to calculate theoretical conversion data during polymerisation reaction and compare the results with laboratory data. Close results prove the accuracy of the experiment and calibration of equipment.

2.3 Mechanism of polymer flooding

Figure 2.10 demonstrates a typical polymer flood schematic (Lindley, 2001). The polymer flood process usually starts with a pre-flush of low-salinity brine. This precaution is taken because of the significant sensitivity of conventional polymers to brine salinity and chemistry. The next step is injecting the polymer solution, followed by driving water to push the polymer solution into the reservoir. Since oil and water are immiscible fluids, neither one can completely displace the other under reservoir conditions. Oil is left behind in the reservoir after water flood either because it is trapped by the capillary forces (residual oil) or because it somehow gets bypassed. Residual oil trapped in the pores is immobilized due to strong capillary forces (Egbogah, 1980).

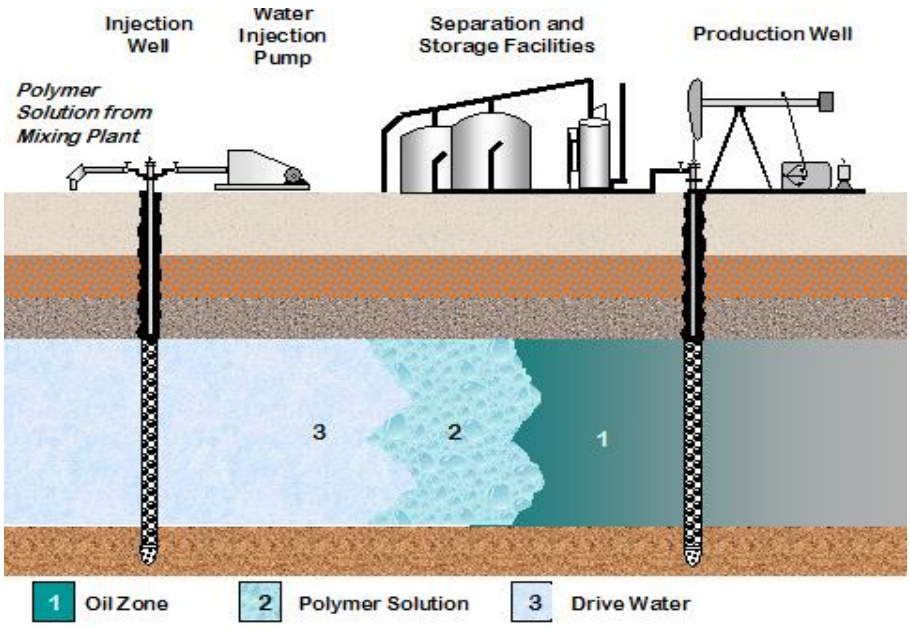

Figure 2. 10: Schematic of polymer flood (Lindley, 2001).

In order to remobilize the trapped residual oil, the interfacial tension between oil and water phases must be lowered to a sufficiently low value. This can be achieved by adding a surfactant to the injecting fluid; but recovering residual oil by this method is the aim of low-tension surfactant flooding (Lake, 1989). Polymer flooding can neither reduce the interfacial tension to sufficiently low value nor greatly increase the viscous-to-capillary force balance between water

and oil phases in the displacement, without which the residual oil cannot be mobilized. Hence, the target of polymer flooding is to recover that portion of oil that is bypassed by waterflood but does not include residual oil (Sorbie, 1991). Even though polymer flooding cannot reduce the residual oil saturation (So_r), it still is an effective way to reach the So_r more quickly or more economically (Du and Guan, 2004).

In order to fully understand and appreciate the mechanism of polymer flooding, it is essential to first gain knowledge about some of the key concepts associated with polymer flooding, such as, mobility ratio, types of sweep efficiency (displacement efficiency and volumetric sweep efficiency) and resistance factor.

2.3.1 Mobility Ratio

Mobility ratio, M, is the ratio of mobility of displacing fluid to the mobility of displaced fluid. It is defined for water floods as follows:

$$M = \frac{\lambda_w}{\lambda_o} = \frac{k_w/\mu_w}{k_o/\mu_o} \qquad (2.2)$$

Where λ_o and λ_w are the mobility of displaced fluid (oil) and the mobility of displacing fluid (water), respectively. μ_o and μ_w are the viscosities of oil and water, respectively. k_o and k_w are the effective permeabilities of oil and water phases, respectively.

During oil recovery, when injecting fluid into the reservoir, it is desirable to have a mobility ratio of less than one. This is because a mobility ratio below one represents a scenario where the oil is more mobile than the displacing fluid. When the mobility number is greater than 1, for example M=10 and with water being the displacing fluid, water is ten times more mobile than the oil which is being recovered. This poor ratio results in an early breakthrough of water and is not desirable when producing oil which, leads to an increase in the amount of water being produced with oil. This early breakthrough that occurs with high mobility ratio is shown in figure 2.11 (a). This commonly occurs during water injection due to the viscosity of water being much lower than the viscosity of the

oil in place. As a result, oil sticks to the reservoir rock while the water pushes through the points of least resistance, leading to an effect called fingering.

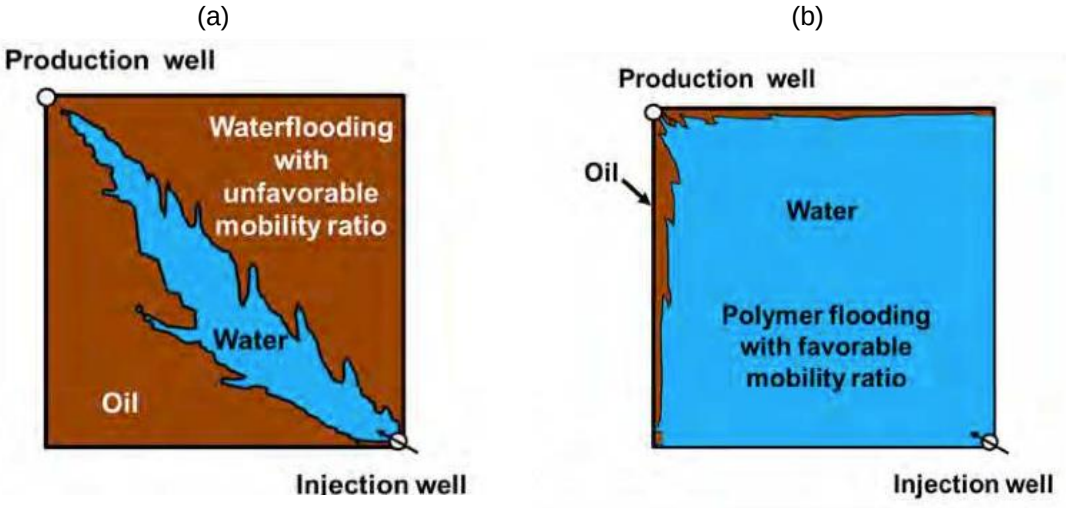

Figure 2. 11: a) Unfavourable mobility ratio (M>>1), b) Favourable mobility ratio (M<1) (Romero- Zeron, 2012).

To lower this effect and decrease the mobility ratio, polymers are added to injected water. As depicted in Figure 2.11 (b), the displacing fluid (water with added polymer) is able to drive the oil more effectively towards to production well. If the mobility of the displacing fluid being less than or equal to the mobility of the displaced fluid (oil) there is normally an increase in the overall recovery process.

2.3.2 Sweep efficiency

The sweep efficiency is a measure of how effective an enhanced oil recovery method is and is represented by the volume of the reservoir that is in contact with the injected fluid (Neil et al 1983). Therefore, with a decrease in the mobility ratio there is an increase in the sweep efficiency. The total sweep efficiency is made of macroscopic (volumetric) displacement and microscopic displacement efficiency (Zekri, 2004)

$$E = E_v E_d \quad \text{Overall sweep efficiency}$$

Where: E_v: Volumetric (macroscopic) sweep efficiency [%]

E_d: Microscopic sweep efficiency [%]

The macroscopic sweep efficiency relates to the amount of displacing fluid that comes in contact with the oil. This is composed of two separate efficiencies; these components are aerial and vertical sweep efficiencies and are represented in the following equation

$$E_v = E_s E_i \quad \text{Macroscopic sweep efficiency}$$

Where: E_s: Aerial sweep efficiency [%]

E_i: Vertical sweep efficiency [%]

The microscopic sweep efficiency (E_d) represents how well that fluid mobilizes the residual oil (Terry, 2011).

2.3.3 Fractional flow

Another important concept associated with two-phase immiscible flow is the fractional flow. In immiscible displacement processes, the mobility ratio does not remain constant; it varies with the saturation of the flowing phase. Assuming that water and oil are flowing simultaneously through a porous medium, the fractional flow equations for water (f_w) and oil (f_o) can be written as:

$$f_o = \frac{1}{1+\frac{\mu_o k_{rw}}{\mu_w k_{ro}}}$$

$$f_w = \frac{1}{1+\frac{\mu_w k_{ro}}{\mu_o k_{rw}}}$$

where k_{ro} and k_{rw} are relative permeability of oil and water, respectively. Figure 2.12 shows the fractional flow curves for the displacement of oil with a viscosity of 15 mPas by water (1 mPas) and a polymer solution (15 mPas) (Littmann, 1988). The saturation at the front of the polymer flood, S_{wp} , and the water flood, S_{wf} , are presented by constructing the tangent line to the fractional flow originate from the irreducible water saturation (S_{wi}) (Hirasaki, 1974). In the polymer flood case, note that the saturations at both the flood front and at the breakthrough are significantly greater than those in the waterflood case. This

increasing in flood front saturation indicates a greater performance of the polymer flood as compared to the water flood.

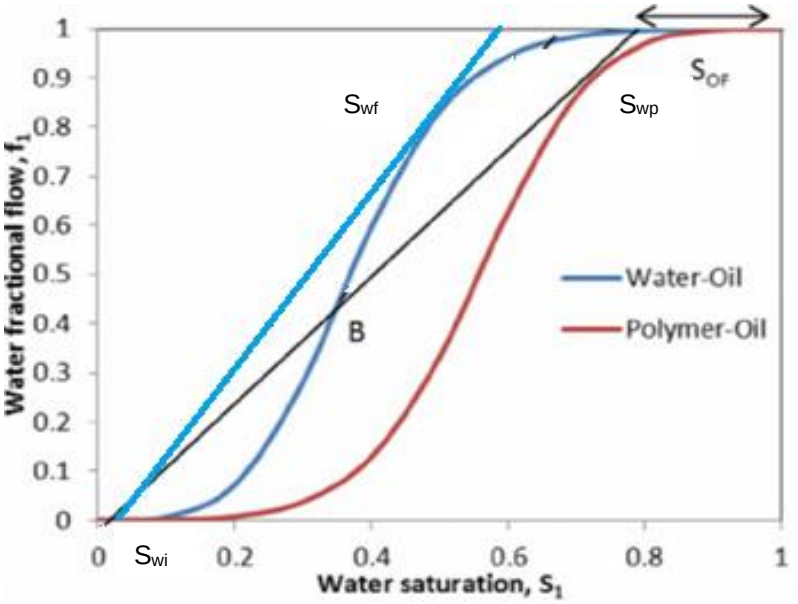

Figure 2. 12: Fractional flow curve (Pancharoen 2009).

2.4 Field applications of polymer flooding

Daqing oil field was found in 1959 and its oil production approached 1,000,000 barrels per day in 1976 which was maintained at that level until 2002. The average water cut reached 87% in 2001 (Rassenfoss, 2014). After decades of laboratory research and pilot tests Daqing extended the polymer floods to the suitable reservoirs of the whole field in 1996. Its production due to polymer flooding approached 200,000 barrels per day in 2002 and increased steadily since then. The polymer flooding production of 2013 reached 270,000 barrels per day accounting for about 1/3 of the total production (Rassenfoss, 2014). Furthermore, polymer flooding has gained country wide field applications during the same period of time, even though other oil fields are in smaller scales compared to Daqing.

The success of the polymer flooding in Daqing should be attributed to the particular reservoirs which are mostly sandstone with amenable properties, similar to many successful polymer flooded reservoirs in the U.S. In Daqing, the average reservoir temperature is low (~45°C); the oil viscosity (~10- 20 mPa.s)

under reservoir conditions is low as well; and the salinity of formation brine ranges from 3000ppm to 7000ppm. The injected water is fresh water or makeup of fresh water with produced water. At these low salinities a polymer solution with higher viscosity than oil can be achieved at a concentration of 1500ppm or lower using high or ultra-high (e.g.~38 million Daltons) molecular weight HPAM polymers and the mobility ratio less than unity can be attained without many difficulties (Taber et al., 1997). The most common screen criteria for polymer flooding is in Table 2.1.

Table 2. 1 : Screen criteria for polymer flooding

Class	Screen Criteria			
	Permeability (md)	Temperature (℃)	Salinity (ppm)	Hardness (ppm)
I	≥500	≤70	≤10000	≤200
II	≥500	70-80	10000-30000	200-400
III	≥100	80-95	30000-100000	>400

As can be seen, unlike Class I reservoir in which most the polymer floods are applied, Class II & III reservoirs are characterized with lower permeability, higher temperature and higher salinity and hardness. The polymer formulations used in Class I reservoirs are much less effective for Class II and III reservoirs. A significant reduction in solution viscosity of HPAM is observed when the polymer is dissolved in salt water. Therefore, new polymers for EOR should be able to resist the presence of salt without a significant reduction in the solution viscosity. New associative polymers (e.g hydrophobically modified polymers) and practices are being investigated and applied to Daqing (Alexis 2016).

The application of polymer flooding also depends on the viscosity of the oil in the reservoir. The viscosity of oil varies significantly, from water like consistency up to bitumen (tar sands). It is desirable to be able to apply polymer flooding for oil viscosities up to 200 cp. The higher the oil viscosity the more polymer is required to match the viscosity of the displacing fluid (water). The higher the

required polymer concentration, the less attractive (higher polymer costs) the oil reservoir is for the application of polymer-based floods. Therefore extensive research has been done, and is still ongoing, to improve the thickening capabilities of water soluble polymers.

The permeability of a reservoir is, as mentioned before, the ability of a fluid to pass through the porous media. A great number of oil reservoirs around the world have porous media whose permeabilities are lower than 50 mD, the so-called carbonate reservoirs. Currently used polymers (e.g HPAM) are high molecular weight polymers and will block the pores of such low permeable reservoirs. Adsorption to the rock surface by the polymer chains lead to injectivity loss. Laboratory core flood testing confirms this by showing a significant increase of the pressure over the core sample increases as more and more polymer solution is flowed through.

The above review of the developments and successes of field polymer floods in the U.S and China at different times reveals some common characteristics. The most important one seems to be the reservoirs and its properties. Polymer flooding is a good EOR choice to be considered for sandstone reservoirs with moderate or high permeability, low salinity and low to moderate temperature.

2.5 Properties of polymer solutions

Estimating polymer solution properties is very important as it affects the molecular behaviour of polymer in solution. Polymer solution in real field application is subjected to parameters such as shear rate, low and high salinity and high temperature resulting in alteration of the initial properties of the polymer solution and affect the polymer performance. Therefore, it is important to have an understanding of these properties as mentioned follow

2.5.1 Polymer concentration

The behaviour of the polymer molecules in the aqueous solutions depends on the polymer concentration (C). The range of polymer concentration can be divided into three different regimes, the dilute, the semi dilute, and the concentrated regime. Since the volume of the polymer coils exceeds the volume of the aqueous solution, the polymer coils are forced to overlap and the

concentration at this point is called the critical aggregation concentration c^*, Figure 2.13 (Ahmed 2002).

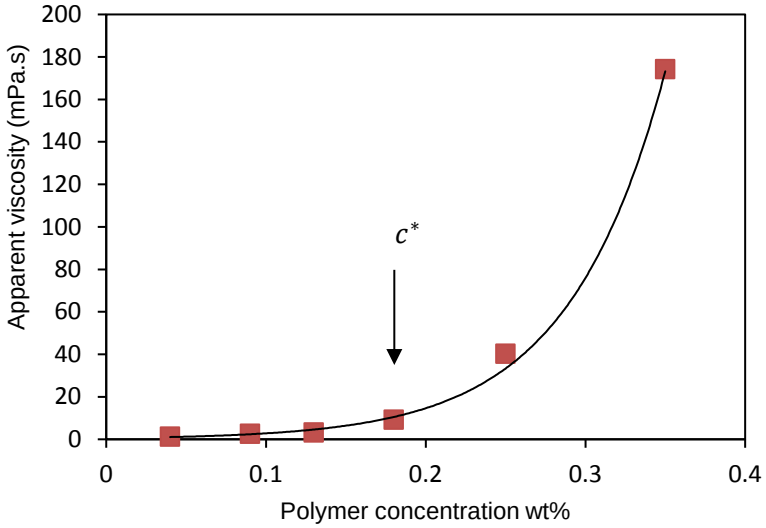

Figure 2. 13: Apparent viscosity as a function of polymer concentration (Ahmed 2002).

In the dilute regimes (C < C*) the polymer chains are expected to move separately in the solution because of the concentration is low and the distance between the polymer coils is larger than the mean radius of one single polymer coil named as the radius of gyration (Figure 2.14). In the semi dilute regimes (C ≥ C*) the radius of gyration is larger than the mean distance between the polymer coils.

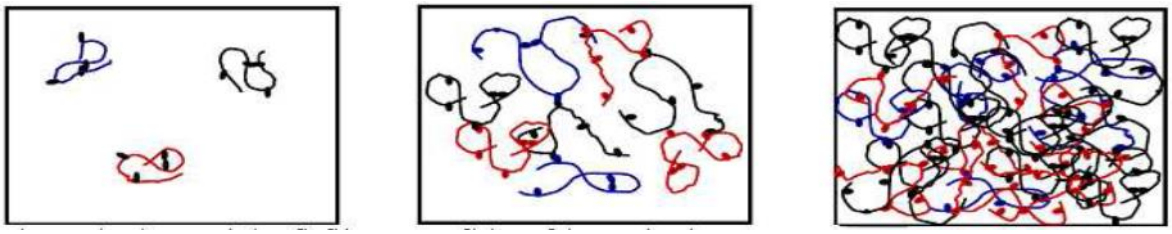

C < C* **C ≥ C*** **C >>C***

Figure 2. 14: Polymer concentration at three different regime (Ahmed 2002).

The hydrophobic group in the copolymer can either form an intra-molecular association by interacting with another hydrophobic group on the same polymer chain, or it can interact with another hydrophobic group on another polymer molecule and form inter-molecular association (Stavland 2010). At low PPAM

concentrations the ability of the hydrophobic group to interact between different molecules is small. Upon increasing polymer concentration, inter-molecular associations become more important and this will raise the viscosity of the solution dramatically. Figure 2.15 shows a schematic of these associations.

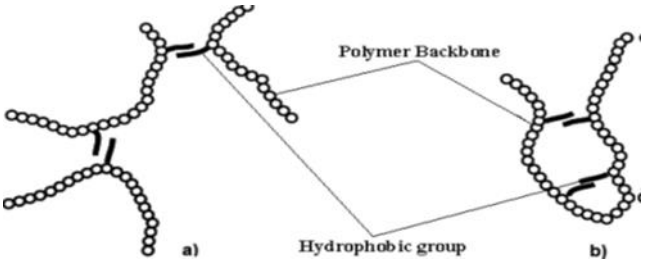

Figure 2. 15: Illustration of a) inter-molecular association, b) intra-molecular association (Stavland 2010).

2.5.2 Viscosity average molecular weight

The viscosity of polymer solution is related to the size of the polymer molecules in solution. The larger the molecules, the higher the viscosity of the polymer in that particular solution. It is obvious that the viscosity in the solution is related to the polymer concentration in the solution. One of the fundamental quantity which is most related to the molecular size of the polymer in solution is intrinsic viscosity $[\eta]$(equ. 2.3) and is used to estimate average molecular weight of polymer. By definition the intrinsic viscosity for polymer is estimated by plotting the reduced viscosity (ratio of specific viscosity to polymer concentration) against polymer concentration and extrapolating the fitted straight line to zero polymer concentration (Blagodatskikh 2004) as shown in Figure 2.16.

$$[\eta] = \lim_{c\to 0} \frac{\eta-\eta_s}{c\eta_s} = \lim_{C\to 0} \frac{t-t_s}{Ct_s} = \lim_{c\to 0} \frac{\eta_{sp}}{c} = \lim_{c\to 0} \eta_R \qquad (2.3)$$

Where η and η_s are solution and solvent viscosity respectively, c is the polymer solution concentration. t and t_s are the time that take the polymer solution and solvent to pass through a capillary viscometer, respectively. In a dilute solution of polymer these times are an indication of the viscosity. η_{sp} is the specific viscosity (dimensionless unit) and η_R is the reduced viscosity (cm^3/g). The SI-unit for intrinsic viscosity is [cm^3/g].

The specific viscosity is a dimensionless viscosity parameter defined as the *relative viscosity* minus unity (Sorbie, 1991):

$$\eta_{sp} = \eta_r - 1 \qquad (2.4)$$

The relative viscosity η_r is also a dimensionless viscosity parameter, and is defined as the ratio between the viscosity of the polymer solution to the viscosity of the solvent (Sorbie, 1991):

$$\eta_r = \frac{\eta}{\eta_s} \qquad (2.5)$$

Where η is the non- Newtonian shear viscosity of the polymer solution [Pa s], and η_s is the solvent viscosity [Pa s]. Sorbie (1991) related the intrinsic viscosity to the inherent viscosity as the polymer concentration goes to zero:

$$[\eta] = \lim_{c\to 0} \frac{\ln\left(\frac{\eta}{\eta_s}\right)}{c} = \lim_{c\to 0} \frac{\ln(\eta_r)}{c} = \lim_{c\to 0} \ln(\eta_I) \qquad (2.6)$$

Where [η] is the intrinsic viscosity at zero polymer concentration with the unit [cm3/g], and η_I is the inherent viscosity with the SI unit [cm^3/g]. The inherent viscosity is defined as the ratio between the logarithmic value of the relative viscosity and the concentration of the solution (Sorbie, 1991):

$$\eta_I = \frac{\ln(\eta_r)}{C} \qquad (2.7)$$

Where the relative viscosity (defined in Eq. 2.5) is a dimensionless viscosity parameter, and the polymer concentration, c, has the unit [g/cm^3].

The intrinsic and inherent viscosity can be measured through viscometry at different concentrations. Since they are limited to zero polymer concentration, the viscosity is determined by extrapolation from the plot. In Figure 2.16 this extrapolation technique is illustrated, and it is only valid at low polymer concentrations such as in the dilute regime where the rheological flow behavior of the polymer solution is Newtonian (Chauveteau, 1984).

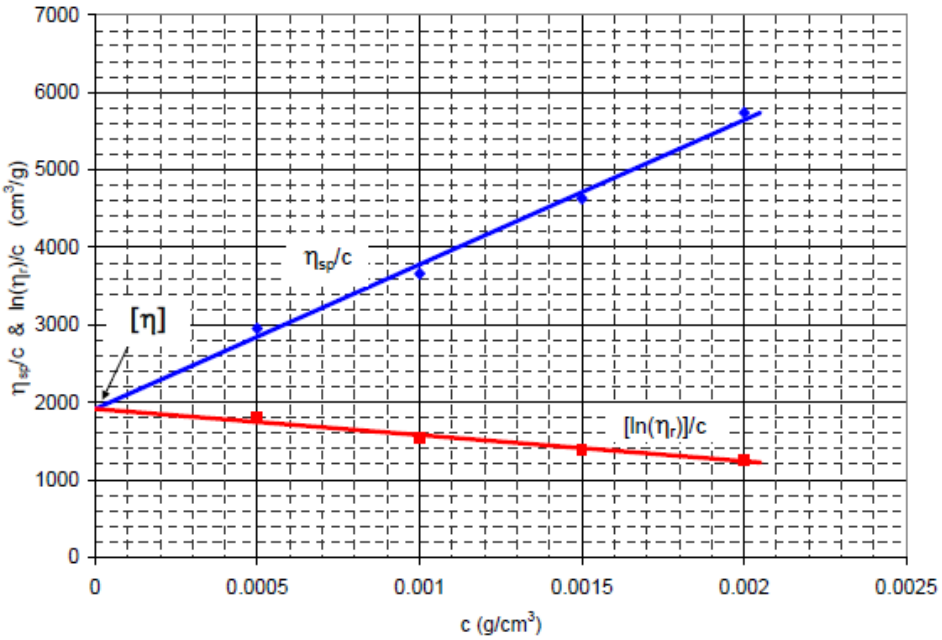

Figure 2. 16: Determination of the intrinsic viscosity (Sorbie, 1991).

The main purpose of capillary viscosity measurement was to calculate average molecular weight of polymer based on the intrinsic viscosity data. Viscosity average molecular weight (M_w) can be calculated by using Mark-Houwink equation.

$$[\eta]=K.M_w^{\alpha} \qquad (2.8)$$

Where K and α are empirical constants for a polymer at a fixed temperature in particular solvent and $[\eta]$ is the intrinsic viscosity (Saaverda 2002).

2.5.3 Polymer viscosity

The viscosity of a fluid may initially be defined as its resistance to shear (Sorbie, 1991). When a fluid is placed between two parallel surfaces moving in the same direction with different velocity, the velocity gradient in the vertical direction of the fluid is found to be linear for many fluid types. This velocity gradient is called the shear rate and is defined as,

$$\gamma = \frac{dv}{dr} \qquad (2.9)$$

The shear stress that causes the movement of the two surfaces is given by,

$$\tau = \frac{F(force)}{A(area)} \qquad (2.10)$$

The viscosity (μ) is then defined as the ratio of the shear stress to the shear rate. The relationship between these parameters is described as,

$$\tau = -\mu \frac{dv}{dr} = \mu\gamma \qquad (2.11)$$

The SI- unit of the viscosity is “Pascal.second” (Pa s), but the field unit used in the petroleum industry is centipoise (cp). Generally, a fluid may be classified as Newtonian or non-Newtonian depending on viscosity. The viscosity of Newtonian fluids, e.g. water, is constant and it is not a function of shear rate. Polymer solution generally classified as non-Newtonian fluids, i.e. the viscosity changes with shear rate and it is not constant.

Figure 2.17 show a standard shape of the complex flow behavior for dilute chain- like polymer solutions, with four distinct regions.

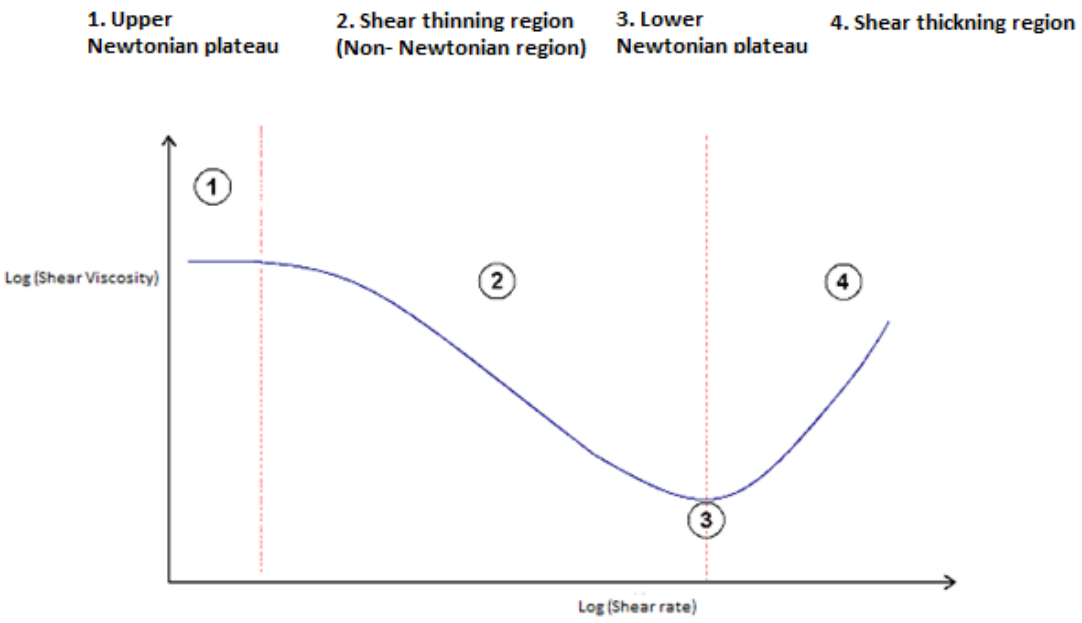

Figure 2. 17: Viscosity of a polymer as a function of shear rate (Sochi, 2010).

The four distinct regions in the above flow curve are described below:

1. The upper Newtonian plateau (Sochi, 2010): This region is also called the plateau of the zero- shear viscosity (μ). At low shear rates, the viscosity is constant, i.e. independent of shear rate. This behavior can be explained through the phenomenon Superposition of two processes (Anton Paar, 2008).

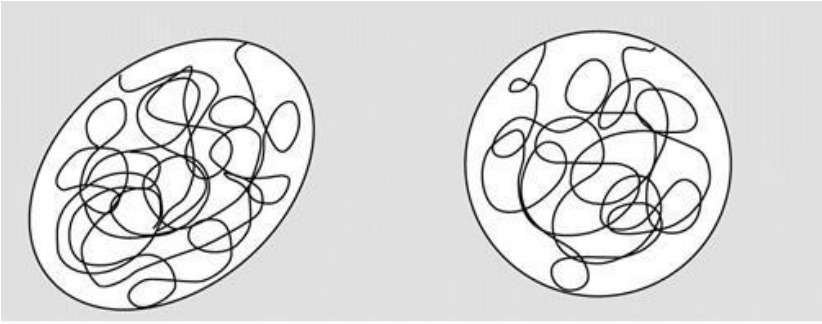

Figure 2. 18: Polymer viscoelastic behaviour under low shear rate (Sochi 2010).

In the low- shear range the macromolecules will start to orient themselves towards the flow, which cause disentanglements. Since the shear force acting on the polymer solution is so weak, the polymers are still able to re-entangle because of their viscoelastic properties (Figure 2.18). These two processes cancel each other out, leading to an area on the flow curve with no change in the total viscosity value.

Chauveteau and Yasuda (1984) defined a transition zone between the Newtonian region (1) and the shear- dominated region (2) at high shear rates. A critical shear rate (γ_c) defined at the end of the upper Newtonian plateau, was estimated to be equal to the inverse proportion of the rotational relaxation time (λ_c). The relaxation time is characteristic for a specific polymer solution, and is defined as the response time for the macromolecules to rearrange back to the originally configuration after the shear stress stops. A long relaxation time indicates a high elasticity in the polymer, caused by the strong interactions in the molecular chains (Sorbie, 1991).

2. *The shear thinning region:* After the critical shear rate defined at the relaxation time for the polymer, the viscosity starts to decrease with increasing shear rate. This non- Newtonian behavior is also referred to a *pseudoplastic* behavior (Sochi, 2010). Now the shear forces starts to break up the equilibrium structure, and uncoils the macromolecules. This results in a deformation in shear direction, which reduces the flow resistance of the polymer solution.
3. *The lower Newtonian Plateau:* At this shear rate region the viscosity of the polymer solution is at its lowest value (μ_∞), due to the strong deformation forces acting on the macromolecules. All the macromolecules in the solution are now stretched out to an aligned conformation and oriented to the shear direction
4. *The shear thickening/ dilatant region:* Odell et al. (1987) reported observations on extremely dilatant effects occurring at high shear rates.

This shear thickening character occurs in any turbulence flows, like thus occurring in the porous media. This viscoelastic effect on the polymer occurs beyond a critical shear rate which is characteristic for a given polymer type, molecular weight and solvent. There exist some disagreement about how this viscosity enhancement phenomenon occurs compared to pure solvent but two of the most supported theories are the coil-stretch transition, and the development of transient entanglement network which is explained as follow;

Coil-stretch transition is the one where the viscosity increases due to stretching of random- coiled molecules. The high shear flow is now regarded as an extensional flow and the stretching continues until the macromolecules are torn apart. A more recent hypothesis to explain this viscoelastic effect is a formation of a transient aggregation network, due to collision of the polymer molecules. As the shear rate increases, the collision frequency increases as well. Since these macromolecules have very flexible chains, they will start to aggregate. This entanglement is thereafter followed by a disentanglement process, which takes longer time. And it is this transient aggregation that may induces the viscosity enhancement.

In this study, hydrolysed polyacrylamide (HPAM) is used as a reference to compare its solution properties with the synthesised poly-phenylacrylamide. PPAM is a hydrophobically modified polymer and is expected to show stronger solution properties in both, bulk solution and porous media than conventional HPAM.

2.6 Polymer flow behaviour in porous media

Polymer flow in porous media is one of the most important concepts in any enhance oil recovery process. It can be achieved through injection of polymer to change displacing fluid (water) viscosity. Oil reservoir rocks are porous media of which part of the total volume (the porosity, φ) is occupied by a fluid, either oil or water. The permeability of the porous media is defined as the ability of a specified fluid to permeate (flow through) the porous media. The permeability can be determined by Darcy's Law (Lake, 1989).

$$k = \frac{q.\mu.L}{\Delta P.A} \qquad (2.12)$$

Where, k = permeability (mD), q = fluid flowrate (ml/s), ΔP= pressure drop (bar), μ = fluid viscosity (cp), L = section length (cm), A = cross sectional area (cm^2).

The permeability of reservoir rocks varies significantly depending on the type of reservoir. Sandstone reservoirs (e.g. Bentheimer or Berea) usually display permeability values higher than 100 mD while carbonate rocks (e.g limestone or chalk) display permeability lower than 10 mD. Permeability of rock might decrease due to building up of polymer on the surface of the rock (e.g by retention/precipitation), which is discussed in the following section.

2.7 Polymer retention

Polymer retention is originated from interactions between the porous medium and the polymer molecules causing the polymer to be retained by the rock. This does not only mean a loss of polymer molecules but also an alteration of rock properties. Retention is defined as the cause of permeability loss after polymer injection. The polymer molecules can either be absorbed to the pore surface, trapped mechanically by narrow channels or trapped hydro dynamically in stagnant zones.

Polymer retention at solid interfaces in reservoir or pore walls in sand pack can cause an additional resistance to flow, and a decrease in polymer concentration which reduces the polymer solution viscosity (Hirasaki 1974). Polymer adsorption, mechanical entrapment and a hydrodynamic retention are the main mechanisms of polymer retention through porous media (Dominguez 1977).

2.7.1 Polymer adsorption

The interaction between the polymer molecules and solid surface of rock causes polymer molecules to be bounded to the surface of the solid mainly by physical adsorption (Dominguez 1977). The polymer sits on the surface of the rock, and the larger the available surface area for polymer to flow, the higher the levels of adsorption.

Polymer adsorption is considered to be an irreversible process; i.e., it does not decrease as concentration decreases. This is not exactly true because continued exposure to water or brine injection can sort of remove some of the polymer adsorbed from porous rock. However, in general, adsorption adds resistance to flow, causes loss of polymeric additive, it also creates the stripped water bank at the leading edge of the slug. The extent to adsorption on the rock surface depends on; the polymer type, mineralogy of the rock, the accessibility to the active surface, relative permeability to water, wettability of the rock, temperature and solvent (salinity).

• Mineralogy of the rock and permeability

Adsorption is higher in calcium carbonate (limestone or dolomite) than silicate surface (sandstone or clay) owing to the presence of calcium carbonate ($CaCO_3$) minerals. For example HPAM type of polymer have the carboxylate group (COO- negatively charged), therefore the higher adsorption occurs due to the strong interactions between the surface Ca^{2+} and the carboxylate groups (Broseta et al, 1995). While silicate surfaces contain negative charge which cause electrostatic repulsion with carboxyl group (COO-) hence adsorption decrease.

The adsorption tests were carried out for HPAM on core surfaces from Dalia field (Morel et al, 2008) in Angola. A sample of clay and 3 samples of sandstone

with different permeability. The maximum adsorption was observed on clays, slightly higher for lower permeability rock and lower for high permeability rocks (Morel et al, 2008). Therefore regardless of mineralogy, lower permeability reservoirs restricts polymer to flow causing polymer to retain hence more adsorption occurs.

Polymer adsorption is a strong function of polymer concentration. Additional of polymer concentration increases the viscosity of the polymer solution and the thick solution creates high chances for polymer to adsorb (Needham 1987).

• Wettability effect

Less adsorption occurs in oil wet rocks since the irregularities in the grain surface are smoothed out by the oil film. This reduces the oil/water interfacial area which decreases adsorption (Broseta et al, 1995).

• Relative permeability to water effect

Polymer adsorption reduces the relative permeability to water because polymer is soluble in water phase and not in oil phase. So when polymers flow through pore throats, some large molecules are retained, at that point polymer blocks water flowing through and reduce relative permeability to water. Another point is; polymers tend to form hydrogen bond with water molecules which enhances the affinity between the adsorption layer and water molecules. This causes the rock surface to become more water-wet thus relative permeability to water reduced (Needham et al, 1987). For this reasons relative permeability curve for polymer solution is expected to be lower than the corresponding relative permeability curve for water before polymer flooding.

• Temperature effect

The combination of electrostatic forces and molecular forces (like hydrogen bond, van der waals, hydrophobicity etc.) causes both anionic and non-ionic polymers adsorption to decrease with temperature. For ionic polymers (HPAM), adsorption is related to electrostatic repulsion and it decreases as temperature increase. This is because high temperature increases negative charge on the rock surface hence high repulsion occurs which lowers adsorption. But for non-ionic polymers (PAM) adsorption is related to hydrogen bond therefore increase

in temperature can easily break the bond causing adsorption to decrease (Smith 1970).

• Salinity effect

Increasing salinity concentration increases the level of polymer adsorption. Ionic polymers such as HPAM are negatively charged due to presence of carboxyl group (COO-). Strong interaction between monovalent ions (e.g Na^{+}, K^{+}) or divalent ions (e.g Ca^{2+}, Mg^{2+}) in brine with carboxyl group may cause higher adsorption or precipitation.

2.7.2 Mechanical entrapment

Retention by mechanical entrapment occurs when polymer molecules get trapped in narrow flow channels (Omar 1983). Assuming porous media as a complex pore structure with large interconnected networks giving lots of possible routes which connects inlet and outlet of the core. As a polymer solution passes through this complex connected network, molecules may go through any available routes and if the route is narrow enough, polymer molecules will get trapped and block the route. Mechanical entrapment is a more likely mechanism for polymer retention in low permeability cores where the pore sizes are small and chance of polymer molecules to be trapped is very high (Omar 1983).

2.7.3 Hydrodynamic retention

Hydrodynamic drag force traps some of the polymer molecules temporarily in stagnant flow regions of the pore space structure as shown in Figure 2.19. In such region it may be possible to exceed the polymer stream concentration. When flow rate stops, these molecules may introduce into main stream channels and increase the concentration. When the flow starts again the effluent concentration shows a peak (Omar 1983).

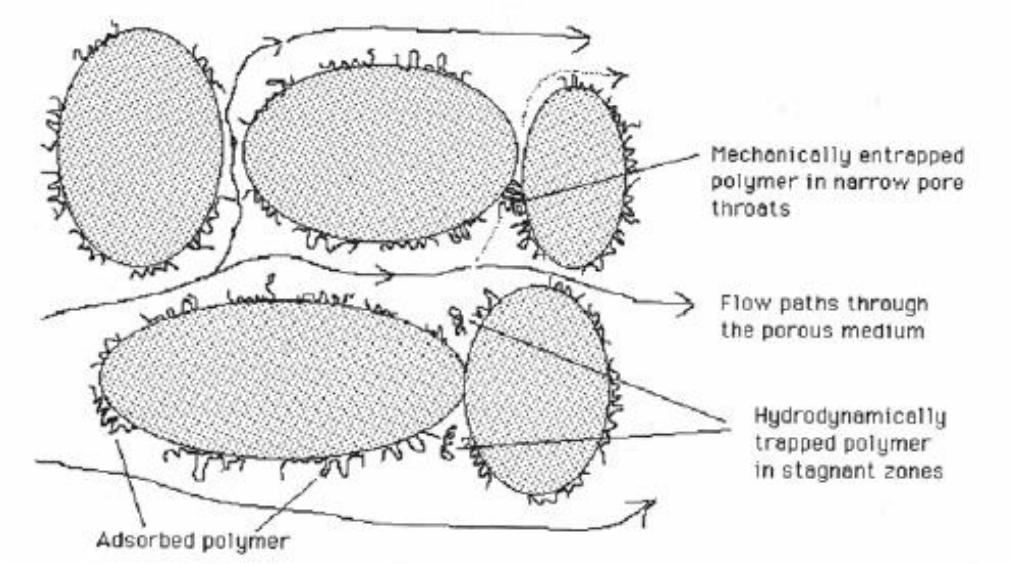

Figure 2. 19: Schematic diagram of polymer retention mechanisms in porous media (Omar 1983).

2.8 Inaccessible Pore Volume (IPV)

Large polymer molecules have less access to small pore (inaccessible pore volume (IPV) in a porous medium (Lake 1989). In the presence of aqueous polymer solution and tracer, polymer molecules will run faster than the tracer because molecules flow only through the larger pores. But in the presence of polymer retention, polymer will lag behind resulting to late polymer breakthrough. Polymer adsorption can be decreased due to presence of IPV since less polymer solution will be in contact with the rock surface than total pore volume. The minimum value of IPV is usually assumed to be equal to irreducible volume of the fluid in the pores. In extreme cases, IPV can be 30% of the total pore volume (Sheng 2010).

2.9 Permeability reduction

Polymer adsorption causes the pore blockage or permeability reduction. The permeability reduction which is also called residual resistance factor (RRF) (Pantus 2012) is defined as the ratio of rock permeability when water flows to rock permeability when aqueous polymer solution flows.

$$RRF = \frac{k_{w(initial)}}{k_{w(after\ polymer\ flood)}} \qquad (2.13)$$

Be noted polymer adsorption assumed to be irreversible process, means even when some of polymer solution is displaced by water or polymer concentration is decreasing the adsorption will still exist. This means the permeability reduction will keep on increasing and the factor would be increasing.

Another factor that is taken under consideration when it comes to permeability reduction is mobility reduction or resistance factor (RF) (Pantus 2012). It can be defined as the ratio of mobility of water to the mobility of a polymer solution. The resistance factor is a term that is commonly used to indicate the resistance to flow encountered by a polymer solution as compared to the flow of plain water. For instance, a resistance factor of 5 means that it is 5 times more difficult for the polymer solution to flow through the system than water.

$$RF = \frac{k_w/\mu_w}{k_p/\mu_p} \qquad (2.14)$$

2.10 Polymer rheology in porous media

2.10.1 Polymer apparent viscosity model

Darcy law (Equ. 2.12) gives a linear relationship between flow rate (q) and pressure drop (ΔP), to define permeability (k) as a measured parameter for conductivity of porous media as:

$$k = \frac{\mu q L}{A.\Delta P}$$

Where A and L are cross sectional area and length respectively, μ is Newtonian viscosity of fluid flowing through porous media which means viscosity is constant and does not change at different shear rate. The relationship between flow rate and pressure drop is linear.

A polymer solution used in EOR is a non-newtonian fluid; therefore, the viscosity term (μ) is not constant. In situ apparent viscosity (μ_p) is often used in polymer flooding and is defined as follow

$$\mu_p = \frac{kA\Delta p}{qL} \qquad (2.15)$$

Apparent viscosity is not constant and changes by shear rate and also the relationship between pressure drop and flow rate is not linear.

It is not possible to measure the apparent viscosity during core flooding experiments. Instead the apparent viscosity is determined by equations that depend on the mobility reduction (RF) and the permeability reduction (RRF) by applying Darcy's law (Equation 2.12) for water and polymer

Initial water flow:

$$q_w = \frac{k_w.\Delta P_w.A}{L.\mu_w} \qquad (2.16)$$

Polymer solution flow:

$$q_p = \frac{k_p.\Delta P_p.A}{L.\mu_p} \qquad (2.17)$$

Water flow after polymer solution flow:

$$q_{wp} = \frac{k_{wp}.\Delta P_{wp}.A}{L.\mu_W} \qquad (2.18)$$

According to the definition the resistance factor (Mobility reduction) RF (Equation 2.14) can be expressed:

$$RF = \frac{k_w/\mu_w}{k_p/\mu_p} = \frac{q_w/\Delta P_w}{q_p/\Delta P_p} \qquad (2.19)$$

Where μ_p is the apparent viscosity of the polymer solution. And if the same flow rate is used for water and polymer, RF can be simplified as:

$$RF = \frac{\Delta P_p}{\Delta P_w} \qquad (2.20)$$

Similarly, residual resistance factor (permeability reuction) RRF (2.13) is expressed as:

$$RRF = \frac{k_w}{k_{wp}} = \frac{{q_w}/{\Delta P_w}}{{q_{wp}}/{\Delta P_{wp}}} \qquad (2.21)$$

And when the same flow rate is used:

$$RRF = \frac{\Delta P_{wp}}{\Delta P_w} \qquad (2.22)$$

The above definitions and equations will be used in the evaluation of the single-phase polymer solution flow in the core flooding.

Figure 2.20 is an illustrative plot of the correlation between permeability and permeability reduction for polymer flood used in UTCHEM software, a chemical flood simulator. As can be seen, at high permeabilities the permeability reduction is close to one. So, the focus of polymer floods in high permeability reservoirs is to increase the solution viscosity as much as economically possible and the permeability reduction is ignored. However, when the permeability is low, or very low, the permeability reduction greatly increase depending on polymer molecular weight, brine salinity, core permeability and lithology (Kasimbazi 2014). At the worst case, the polymer flow in porous media cannot reach stable state, or even simply plugs the core.

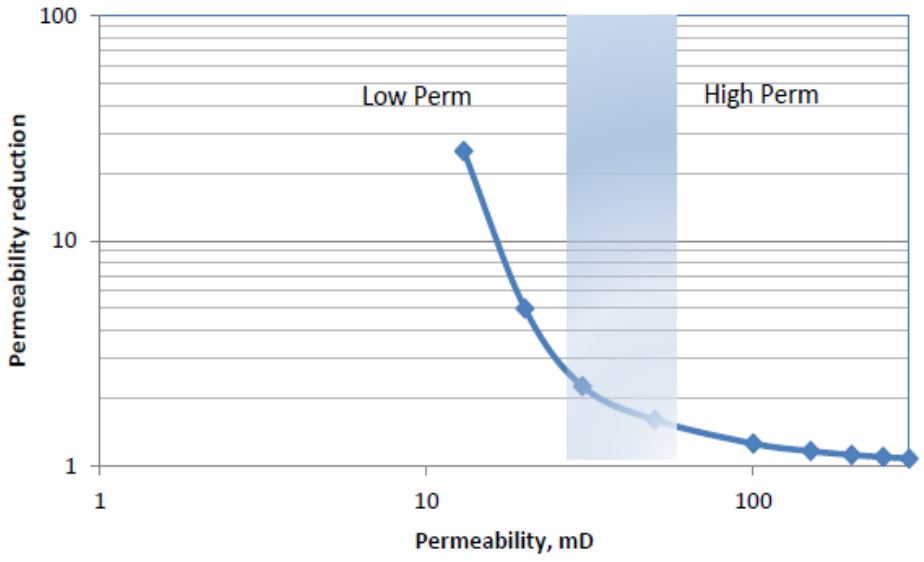

Figure 2. 20: Permeability versus permeability reduction for a polymer flood in UTCHEM (Kasimbazi 2014).

The apparent viscosity can be calculated by an assumption made where the brine permeability after polymer flow is the same as the polymer permeability. This assumption has been made due to non-consistency of apparent viscosity for polymer solution (Pancharoen et al 2010, Guillaume 2010).

$$\mu_p = \frac{RF}{RRF} . \mu_w \qquad (2.23)$$

2.10.2 Shear rate of flow in porous media

Porous media is a complex networh of channels and poe sizes in microscopic scale.Therefore both molecular structure of polymer and pore structure play very important role in detemining rheological behavior. The simple model to describe fluid behaviour in porous media is like a bundle of capillary tubes. Several workers (Hirasaki, 1974 and Gramain, 1981) used this model to calculate the shear rate applying on non-Newtonian fluid flows through porous media.

$$\gamma = \alpha \frac{4u}{\sqrt{8k/\phi}} \qquad (2.24)$$

Where α=2.5 is a shape parameter refers to characteristics of porous media with angular particles (Zitha et al 199

5), u is an interestitial velocity ($u = \frac{q}{A}$) and ϕ is the porosity of porous media. This relationship is useful and valid for both Newtonian fluids and non-Newtonian fluids. Equation 2.24 is used in the experimental calculations.

Chapter 3

Methodology

3. Methodology

This chapter is divided in two sections;

The first section presents the process to synthesise and characterise phenyl-polyacrylamide (PPAM), and to investigate the rheological properties of the synthetic polymer in bulk solution. The viscosity of polymer solution is also investigated in both distilled water and brine and the results were compared with those of HPAM. A flow chart for the experiments is shown in Figure 3.1.

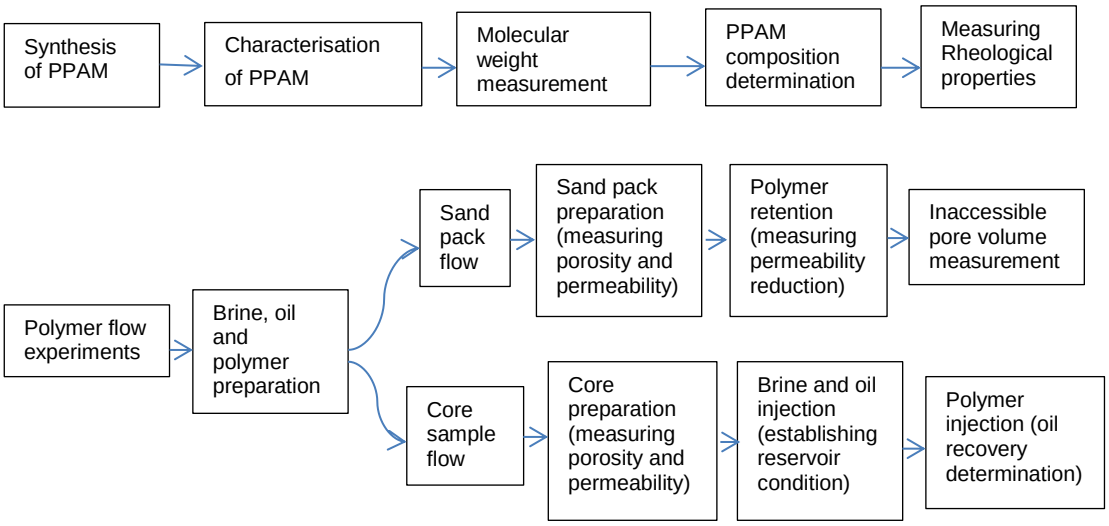

Figure 3.1: Experimental flow chart

In the second section, the methodology to investigate the properties of PPAM solutions when they flow through porous media is presented. The interaction mechanism between PPAM and sand pack under dynamic flow condition was investigated and parameters such as permeability reduction, inaccessible pore volume and polymer retention on rock surface and plugging of the formation were estimated. The performance of polymer solution on oil recovery was also investigated in Benthemier sandstone in a coreflood system.

3.1 Synthesis of PPAM

3.1.1 Materials

• Acrylamide (C_3H_5NO) with 99% purity was used as supplied by Sigma-Aldrich.

• Sodium dodecylsulphate ($NaC_{12}H_{25}SO_4$) with 99.5% purity from Fisher chemical was used. Its critical micelle concentration at 25 °C was measured by tensiometer (DCA-100) to be 9×10^{-3} mole/L which is in good agreement with known literature values confirminig the purity of the SDS used here.

• Potassium persulphate ($K_2S_2O_8$) ≥ 99% was used as supplied by Sigma-Aldrich.

• N-phenyl acrylamide (C_9H_9NO) as a hydrophobic monomer with 99% purity was used as supplied by Sigma-Aldrich.

• Methanol 99.9% (Fisher chemical) was used for precipitation.

• Hydrolyzed polyacrylamide (HPAM) from SNF FLOEGER was used as supplied.

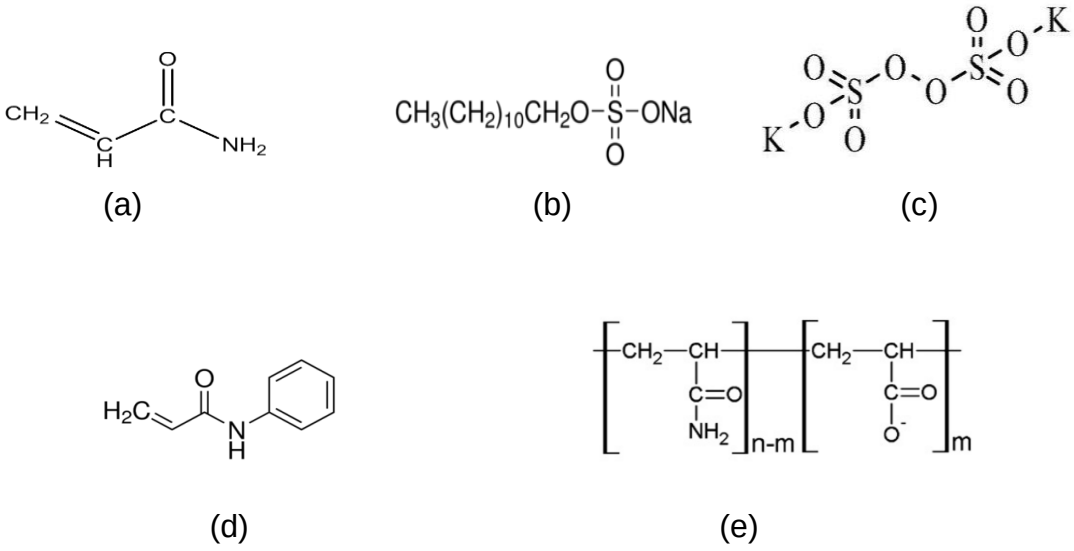

Figure 3. 2: Chemical structure of (a) acrylamide, (b) potassium persulphate, (c) sodium dodecylsulphate (SDS), (d) N-phenyl-acrylamide, (e) hydrolysed-polyacrylamide (HPAM).

3.1.2 Polymerisation

In this study, polyacrylamide (C_3H_5NO) is hydrophobically modified with a low amount (1-3 mole %) of phenyl-acrylamide. The polymerisation was conducted through a micellar radical copolymerisation in water, with sodium dodecyl sulfate (SDS) which is an ionic surfactant, and the potassium persulfate ($K_2S_2O_8$) as the initiator. Phenyl-acrylamide needs to be solubilized in distilled water by means of surfactant to become a part of polymerisation chain. However, a maximum solubility for phenyl-acrylamide is achieved in presence of surfactant. It means no more phenyl-acrylamide monomer is solubilized in surfactant micelles. To achieve this, critical micelle concentration (CMC) of the surfactant needs to be measured first.

Each reaction is conducted in a five-necked glass reactor (Figure 3.3) equipped with a condenser, a mechanical stirrer, nitrogen inlet and outlet, and a thermometer (Figure 3.4). The reactor containing surfactant solution and phenyl-acrylamide monomer is added. Then, the solution was heated to 50°C from ambient temperature using a water bath with continuous stirring under nitrogen flow until the phenyl-acrylamide monomer is solubilized in surfactant micelles and solution is transparent. Nitrogen is also bubbled separately through an aqueous acrylamide solution within a flask, the acrylamide solution then is transferred into the reaction vessel. The mixture is kept at a constant temperature 50°C with continuous stirring and under a nitrogen purge for 30-45 minutes to ensure the complete removal of trapped air due to strong foaming arising from the presence of surfactant in the solution. When the mixture is homogenous, an aqueous solution of $K_2S_2O_8$ is added into the reactor. The reaction is carried out for 7-8 hours with purging nitrogen and vigorous stirring.
The progress of the reaction is monitored by taking several samples of polymer solution out for composition analysis and precipitated in six times (18 ml) excess of methanol, and after filtration each sample was washed repeatedly in methanol to remove all traces of surfactant, water and all residual unreacted monomers. Then all samples were dried under reduced pressure at 50°C for two days in a vacuum oven (Biggs et al. 1991).

The sequence distribution of the hydrophobic monomer in the copolymer chain depends on the initial number of hydrophobe per micelle, N_H, calculated as follow

$$N_H = \frac{[M_H] \times N_{agg}}{[SDS] - CMC} \qquad (3.1)$$

where $[M_H]$ is the molar concentration of hydrophobic monomer in the solution, $[SDS]$ is the molar surfactant concentration and CMC is the critical micelle concentration (Huang 1995). In this study CMC at 50℃ is 9.2×10^{-3} mol.L^{-1} and aggregation number N_{agg}=60 was used for SDS at 50℃ (Candau 1999).

Figure 3.3: Five-neck glass reactor

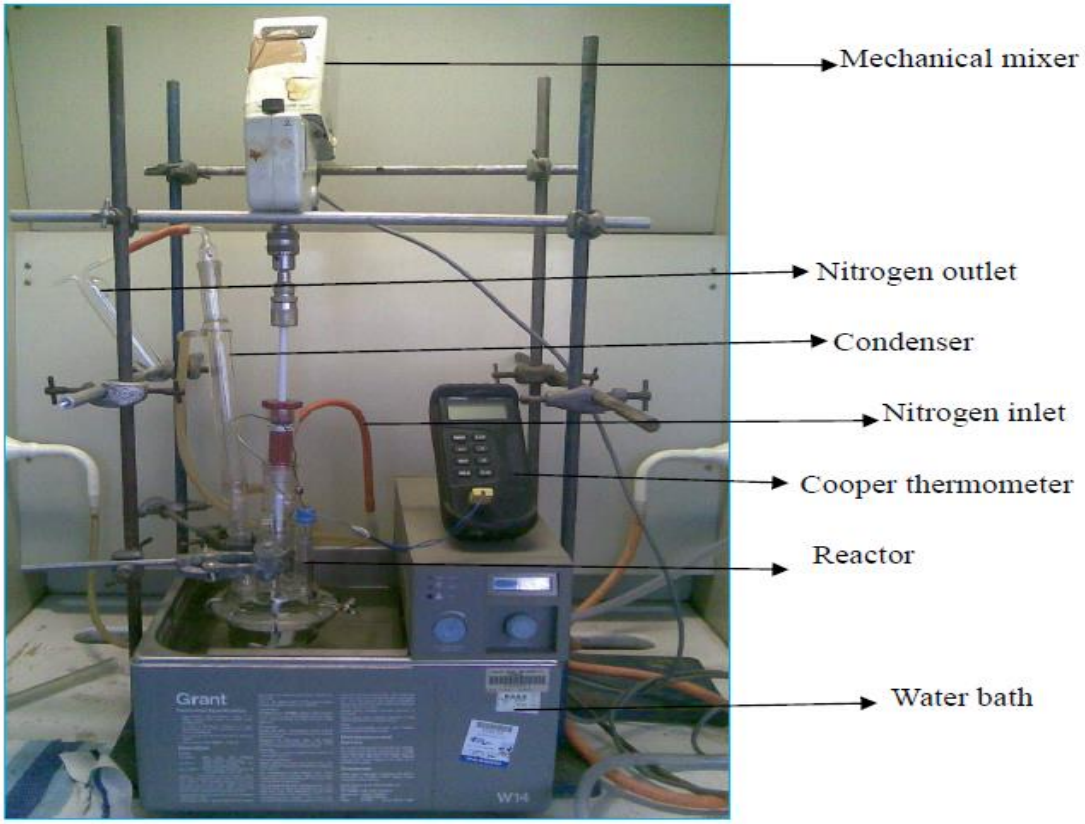

Figure 3.4: Experimental set-up (mechanical mixer, nitrogen inlet and outlet, condenser, thermometer, reactor and water bath).

3.1.3 CMC measurement

Critical micelle concentration (CMC) of surfactant was determined with a contact angle tensiometer DCA (Figure 3.5) by measuring the surface tension of different surfactant concentration. A sensitive ring was used when it touches the surface of the liquid (1), driving it further under the surface to completely wet it (2), and then pulling it from the liquid (3), until the lamella breaks (4). The maximum force measured is used to calculate surface tension and this occurs just before the lamella breaks.

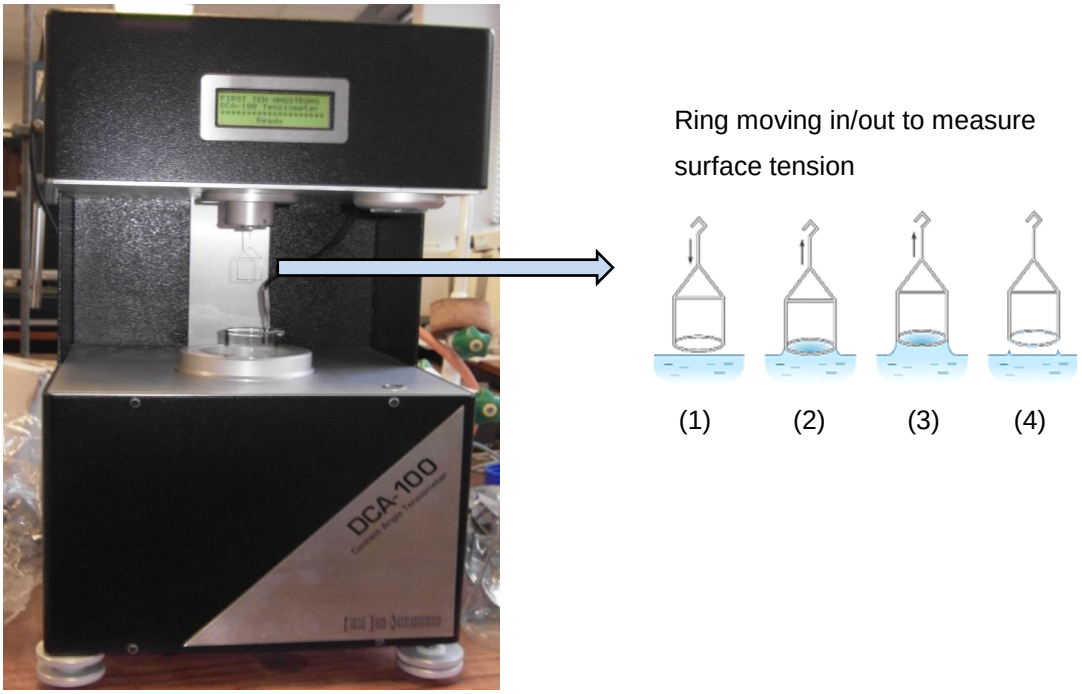

Figure 3.5: Contact angle tensiometer

3.2 Polymer Characterisation

Polymer characterisation tests were carried out using two analytical techniques, Fourier transform infrared spectroscopy (FT-IR) and nuclear magnetic resonance spectroscopy (HNMR).

3.2.1 FT-IR spectroscopy

FT-IR spectrometer (Mattson Satellite 5000 FT-IR) was used for the Fourier transform infrared (FTIR) spectroscopic analysis (Figure 3.6). In infrared spectroscopy, IR radiation is passed through a sample; some of the infrared radiation is absorbed by the sample and some of it is passed through (transmitted). The resulting spectrum represents the molecular absorption and transmission, creating a molecular fingerprint of the sample. Like a fingerprint no two unique molecular structures produce the same infrared spectrum. Infrared spectroscopy was used for qualitative analysis of the polymer.

Figure 3.6: Mattson satellite FT-IR

3.2.2 H-NMR spectroscopy

NMR (Figure 3.7) analysis is used to confirm the chemical structure of an organic compound. Different functional groups are distinguishable, and identical functional groups with differing neighbouring substituents still give distinguishable signals. The principle behind NMR is that many nuclei have spin and all nuclei are electrically charged. If an external magnetic field is applied, an energy transfer is possible between the base energy to a higher energy level (generally a single energy gap). The energy transfer takes place at a wavelength that corresponds to radio frequencies and when the spin returns to its base level, energy is emitted at the same frequency. The signal that matches this transfer is measured and processed in order to yield an NMR spectrum for the nucleus concerned.

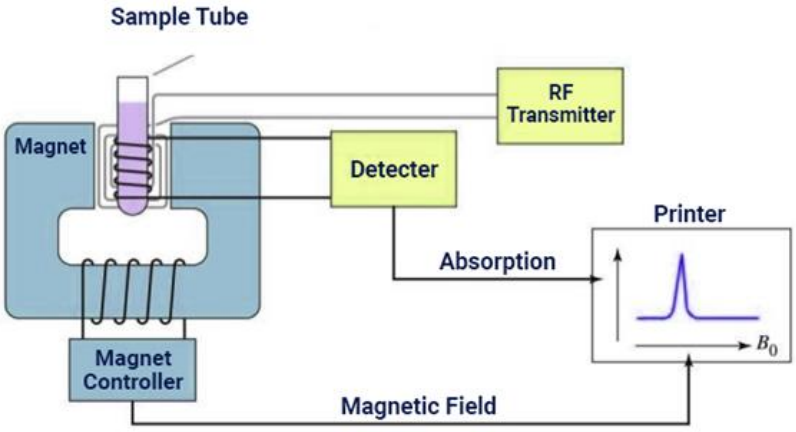

Figure 3. 7: NMR Spectrometer (Pulsar) for High Performance NMR Spectroscopy

3.3 Viscosity average molecular weight measurement

An estimation of viscosity average molecular weight is obtained by using an Ubbelohde capillary viscometer (Technico size 13) shown in Figure 3.8 at 25°C. In this method, polymer solutions with different concentrations flow through the Ubbelohde viscometer and the flow time of solutions are recorded between the start and stop mark. Intrinsic viscosity is estimated by plotting the reduced viscosity of polymer solutions against concentration and extrapolating to infinite dilution. Molecular mass is calculated by Mark-Houwink equation $\eta=K.M_w^{\alpha}$ where K and α are Mark Houwink constants and depend on the particular polymer-solvent system, η is the intrinsic viscosity (ml/g), and M_w is viscosity average molecular weight in gr per mole (Blagodatskikh et al 2004).

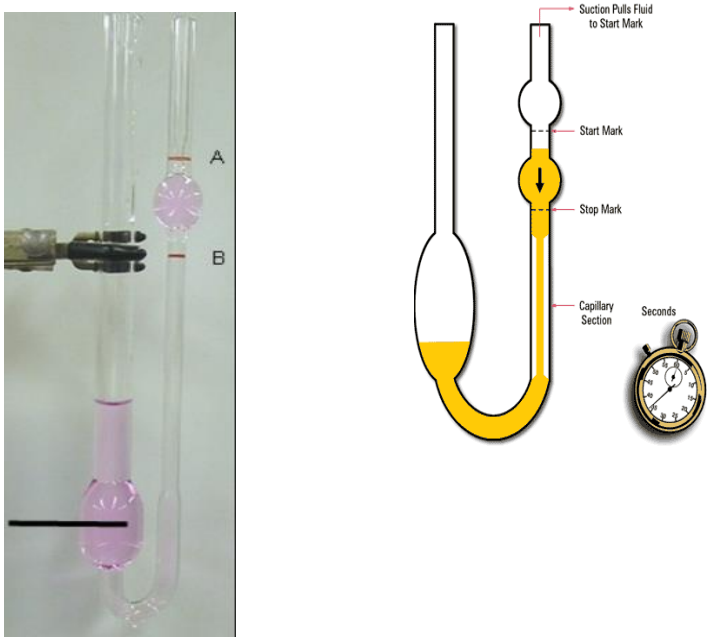

Figure 3. 8: Ubbelohde capillary viscometer (Blagodatskikh 2004).

3.4 PPAM composition analysis

PPAM composition determined by using a UV-vis spectrophotometer 1800-(SHIMADZU) shown in Figure 3.9. Spectrophotometer measures the amount of light that a sample absorbs at a particular wavelength. Two glass cuvettes are typically used in the wavelength range of visible lights. One is filled with the diluted polymer solution and the other one with distilled water as the reference solvent. Solvent gives a base line to compare the light adsorption for monomers. The instrument operates by passing a beam of light through a sample and measuring the intensity of light reaching a detector. This equipment is used in analytical chemistry for the quantitative determination of different components such as organic compounds and macromolecules. The results shown as an absorbance spectrum at different wavelength.

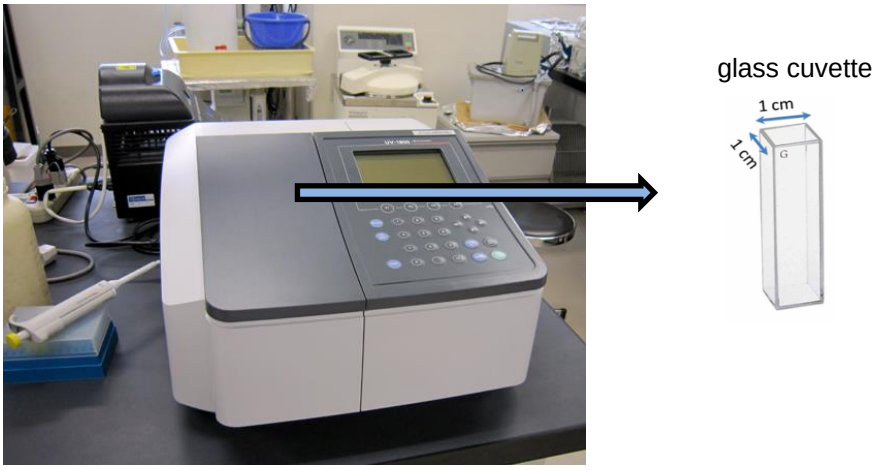

Figure3. 9: UV Spectrophotometer.

3.5 Rheological properties measurement

Rheological measurements were carried out by using a BOHLIN 200 Rheometer shown in Figure 3.10. The viscosity of the polymer solution is measured at different shear rate range (0.1 s^{-1}-1000 s^{-1}) and also the effect of temperature and salinity on the viscosity is determined. Loading the polymer solution into the plate of the viscometer and leave it for 1-2 minutes to settle before running the viscometer. The measuring system consists of a cone and a plate with 4 ° angle and 40 mm diameter of plate.

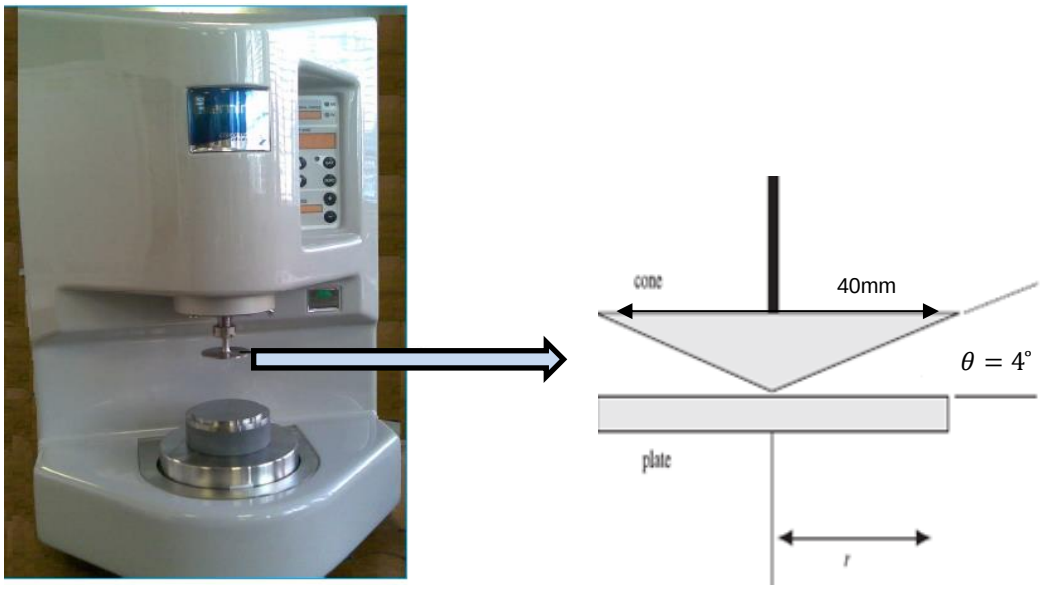

Figure 3. 10: Bohlin Rheometer

The viscosity measurements carried out on the rheometer was performed at 22 ° C, and the apparatus had an uncertainty of 0.1 ℃. The required sampled volume was dispensed with a pipette onto the plate. For each measurement performed on the rheometer, only fresh samples of the solution were used since a measured sample becomes mechanically degraded at high shear rates. Some difficulties arise for very viscous fluid samples regarding use of the pipette to sample the required volume from the solution, and thereafter injecting it into the plate.

3.6 Polymer flow experiments

Polymer flow tests were carried out in both sand packs and sandstone cores. The PPAM and HPAM solutions flow experiments and two synthetic brines, soft brine and hard brine, were prepared in the laboratory. The brines composition is listed in Table 3.1 and 3.2.

Table 3. 1: Synthetic brine (soft brine)

Composition	Concentration(g/l)
NaCl	23.49
KCl	0.75
$MgCl_2.6H_2O$	2.15
$CaCl_2.6H_2O$	1.91
Total dissolved solids	28.3

The only difference between these two brines is the greater concentration of calcium chloride hexahydrate (Ca^{2+}) in hard brine compare to soft brine.

Table 3. 2: Synthetic brine (hard brine)

composition	Concentration (g/l)
NaCl	23.49
KCl	0.75
$MgCl_2.6H_2O$	2.15
$CaCl_2.6H_2O$	10.12
Total dissolved solids	36.51

All brines were filtered by 0.2 μm filter paper to remove any undissolved solids before any experiment.

The crude oil was provided by Maersk Oil Company from North Sea in the UK. Oil properties are in Table 3.3

Table 3. 3: Crude oil properties

Crude Oil	API	Density (g/cm^3) @22℃	Viscosity (mPa.s) @ 22℃
North sea	21	0.925	115

3.6.1 Polymer solution preparation

The preparation of all polymer stock solutions during this thesis, regardless of type of polymer and solvent, followed the American Petroleum Institute (API) standard procedure (Dupuis 2010). Here is an example of preparation of 5000 ppm polymer solution in brine/distilled water.

- Fill a suitable open glass container (e.g beaker) with 500g of brine/distilled water.

- Drop a suitable magnet into the container.

- Use a magnetic stirrer to create a vortex (Figure 3.11) almost reaching the bottom of the container.

- Carefully sprinkle 2.5 g of polymer powder into the wall of the vortex, not the bottom. This careful sprinkling

process was carried out during 30 seconds.

- Right after the addition of the polymer granulate, the stirring speed was reduced to the lowest possible rotation to avoid any mechanical degradation of polymer and also to prepare a homogeneous polymer solution.

- Turn the magnetic stirrer down to the lowest, yet smooth turning level.

- The polymer solution was left on adequate stirring overnight and then the stock solution is ready to use.

-The polymer solutions were filtered through a 3μm millipore fiberglass filter in order to remove any microgels or high molecular weight clumps that may have formed during the polymer preparation.

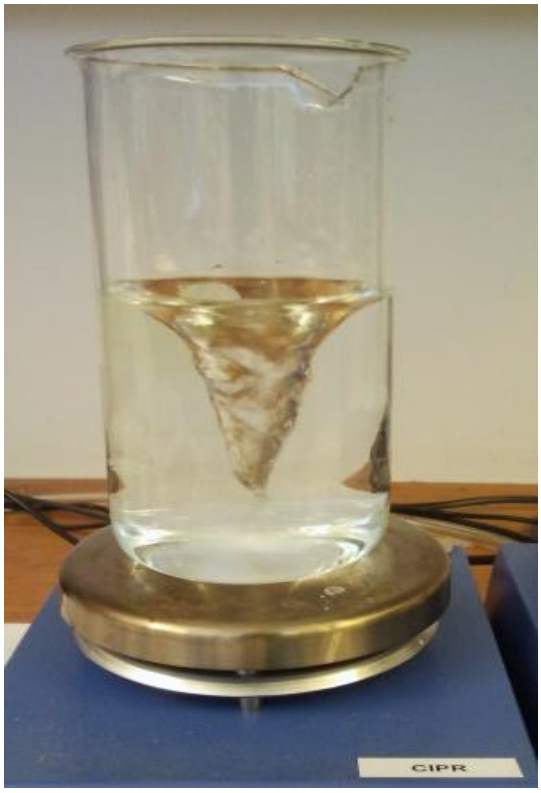

Figure 3. 11: Polymer solution preparation by using a magnet stirrer.

The stock solution was diluted when solutions with lower concentrations were prepared, using the magnetic stirrer at low speeds to avoid possible mechanical degradation. Solutions older than a couple of weeks, especially lower concentrations, were disposed and replaced by a freshly made solution.

3.7 Study of polymer solution flow in sand pack

This section describes detailed experimental procedure used during the research Including the preparation and characterisation of sand pack, displacement procedure, and analytical testing of samples. Rheological behaviour of polymer solutions in sand pack is studied and parameters such as permeability reduction, polymer retention and inaccessible pore volume (IPV) are investigated. This procedure has also been done by other authors such as Zheng 2013 and Stavland 2013.

3.7.1 Sand pack preparation

The sand used for the sand packs, was crushed Berea sand. The sand was sieved, washed with distilled water and dried before use. The particle size

distribution of the sand was measured by means of sieve analysis. Two sands with average size of 50-110 µm and 280-355 µm were used for sand pack flooding tests. Figure 3.12 shows sieves and shaker.

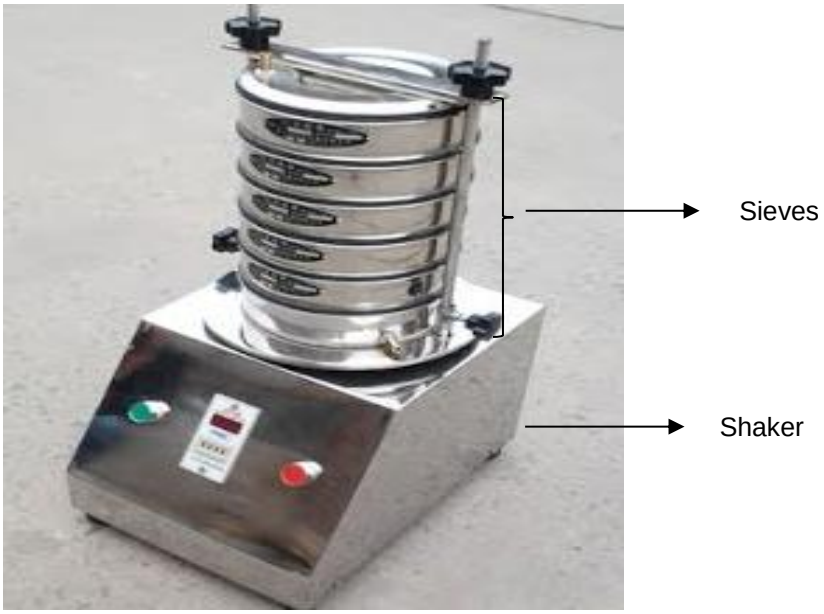

Figure 3. 12: Sieve analysis of soil (www.civilblog.com).

Sands with different particle size was packed in a chromatography column (L15 cm ˣ I.D 2.5 cm) used as a horizontal porous medium in this experiment. The sand pack was vacuumed for 15-20 minutes to remove air in order to have a better brine saturation. When saturation was completed, the porosity was calculated using the following equation (Zhang 2013):

$$porosity\ (\emptyset) = \frac{Pore\ volume\ (V_p)}{Bulk\ volume\ (V_b)} \qquad (3.2)$$

Where

$$Pore\ volume\ (V_p) = \frac{\text{Saturated weight – Dry weight}}{\text{Density of the saturated brine}} \qquad (3.3)$$

$$Bulk\ volume\ (V_b) = \left(\frac{sand\ weight}{\text{grain density}}\right) + Pore\ volume \qquad (3.4)$$

The dry weight was measured after the sand was packed and the wet weight was recorded after the sand pack was completely saturated. The grain density

was measured by filling a volumetric flask with a known weight of sand and then filling the rest of the volume with water.

A syringe pump (KDS 210) (Figure 3.13) was used for the sand-pack flooding experiments. It has a maximum injection rate capacity of 20 ml/min.

A low pressure transducer Omega (PX2300), with a measuring interval 0 to 1.7 bar was used to measure differential pressure across the sand pack holder.

Pressure data is recorded on a data acquisition system as a function of current intensity (mAmp) versus time.

Figure 3. 13: KDS syringe pump (www.sisweb.com).

3.7.2 Permeability of sand pack to brine

Permeability tests were done with solely brine injection. The syringe pump was used to determine permeability because of its ability to accurately change the volumetric flow rate in small increments. The air was evacuated from sand pack by using a vacuum pump to ensure fully saturation of sand pack. Sand pack holder was weighed before and after saturation to determine sand pack porosity and then brine injection was performed at different flow rates. Each flow rate was maintained long enough to fully reach a steady state pressure drop. The pressure drops were measured by the pressure transducer and the effluents were collected in the fraction collectors. The injection rate could be checked by the effluent volume because the samples were taken on a time basis. Once the brine injection was completed at different flow rates, the data from the

experiment was collected and the permeability was determined using Darcy's law. A schematic diagram is shown in Figure 3.14.

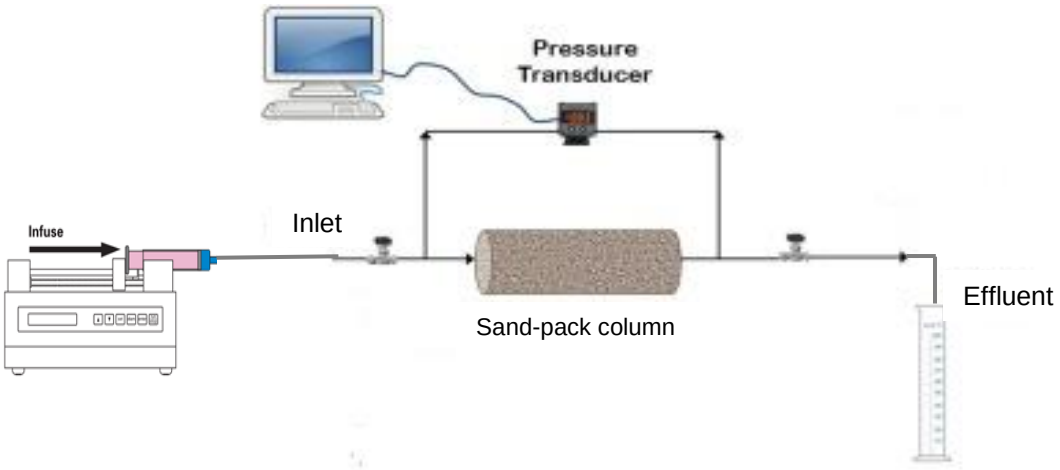

Figure 3. 14: Sand-pack flooding system**.**

3.7.3 Polymer retention experiments in sand pack

To conduct polymer retention experiments, the sand pack is initially weighed and saturated with brine and then pore volume of sand pack is also calculated. Polymer solutions were then injected through the sand pack at a low flow rate of 1 ml/min until the pressure drop remained stable. Low injection rate is applied to ensure homogenous propagation of polymer solution in the sand pack. For each run of polymer injection, a new sand pack was prepared and the effluent samples were collected by fraction collectors. The effluent samples are analysed by UV spectroscopy to determine the concentration of polymer solution in each sample. A calibration (standard) curve of polymer concentration versus absorbance is plotted by using fresh polymer solution at various concentrations and the polymer concentration is determined in each effluent sample. The area under the absorbance curve at each particular wavelength is an indication of polymer concentration. Polymer retention was calculated by a material balance equation as follows (Hatzignatiou 2013):

$$\text{Retention (Rp)} = \frac{(\text{C inf} - \text{C eff})}{\text{Ws}} * \text{Vp} \qquad (3.5)$$

Where c_{inf} and c_{eff} are influent and effluent polymer concentrations (ppm) respectively, Vp is pore volume (cm^3) and w_s is sand weight (g).

3.7.4 Inaccessible pore volume (IPV) experiment for sand pack

To determine the IPV in the sand pack, potassium nitrate (0.1 M KNO_3) solution was used as a tracer to evaluate the uniformity of sand pack. KNO_3 solution was used with polymer solution and UV spectrophotometry was used to measure the absorbance of the tracer solution in the effluent line of the sand pack. The tracer output was recorded using the data acquisition system. The UV spectrophotometry was zeroed at the beginning of the tracer test using brine without KNO_3. A standard curve was developed using the absorbance of different tracer concentration to calculate the concentration of tracer in the effluent samples. Finally, the inaccessible pore volume (IPV) of polymer solutions was acquired by calculating the difference in break-through time between the polymer and the tracer according to (Manichand 2014).

3.8 Study of the effect of polymer on oil displacement in core samples

In this section, a series of oil displacement experiments were conducted on sandstone core samples. Two Benthemier sandstone cores with absolute permeability of 100 mD and 500 mD were used. The tests were carried out for both PPAM and HPAM solutions and parameters such as permeability reduction, mobility reduction and oil recovery were studied. Polymer retention tests were also conducted for both PPAM and HPAM in core samples.

A complete high pressure core flooding apparatus shown in Figure 3.15 was used to conduct the experiments. It composes of a core holder, pressure transducer, pumps and piston cylinder for fluids, back pressure regulator, sample fraction collector and data acquisition system.

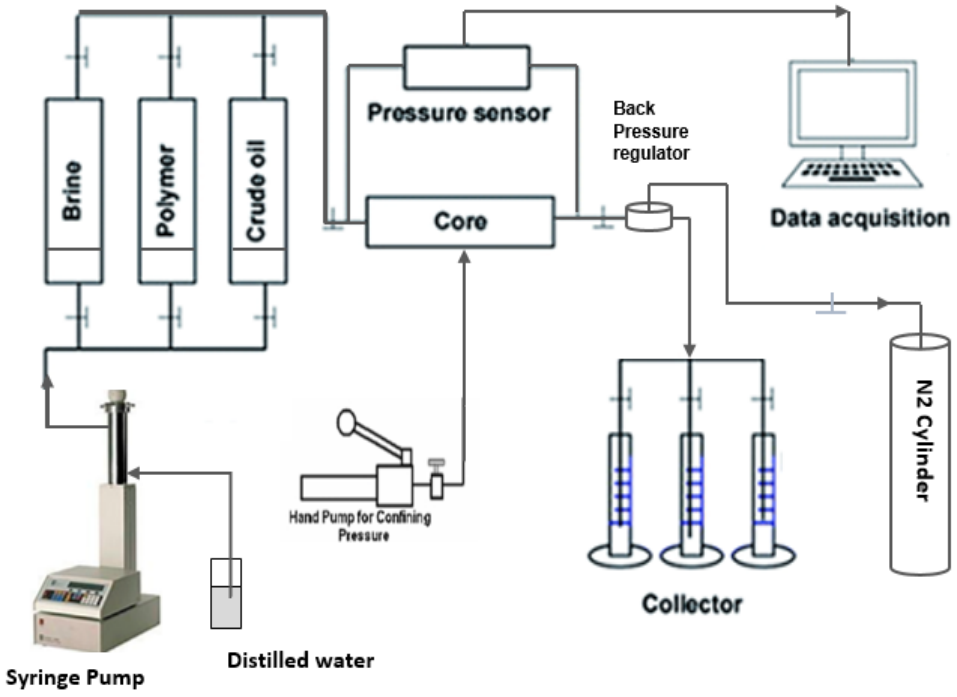

Figure 3. 15: Schematics of the sandstone core holder set-up

• Core and Core holder

The core holder used have both inlet and outlet mandrels as shown in Figure 3.16. One mandrel at left was fixed attaching to the cap and another mandrel at right can slide inside the core holder barrel to accommodate cores of different lengths. Dismounted core holder can be seen to the right in Figure 3.16 and shows the sleeve, a sand stone core and the two inner end pieces before mounting.

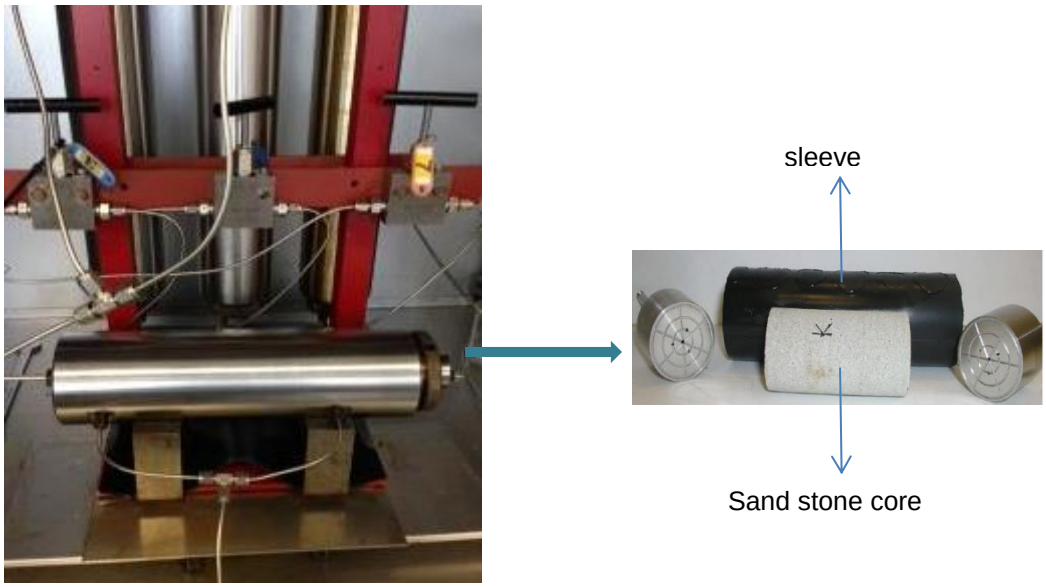

Figure 3. 16: Core holder cylinder and as dismanteled to the right

• Pressure transducers

Pressure transducers were used to measure the pressure of core inlet, core outlet, pump, back pressure regulator, and overburden. One differential pressure transducer was connected to the core inlet and outlet for the measurement of pressure drop across the core. The pressure transducer and pressure gauges were supplied by Bronkhorst pressure controller Inc with a range of $\pm$0.25 % accuracy for transducer and $\pm$1% accuracy for pressure gauges, respectively. The pressure transducer was connected to a data acquisition system for converting the electrical signals into pressure readings.

• Pump and injection cylinders

ISCO 500D digital syringe pump was used with a capacity of 500 cm^3 was used to inject fluids. The pump flow rate was approximately set with a percentage dial and a range switch (maximum 100 cm^3/min). The pump pressure was displayed on the pump controller. The pump volume, flow rate and pressure can be logged into the DAS computer through a data cable.

The DI water was pumped into one side of piston cylinder and the brine, oil or polymer solutions flowed out from the other side of the piston cylinder to injection lines of the core holder.

• Back pressure regulator

Back pressure regulator (BPR) was used to control the pressure inside the system especially when high viscous fluids were running inside. The back pressure was set manually using a nitrogen cylinder to supply the required pressure for the experiment.

• Confining Pressure

After the core is placed into the core holder, the sleeve was pressurised to simulate the 3D axis stresses that the core was under in real reservoir conditions. Some of these stresses are caused by the weight of the material above the core which is called “overburden” pressure. In this experiment hydraulic oil was used to provide an overburden pressure of around 700 psi.

3.8.1 Experimental procedure

In this experiment, initial reservoir condition needs to be applied on the core sample to determine oil recovery. After cleaning the core and measuring its porosity, brine is injected at low flow rate to estimate the brine permeability of the core, followed by oil injection to establish reservoir condition for the core. At this stage, original volume of oil in core sample can be calculated by measuring the effluent volume. The test was further carried out by initial water flooding (IWF) into core sample and volume of recovered oil was measured. Irreducible water saturation (Sw_i) and residual oil saturation (So_r) can be calculated through measuring of the volume of effluent samples. Then, polymer flooding (tertiary oil recovery) was conducted to produce more oil and effect of polymer solutions on oil recovery was investigated. Details of the experimental procedure are as follow

• Core preparation

- The core was soaked in methanol using a vacuum pump (Figure 3.17) for at least 24 hours. This allows any air trapped in void spaces of core to escape.

- Remove the core from methanol and allow it to air dry for at least 48 hours.
- Submerge the core in distilled water in a vacuum pump for at least 24 hours, then remove it and wipe it off gently before measure its wet weight.
- Place the core in a vacuum oven set to 70℃ for 8 hours and then measure the dry weight to be able to calculate the pore volume of the core sample.

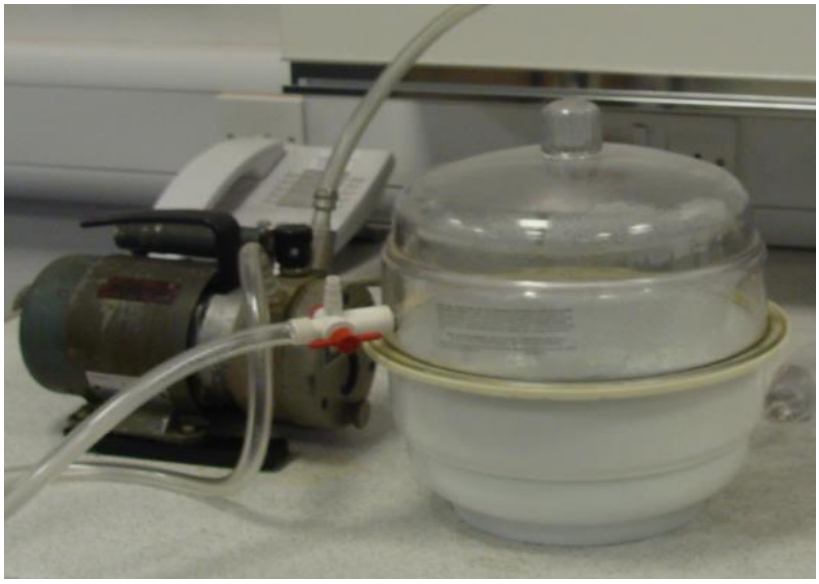

Figure 3. 17: Vacuum pump for core saturation.

• Brine injection

The same synthetic soft brine for sand pack flooding was used in the core flooding experiment. The prepared brine was filtered through a 0.45 μm Millipore filter paper and then transferred to the injection cylinder (accumulator). The brine was then injected into the core sample at different flow rates by using ISCO syringe pump.

• Steps of oil injection procedure:

i) Fill in the accumulator with oil, attach all lines and purge oil into the line to make sure there is no air in the system before use.

ii) Apply the confining pressure in the system by closing the hand pump valve first. Then start pumping hydraulic oil until the confining pressure reaches 700 psi.

iii) Increase the back pressure by opening the nitrogen tank valve and set the regulator to 2 bar.

iv) Ensure all lines have been purged and pressure is monitored during the experiment.

v) Apply a low flow rate of maximum 0.5 ml/min to make sure a homogeneous propagation of oil in the core sample for better saturation. Oil injection carried on until a constant pressure drop across the core achieved. At this point the original oil in place (OOIP) that is the total volume of oil in the sample and the volume of brine displaced can be determined.

vi) After this the pump is shut off and the oil valve should be closed to stop any further flow of oil into the core.

• Steps of Initial water flooding (IWF) procedure:

i) The brine accumulator must be filled with brine solution. Then the lines must be properly reattached to ensure there is no loss of pressure or fluid during the experiments.

ii) Set the pump flow rate to 0.5 ml/min and make sure the pressure data is recording on the computer.

iii) The brine in injected at the constant flow rate and the effluent is collected in 10 ml graduated cylinders.

iv) Brine injection continued until the pressure drop across the core sample remains constant.

v) The volume of oil recovered by brine injection can then be determined after completing these steps.

• Steps of polymer flooding (tertiary oil recovery) procedure:

The same sequence of brine injection followed for polymer injection. Two kind of polymer solution were used in this experiment, PPAM and HPAM. However, a lower flow rate is required to keep the inlet pressure constant due to the high viscosity of the polymer solution (0.1- 0.2 mL/min). Polymer injection continued until the pressure drop across the core remains constant. For each trial roughly

two pore volumes of polymer are injected as the final phase to represent the tertiary oil recovery step.

After the polymer injection is completed the trial is finished and the system can be cleaned and reset for a new core.

3.9 Core cleaning process

The field cores contained residual oil and brine which needed to be removed for subsequent experiments. The cores were cleaned by a soxhlet extractor (Figure 3.18) with toluene for the oil/water removal and acetone/methanol for the salt removal. Sufficient time (~one week) was allowed for both the toluene and acetone/methanol cleaning.

Figure 3. 18: Soxhlet extractor for core cleaning

3.10 Source of Errors in the experiments

The following factors could cause errors during the experiment

• Air could get trapped in the apparatus and affect the flow of the fluids and also the displaced volume.

• Misreading the volume of the produced fluids on the graduated cylinders.

• The existence of “dead volume” in the system could cause errors in the final calculations.

• Assurance of no liquid residual, especially oil, left in the system which could cause errors in experiments.

Chapter 4

Results and Discussion

4. Results and Discussion

The results are presented in two sections;

The first section (4.1) presents the results of polymerisation of the PPAM, synthesis and characterisation. The results for the study of the average molecular weight are also discussed and the findings of the investigation for PPAM composition analysis are presented.

The second section (4.2) presents the findings of the study of PPAM and HPAM flow in porous media, sand packs and sandstone cores. The results of the investigation of rock interactions with brine and PPAM are also presented and compared with HPAM. Oil displacement results in sandstone cores are also shown and discussed.

4.1 Synthesis and characterisation of PPAM

4.1.1 Solubility of phenyl-acrylamide monomer in surfactant solution

Figure 4.1 shows the results for the determination of the critical micelle concentration (CMC) of the surfactant (SDS). At surfactant concentration of about 0.008 mol/l (2.3 g/l) the minimum concentration of surfactant at which micelles start to form is achieved.

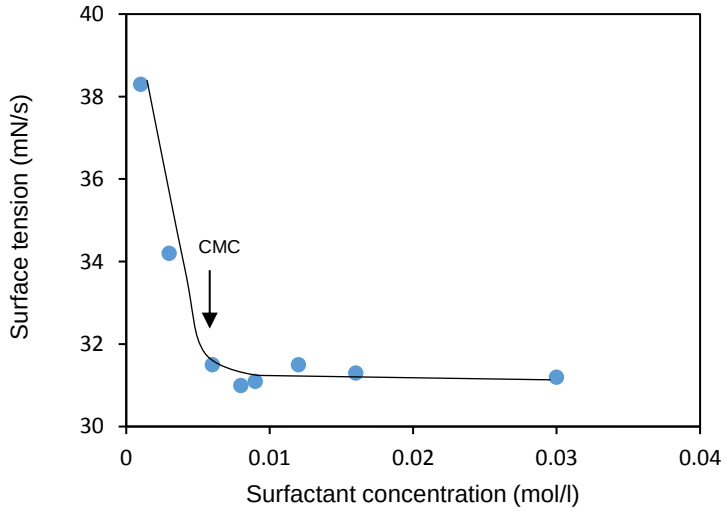

Figure 4. 1: Effect of SDS concentration in the surface tension (CMC estimation).

The effect of SDS at concentration higher than CMC in the solubility of the phenyl-acrylamide was studied and the results are presented in Figure 4.2.

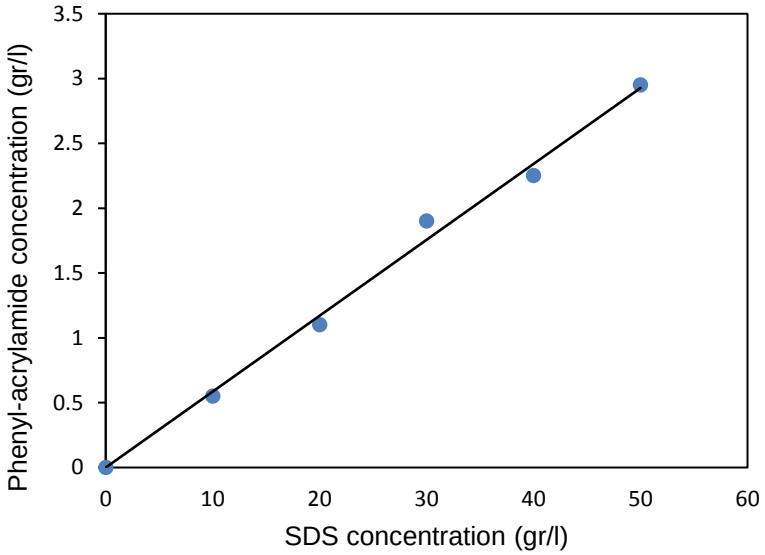

Figure 4. 2: Effect of surfactant concentration in solubility of phenyl-acrylamide

To initiate polymerisation of acrylamide and phenyl-acrylamide in the solution, solubilisation of phenyl-acrylamide monomer in the surfactant needs to be ensured. To achieve this, SDS concentration used has to be above CMC to make sure enough micelles exist is the solution otherwise, the phenyl-acrylamide is not going to incorporate in the polymerisation reaction.

4.1.2 Polymerisation of acrylamide

Table 4.1 shows the laboratory results for polymerisation of acrylamide monomer. This experiment has been done as a reference experiment to monitor the progress of the reaction and ensure the equipment is fully calibrated. Acrylamide monomer conversion to polyacrylamide is calculated by mass of dried polymers obtained divided by mass of monomers in each sample. The total mass of monomer in each solid sample is the weight of each sample multiplied by mass fraction of monomer ($\frac{\text{weight of initial monomer}}{\text{Total weight of solution}}$) in initial solution.

Table 4. 1: Monomer conversion-time

No	Sample weight (g)	Dried polymer weight (mg)	Total mass of monomer in the sample (mg)	Conversion rate	Time (min)
1	1.40	12	41	0.28	30
2	1.34	19	39	0.49	60
3	1.79	22	52	0.41	90
4	1.82	32	53	0.60	120
5	2.20	38	64	0.60	150
6	1.82	39	53	0.74	180
7	1.62	38	47	0.80	210
8	1.58	34	46	0.74	240
9	1.80	44	52	0.85	270
10	1.92	51	56	0.91	300
11	1.78	48	52	0.92	330
12	1.65	44	48	0.92	360
13	1.82	49	53	0.93	390
14	1.99	56	58	0.97	420

Figure 4.3 shows the conversion rate during polymerisation. Close agreement between the theoretical model (Shawki-Hamielec) and the laboratory results is observed which confirms the progress of the reaction and calibration of the equipment is accurate.

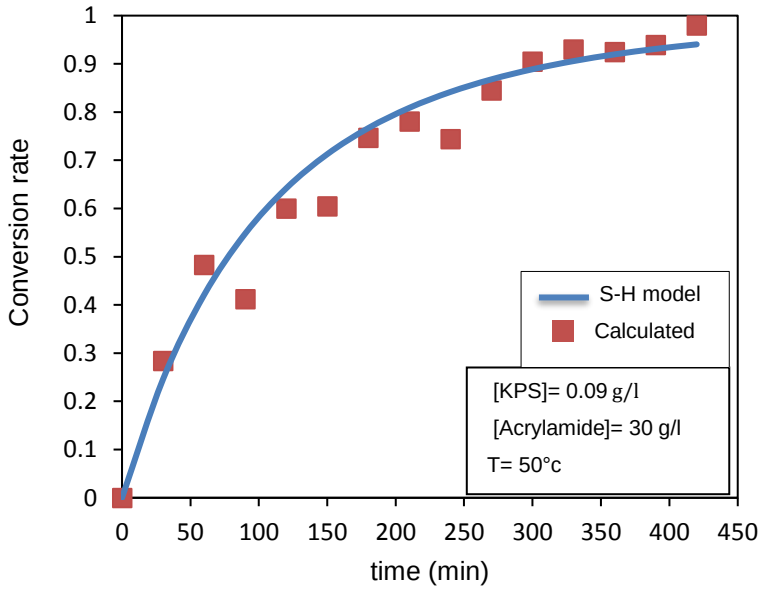

Figure 4. 3: Conversion rate of acrylamide during polymerisation using initiator (KPS) at 50℃.

4.1.3 Micellar copolymerisation of acrylamide with phenyl-acrylamide

Figure 4.4 presents the conversion rate during polymerisation of acrylamide with phenyl acrylamide (micellar copolymerisation). Shawki-Hamielec model developed for homopolymerisation of acrylamide is also applied to copolymerisation of acrylamide with phenyl-acrylamide. As Figure 4.4 shows a very good match of experimental results and S-H model is observed. It can be concluded that a small percentage of hydrophobe incorporation into polyacrylamide chain did not have a significant effect on the total rate of monomer conversion to polymer. Therefore, S-H model can be applied to micellar copolymerisation of acrylamide with phenyl-acrylamide. This has been reported by other authors such as Hill and Selb (1996), Biggs and Candau (1991).

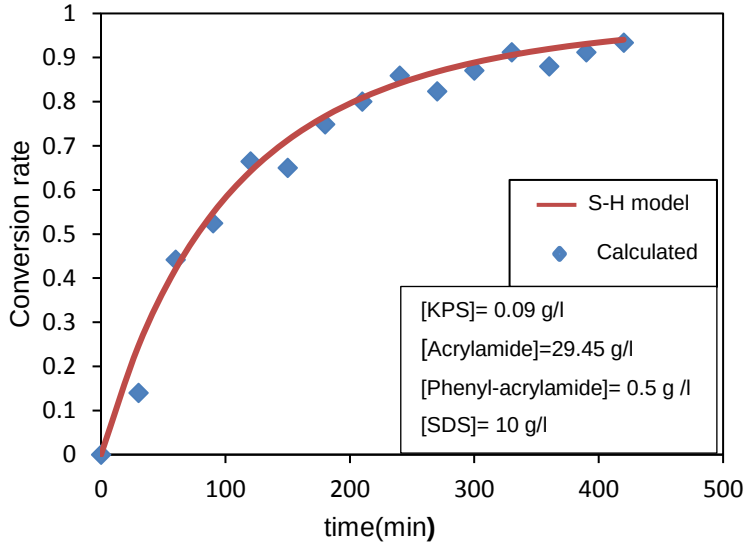

Figure 4. 4: Conversion rate for micellar copolymerisation of acrylamide (3% wt of solution) with phenyl-acrylamide (1% mol of total monomers), using KPS (0.3 %wt of total monomers) and SDS (1% wt of solution) at 50℃ in 200ml of distilled water.

Concentration of SDS and phenyl-acrylamide monomer need to be chosen to ensure the solubility of phenyl-acrylamide monomer in surfactant micelles. Effect of different components concentration on rate of monomer conversion during polymerisation is studied and the results are as follow;

4.1.3.1 Effect of initiator (KPS) concentration on rate of monomer conversion

Polymerisation reactions were carried out with different concentrations of initiator. Figure 4.5 illustrates the experimental data that is close to S-H model. As it can be seen, increasing the initiator (KPS) concentration while the concentration of other components is constant causes speeding up the reaction and more monomers are converted into polymer in a shorter period of time. As the initiator concentration increases more free radicals are produced which causes more active acrylamide monomers in the solution. These active monomers have higher chance to react with other monomers so there will be more chain propagation and termination occur more quickly as it has been reported by Candau (1994).

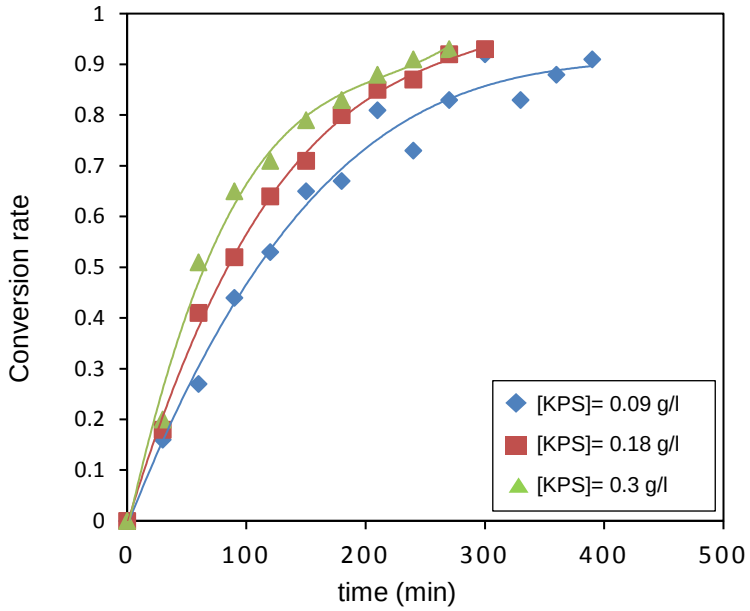

Figure 4. 5: Effect of initiator (KPS) concentration on total monomer conversion rate. Concentration of SDS, acrylamide and phenyl-acrylamide is constant at 50℃.

4.1.3.2 Effect of surfactant concentration on rate of monomer conversion

Conversion-time results are shown in Figure 4.6 for the polymerisation at different surfactant concentration. In this experiment, all SDS concentrations used is above CMC and the other components concentration remained constant. As it is evident, increasing SDS concentration causes a decrease in monomer conversion rate. This has been observed and explained by Mansri

(2007) and Candau (1993). Higher concentration of surfactant means greater number of micelles in the solution which might interfere with the progress of the polymerisation reaction. Also, it is known that alcohols are always present within SDS, as residual reagents from the synthesis or as subsequent hydrolysis products of the surfactant. Hydrolysis of SDS probably occurs to some extent under the polymerisation conditions which prevent the progress of polymerisation.

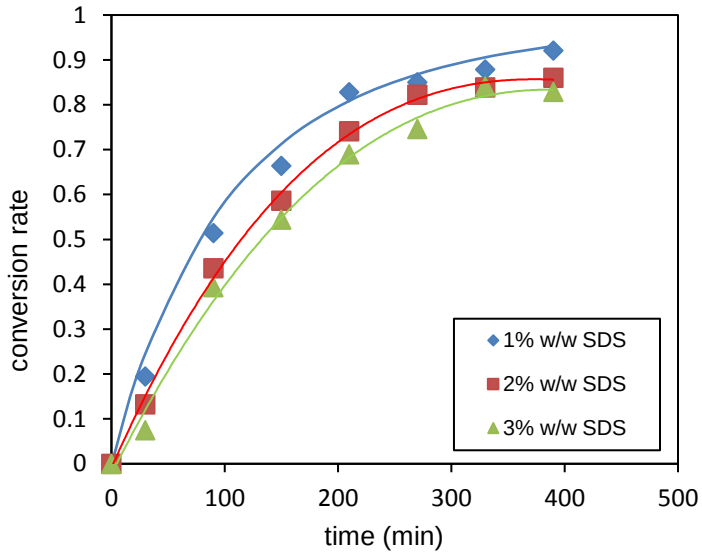

Figure 4. 6: Effect of SDS concentration on total monomer conversion rate. Concentration of acrylamide, Phenyl-acrylamide and initiator (KPS) is constant at 50℃.

4.1.4 PPAM characterisation

4.1.4.1 FT-IR spectroscopy

The FT-IR spectrum of the synthesized polymer is displayed in Figure 4.7. PPAM structure made up of carboxylate functional group (C=O), amide group (N-H) and phenyl group (C_6H_5-). Peak observed at 2982 cm^{-1} is assignable to the C-H stretching from the phenyl group. The IR spectrum also indicated the existence of the carboxylate (C=O) and amide (N-H) groups by absorption peak at 1623cm^{-1} and 3356 cm^{-1}, respectively. Therefore, PPAM composition analysis is accurate with FT-IR. Handbook of polymer (1999) was used to extract functional groups relationship with wavelength.

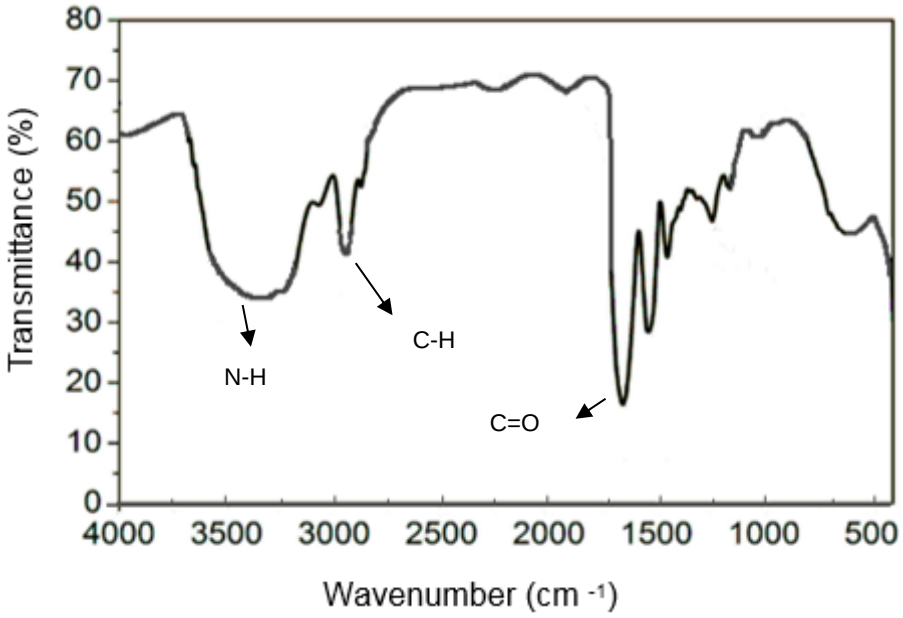

Figure 4. 7: FT-IR spectrum of sample of P(acrylamide/phenyl-acrylamide).

4.1.4.2 H-NMR spectroscopy

The H-NMR spectrum for PPAM is presented in Figure 4.8. This indicates the presence of methylene CH_2 group (A), CH (B) and phenyl (C) group. Data also confirms the absence of any surfactant molecule after drying the polymer as no more peaks was observed in the spectrum. This observation supports the formation of multi-block copolymers including long sequence of acrylamide and short sequence of the hydrophobic monomers.

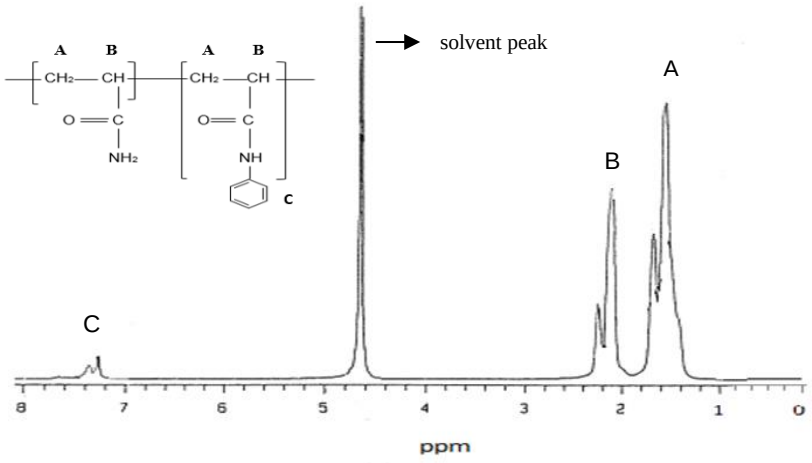

Figure 4. 8: H-NMR spectrum of a sample of P(acrylamide/phenyl-acrylamide) containing 1.2 mol % hydrophobe.

4.1.5 PPAM Polymer Composition

UV spectroscopy is used to estimate the phenyl-polyacrylamide composition (Concentration of acrylamide and phenyl-acrylamide in copolymer). Different concentrations of polymer solution ranged from 100-500 ppm were prepared. The UV spectra for these solutions are examined in the range 200-400 nm. Phenyl-acrylamide monomer gives an absorbance maximum in the range of 312-314 nm and acrylamide absorbance is around 206-208 nm, as shown in Figure 4.9. Phenyl-acrylamide blocks show a smaller peak than acrylamide blocks due to the presence of chromophoric groups and bonding.

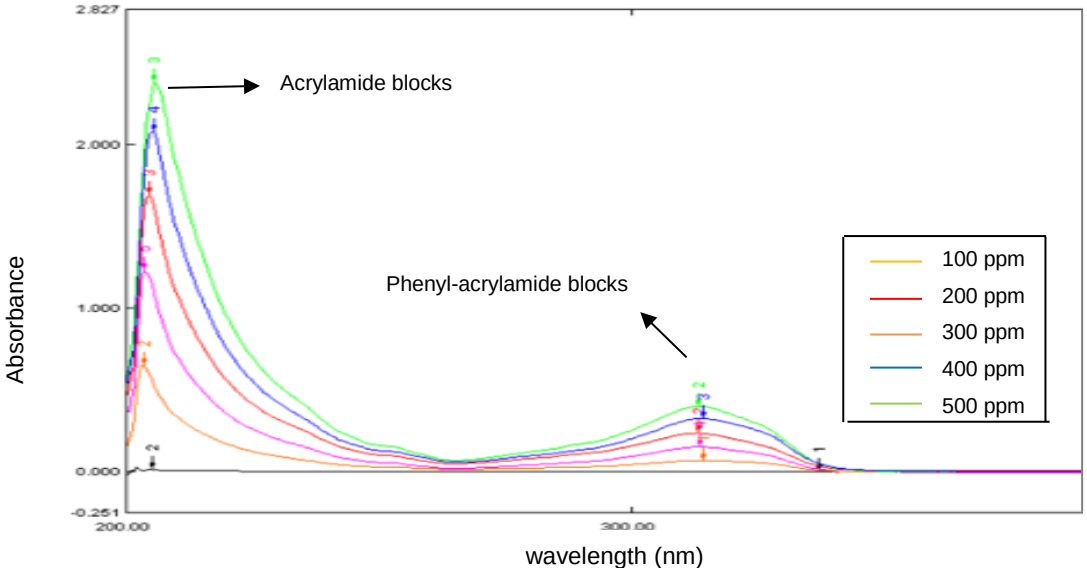

Figure 4. 9: Absorbance at different concentration of phenyl-polyacrylamide.

Phenyl-acrylamide molar content in copolymers was calculated from maxima absorbance of copolymer at 312 nm, according to Eqs (4.1) and (4.2) (Mansri et al 2007) and (Zhang 2011).

$$w\% = \frac{A_0}{\varepsilon}\frac{M_2}{y} \times 100 \qquad (4.1)$$

$$\text{mol}\% = \frac{\left(\mathbf{w}/\mathbf{M_2}\right)}{\left[\left(\mathbf{w}/\mathbf{M_2}\right)+\left(\mathbf{(100-w)}/\mathbf{M_1}\right)\right]} \times 100 \qquad (4.2)$$

Where y is the concentration of copolymer in g/L and ε is 2633.6 ($mol^{-1}.cm^{-1}.L$), the value of the molar absorption coefficient determined from the

corresponding monomer phenyl-acrylamide, A_0 is the maxima absorbance of copolymer at 312nm. The values M_1 and M_2 are the molecular weights of acrylamide and hydrophobe phenyl-acrylamide, respectively.

A series of copolymers containing various fractions of hydrophobic monomer (phenyl-acrylamide) at constant surfactant (SDS) concentration (3%w/w) were synthesised and the results are given in Table 4.2.

Table 4. 2: Characteristics of synthesised copolymers PPAM

Sample	Monomer feed, Phenyl-acrylamide (mol %)	SDS (wt %)	Polymer composition, phenyl-acrylamide (mol %)	N_H	[η] mL.g^{-1}	K_H
PPAM1	0.21	3	0.18 (±0.01)	0.54	422.6	0.41
PPAM2	0.38	3	0.36 (±0.01)	0.98	395.3	0.47
PPAM3	0.62	3	0.64 (±0.01)	1.58	381.6	0.42
PPAM4	0.78	3	0.86 (±0.01)	2.02	332.7	0.58
PPAM5	1.23	3	1.24 (±0.01)	3.18	320.4	0.82
PPAM6	2.10	3	2.16 (±0.01)	5.44	308.1	0.76
PPAM7	3.0	3	2.85 (±0.01)	7.59	273.5	0.80
PAM	0.0	0.0	0.0	0.0	452.2	0.61

N_H, Number of hydrphobe monomer per micelle in the synthesis. [η], calculated intrinsic viscosity. K_H, Huggin constant.

Some properties of copolymer PPAM in dilute solution are also shown in Table 4.2. Intrinsic viscosity [η] (equ.2.3) and Hugging constants K_H were calculated in 1 M NaCl aqueous solution at 25℃ by using an Ubbelohde capillary viscometer. Number of hydrophobe per micelles (N_H) were calculated using (equ.3.1) and the viscosity average molecular weight of samples were determined by Mark-Houwinks equation (equ. 2.8). The values for homopolymerisation of acrylamide (PAM) are also given as reference.

At low hydrophobe content (< 1.2 mol %) the Huggins constant values are between 0.4-0.65 that indicates a good water solubility of copolymers however, at higher hydrophobe content a deviation occurs; the lower intrinsic viscosity and higher K_H shows the contraction of the polymer coils due to their intra-molecular hydrophobe association. These results are close to finding of Volpert (1997) and Wever (2011).

Figure 4.10 shows the variation of the mole percentage of hydrophobe in the copolymers as a function of mole percentage of hydrophobe in feed. An almost unit molar ratio of hydrphobe was observed in feeds and copolymers at low concentration of hydrophobe; however, this started to decrease slightly at higher concentration of hydrphobe in feed. This behaviour can be attributed to reactivity ratios, r_1 and r_2, of acrylamide and phenyl-acrylamide monomers. By keeping the amount of hydrphobe low in feed, a constant reactivity ratio was observed for both monomers. However, no accurate data are available on this ratio (Gouveia 2009).

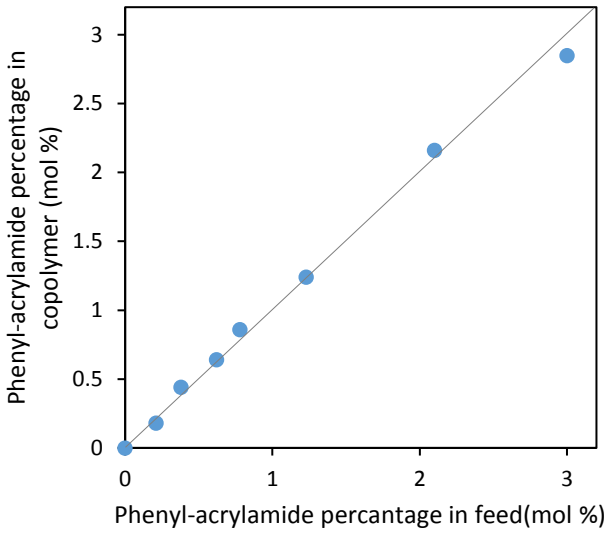

Figure 4. 10: Mole percentage hydrophobe in copolymers as a function of hydrphobe percentage in feeds.

4.1.3.3 Effect of hydrophobe concentration on rate of hydrophobe monomer conversion.

Phenyl-acrylamide conversion versus time for polymerisation reactions are shown in Figure 4.11 for three copolymers with different initial hydrophobe concentration. Other components concentration remained constant. Theoretical conversion-time variation for acrylamide monomer conversion was also calculated using Shawki-Hamielec equation. A rapid incorporation of hydrophobe monomer into copolymer was observed at higher hydrophobe content. But it slows down as the hydrophobe concentration decreases. As it

can be seen in Figure 4.11, almost all of hydrophobe monomer was consumed less than 80 minutes up to 50% of total monomer feed conversion in copolymer with 3 mol% of hydrophobe. This fast reaction causes a heterogeneity in copolymer structure and growing polymer chain will have mainly acrylamide monomer (Hill 1993; Biggs 1991).

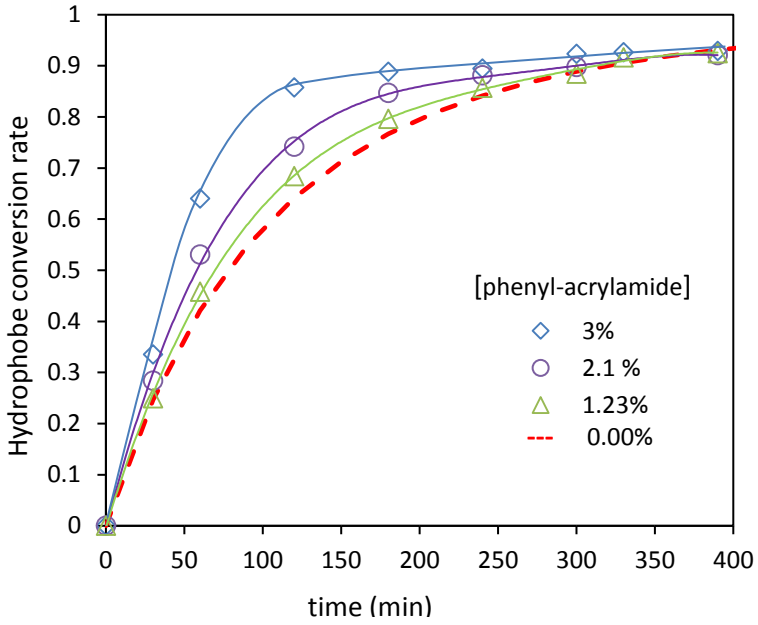

Figure 4. 11: Effect of phenyl-acrylamide concentration on the rate of hydrophobe monomer conversion. Concentration of acrylamide, SDS and initiator (KPS) is constant at 50℃.

Figure 4.12 and 4.13 show phenyl-acrylamide percentage data for copolymer samples PPAM5 and PPAM6 as a function of monomer conversion. In Figure 4.12 Initial hydrophobe content is 1.23 mol% and in Figure 4.13 is 2.1 mol% at a constant surfactant concentration (3%w/w). It can be seen that initial incorporation of hydrophobe content at the beginning of polymerisation is high and this value decreases to feed phenyl-acrylamide content at higher conversion. The larger the initial hydrophobe content the more deviation from initial hydrophobe content. The initial rapid incorporation of hydrphobe monomers ensure that the hydophobe is accessible to other active radicals in the bulk solution (Candau 1999) and Baojiao (2008).

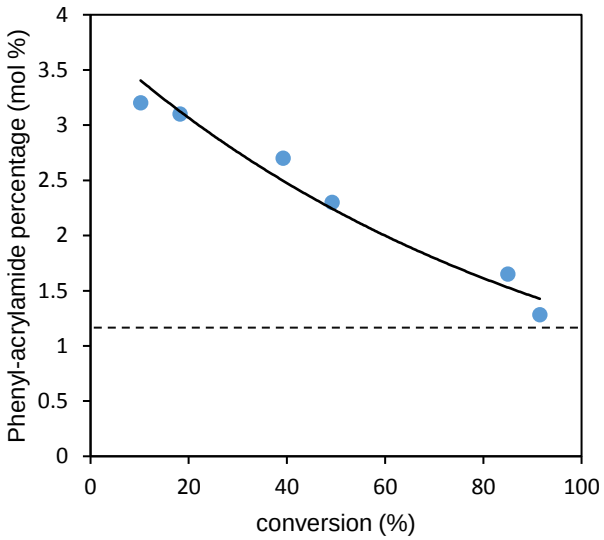

Figure 4. 12: Hydrophobe percentage as a function of monomer conversion for PPAM5.

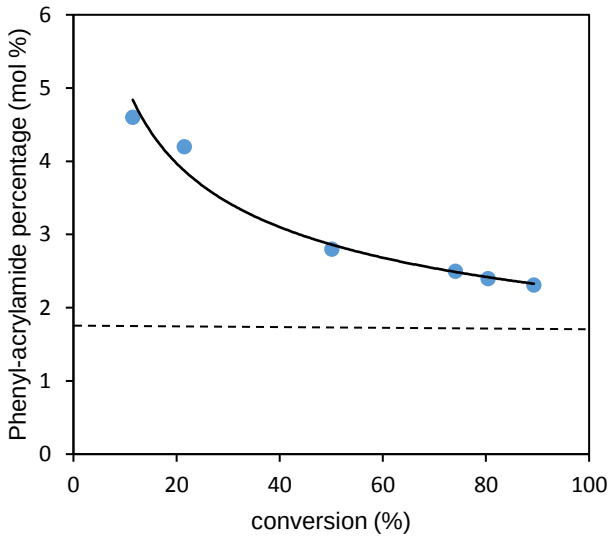

Figure 4. 13: Hydrophobe percentage as a function of monomer conversion for PPAM6.

4.1.6 Viscosity average molecular weight estimation

Flow time of diluted polymer solutions from 1×10^{-4}- 6×10^{-4} g/ml and solvent (distilled water) is measured by using ubbelohde viscometer to calculate average molecular weight of polymer. Reduced viscosity was calculated at different surfactant concentration from 1-3% w/w. Figure 4.14 represents the

variation of the reduced viscosity of the copolymer according to its concentration in dilute solution and intrinsic viscosity is estimated.

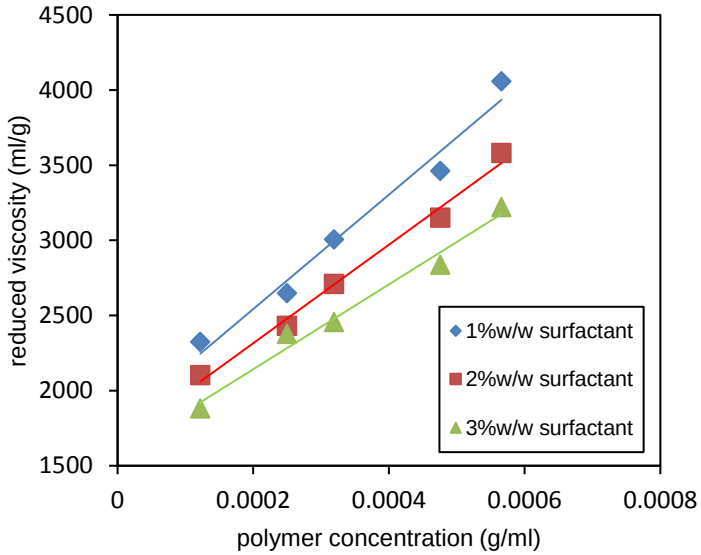

Figure 4. 14: Reduced viscosity of PPAM versus the polymer concentration

Intrinsic viscosity [η] (intercept of reduced viscosity at zero polymer concentration) is reduced by increasing the surfactant concentration. Based on Mark-Howink (equation 2.8) Ƞ=K.Mw^{α} where K and α are 1×10^{-2} and 0.76, respectively, the average molecular weight (M_w) values can be calculated and the results shown in Table 4.3. K and α are extracted from Wiley encyclopaedia for homopolyacrylamide (1994).

Table 4. 3: Average molecular weight of polymer solutions at different surfactant concentrations

Polymer solution	Intrinsic viscosity [η] ml/g	Average M_w (g/mol)
1% w/w surfactant	1724 (±5)	7.8×10^{6}
2% w/w surfactant	1646 (±5)	7.3×10^{6}
3% w/w surfactant	1611 (±5)	7.1×10^{6}

Increasing the surfactant concentration results in a decrease in the observed average molecular weight. One possible explanation for reducing the molecular weight could be the presence of excess free micelles by increasing

surfactant concentration (Mansri et al. 2007). Large amount of free micelles in the solution may interfere with chain propagation and as a result, termination occurs more rapidly. This may lower the average molecular weight of polymer.

4.1.7 Rheological properties of PPAM solution

4.1.7.1 Effect of phenyl-acrylamide concentration on viscosity

The aim of this experiment is to increase the concentration of phenyl-acrylamide so that change the number/length of the hydrophobe content in the molecular structure and consider the effect of this change on the viscosity of final polymer solution. Figure 4.15 shows a viscosity maximum is reached at the hydrophobe content of approximately 1% mole. This can be related to the competition between inter- and intra- molecular association (Figure 4.16). At low hydrophobe content (below 1% mole) the molecular structure of the polymer tends to form inter-molecular association (cluster) leading to a strong viscosity enhancement, while at the higher hydrophobe content, intra-molecular associations begin to become dominant, resulting in a constriction of polymer coils and decrease in viscosity (Wever 2011).

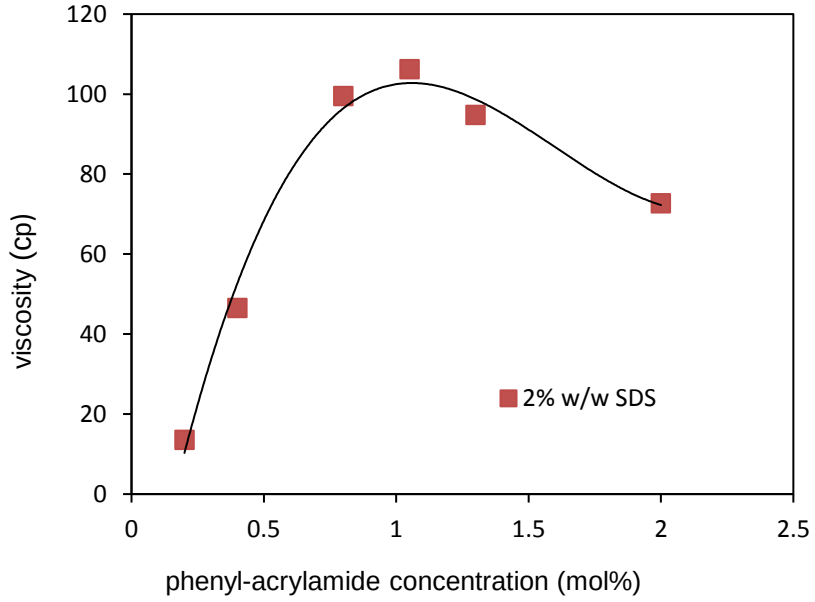

Figure 4. 15: Effect of phenyl-acrylamide on viscosity of PPAM solution.

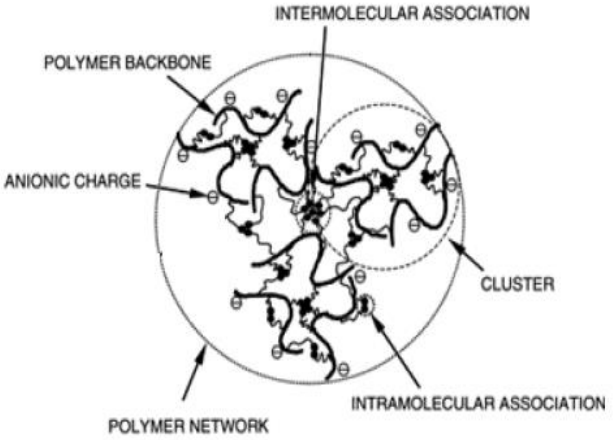

Figure 4. 16: Associative polymer in aqueous solution (Wever 2011).

4.1.7.2 Effect of SDS on the viscosity of PPAM solutions

In this experiment, the effect of external surfactant (SDS) concentrations on polymer viscosity was measured as shown in Figure 4.17. Initially, by adding SDS at concentration lower than CMC to the copolymer solution, the surfactant molecules associate with the hydrophobic regions of the copolymer (Figure 4.18 region 1). As there is not enough surfactant to solubilize each region of the hydrophobe, mixed surfactant micelles are formed containing several regions either of the same chain or others (Region 2) which cause a dramatic increase in viscosity. As further surfactant is added above CMC, each hydrophobe region is solubilized by a single micelle leading to a decrease in the viscosity (Region 3) therefore a maximum in viscosity is achieved by adding surfactant lower than CMC to a hydrophobically modified polymer solution (Wever 2011).

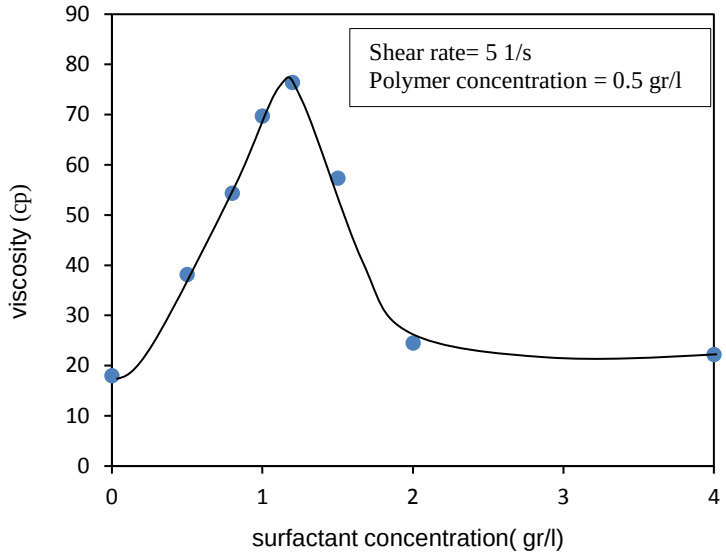

Figure 4. 17: Effect of surfactant concentration on polymer solution viscosity.

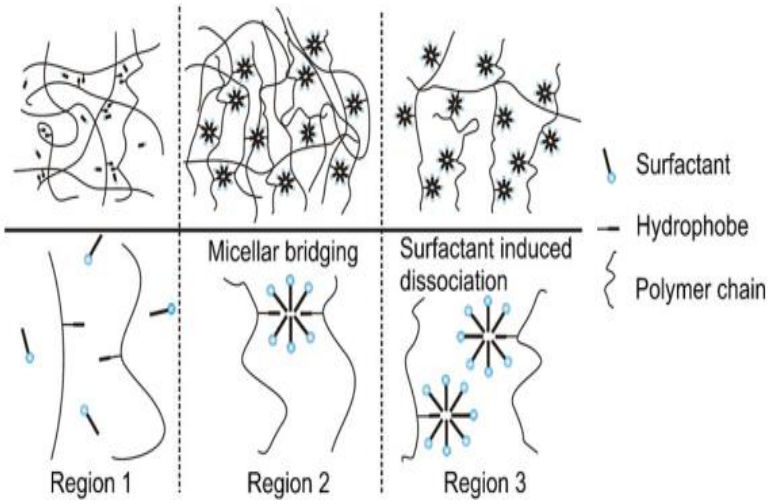

Figure 4. 18: Schematic of mixed micelle formation (Wever 2011).

4.1.7.3 Effect of shear rate on viscosity

Viscosity of bulk polymer solution at different concentration in distilled water is measured against shear rate by using a rheometer; the results are shown in Figure 4.19. Initially, the polymer solution shows a Newtonian (viscosity value is almost constant) behaviour at low shear rate. This behaviour explained by the polymer molecule coils are moving freely inside the solution. As the shear rate continue to increase, the polymer solution shows a non-Newtonian behaviour and the viscosity drops significantly. The polymer

solution displays a shear thinning behaviour which is a result of polymer molecules alignment that occurs when macromolecules are elongated at high shear rate. At this stage, shear forces starts to uncoil the macromolecules which reduces the flow resistance of the polymer solutions. Similar results for the viscosity behaviour of HMPs were observed by authors such as Guillaume (2010) and Stavland (2010) at different shear rate.

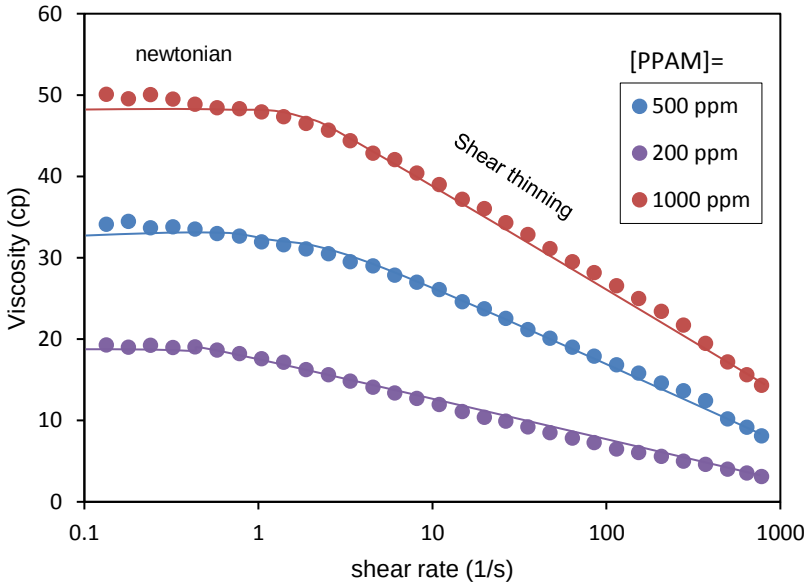

Figure 4. 19: Viscosity of PPAM at different concentrations.

4.1.8 Comparing PPAM with HPAM

In this section, some experiments are conducted to compare HPAM with PPAM in terms of the effect of polymer concentration, water salinity and temperature on the viscosity of polymer solutions.

4.1.8.1 Effect of polymer concentration on viscosity

The results for solutions of HPAM and PPAM at different concentrations and fixed shear rate of $10s^{-1}$ are presented in Figure 4.20. They indicate that at low polymer concentration (< 200 ppm) the viscosity of both polymer solutions is almost the same, however, the viscosity of PPAM solutions begin to increase faster than HPAM solution after a concentration roughly 200 ppm. This concentration for PPAM and HPAM is called critical aggregation

concentration (CAC) and different mechanisms may cause these viscosity enhancements. A higher concentration of HPAM solution is required to obtain the same viscosity value as PPAM solution. Increase in viscosity for PPAM occurs due to the entanglement of hydrophobic regions and intermolecular associations. However, the viscosity increase for HPAM solutions occurs due to the repulsion of negative charges (COO^-) in macromolecule structure. This causes the polymer chain to stretch and increase the viscosity (Pandey et al 2008).

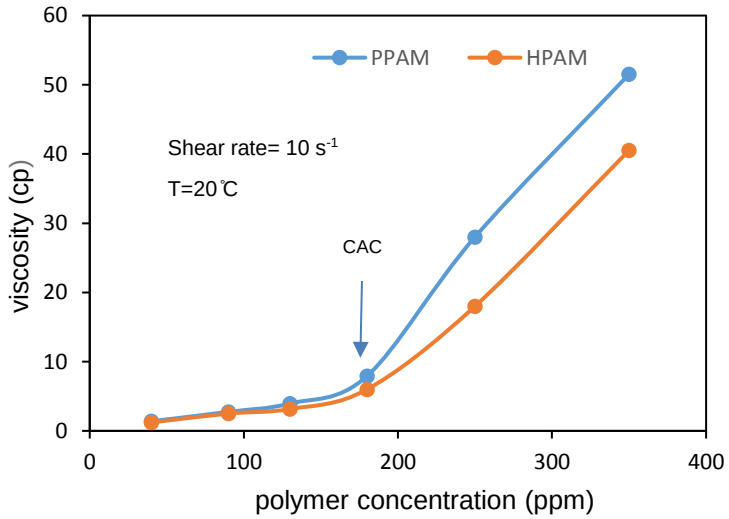

Figure 4. 20: Effect of polymer concentration on viscosity.

4.1.8.2 Effect of NaCl concentration on polymer viscosity

Figure 4.21 shows the effect of NaCl concentration on the viscosity of PPAM and HPAM solutions at different shear rates. As it can be seen, adding NaCl concentration causes a reduction in the viscosity of both polymer solutions. The reduction in viscosity of PPAM solution is due to an enhancement in the intramolecular hydrophobic associations compared to inter-molecular associations which reduce the hydrodynamic volume of the polymer (Wever, 2011).The hydrophobic monomer units contain ion groups, so the addition of salt shielded the inter-molecular repulsion and made the polymer molecule contract. However, viscosity reduction in HPAM solution is due to the electrolyte ions (Na^+) in the salt forms a layer that shields the repulsion between the negative charges (-COO-) of the polymer backbone which

makes the polymer less stretched as it used to be (Mansri 2007). PPAM solution shows a higher salinity resistance in presence of NaCl than HPAM solution.

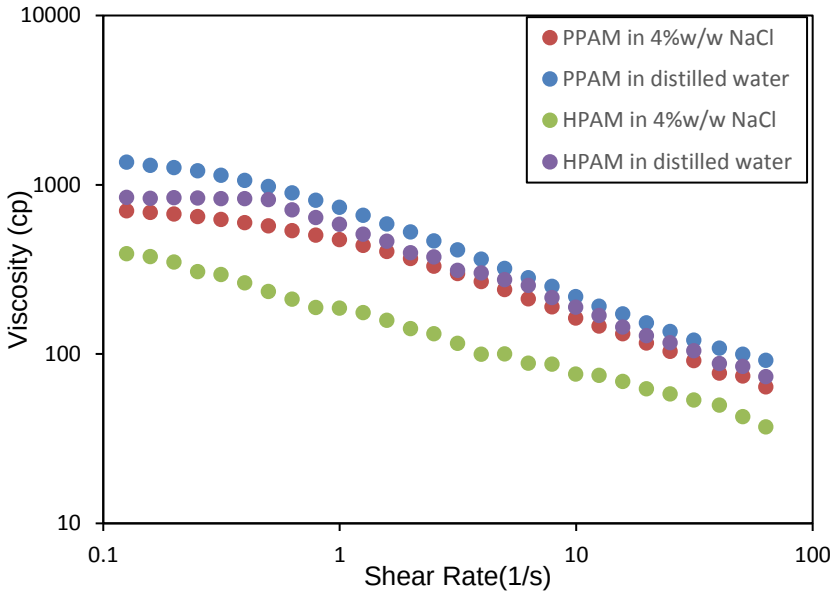

Figure 4. 21: Viscosity at different shear rate in distilled water and NaCl (4% w/w).

4.1.8.3 Effect of temperature on polymer solution viscosity

The effect of temperature on viscosity is shown in Figure 4.22. The apparent viscosity for HPAM decreases by increasing temperature, which is a result of polymer chain degradation. For PPAM polymers, the viscosity increases by increasing temperature and reaches a maximum at about 38-48℃ and then decreases as the temperature continues to increase. These results show the intermolecular association of hydrophobe increases by increasing temperature. It can also be seen that with increasing hydrophobe content, the maximum temperature is shifted in order PPAM 2 at (38℃) < PPAM 3 at (43℃) < PPAM 5 at (48℃). Therefore, the introduction of hydrophpobe monomer into polymer chain can enhance the temperature resistance of PPAM. Similar behaviour have been reported by other authors such as Huang (2004) and Fei-peng (2008) for other hydrophobically modified (HM) polymers which proves the suitability of PPAM in reservoirs with higher temperature. Increasing the temperature may increase the movement of

hydrophobic groups and weaken the intermolecular association which leads to decreasing viscosity.

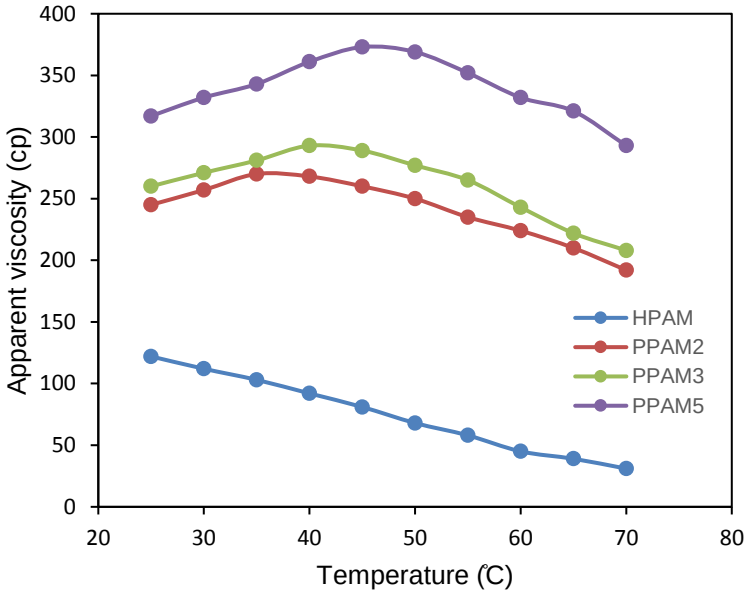

Figure 4. 22: Effect of temperature on the apparent viscosity of 0.6 g.dL^{-1} polymer solutions (25℃, shear rate 10 s^{-1}).

4.2 Experimental study of polymer solutions flow in porous media

In this section, polymer solution flow tests were conducted in both porous media, sand packs and sandstone cores. Sand packs are used to provide a high porosity (40-50%) and permeability (3000-4000 mD) porous medium, however, core samples used in these tests have much lower porosity (15-20%) and permeability (400-500mD). Oil displacement tests were conducted in sand stone cores.

4.2.1 Polymer solutions flow in sand packs

The sand packs properties are shown in Table 4.4. Porosity, pore volume and density of the sand pack calculated by using equations 3-2 and 3-3. Three sand packs of crushed Berea sand were prepared to ensure the repeatability of the tests and reduce errors.

Table 4. 4: Sand pack properties

Length (cm) L	Section area (cm^2) A	Pore volume (cm^3) PV	Sand density (g/ml)	Porosity %
15	4.9	31	2.65	42.9
15	4.9	30.2	2.64	42.7
15	4.9	31.4	2.65	43.0

Sand pack porosity (≈ 43 ±0.5%) is normally very high compared to core samples which provide a high porous environment to avoid polymer trap in porous media. Therefore, it is much easier to investigate polymer solutions flow properties.

4.2.1.1 Permeability of sand pack to brine

Pressure drop data versus flow rates are plotted in Figure 4.23 and brine permeability is calculated to be 3100 mD from the slope of the line by using Darcy equation.

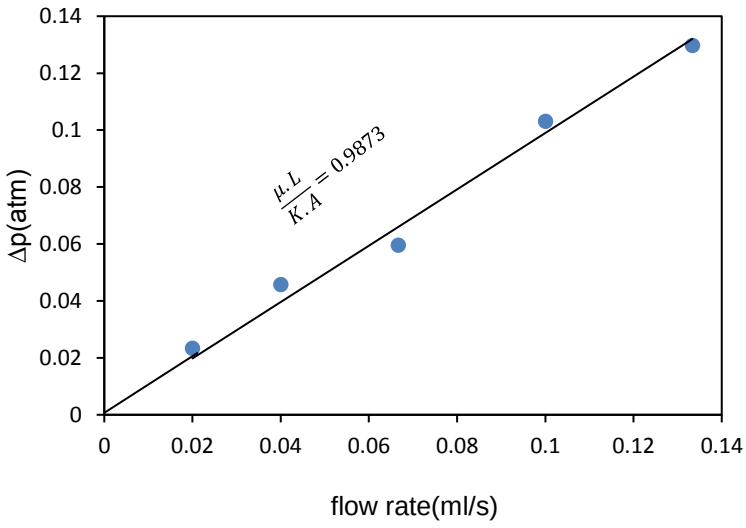

Figure 4. 23: Pressure drop versus brine flow rate in sand pack.

Sand pack is used as an unconsolidated core sample with greater porosity and permeability to investigate the polymer flow behaviour in porous media and investigate the interaction of fluid (brine, polymer) with porous media such as viscosity, permeability reduction, mobility reduction and polymer retention which are discussed below more in detail.

4.2.1.2 Polymer viscosity in sand pack

Table 4.5 presents experimental pressure drops data for polymer injection (∆Pp), brine injection before polymer injection (∆PBb), brine injection after polymer injection (∆PBa), estimated bulk viscosity and shear rate for single phase polymer flow.

Table 4. 5: Pressure drop results for single-phase polymer injection

Flow rate (ml/min)	∆PBb (mbar)	∆Pp (mbar)	∆PBa (mbar)	Mobility reduction (RF)	Permeability reduction (RRF)	Calculated apparent Viscosity (cp)	Calculated shear rate (1/s)
0.05	21.55	47.84	53.16	2.22	2.47	0.90	2.29
0.2	24.78	43.59	53.16	1.76	2.14	0.82	9.15
0.4	31.24	38.28	52.10	1.22	1.67	0.73	18.30
0.8	35.55	51.03	53.16	1.43	1.49	0.96	36.60
1.2	40.94	57.41	54.22	1.40	1.32	1.06	54.90
2.4	46.32	86.12	55.29	1.86	1.19	1.56	109.81
4	53.86	127.59	58.48	2.37	1.08	2.19	183.01
5	75.41	191.38	75.49	2.54	1.00	2.54	228.77
6	104.50	265.80	96.75	2.54	0.93	2.73	274.52
8	131.43	435.92	120.14	3.32	0.91	3.65	366.03
9	147.59	520.98	137.16	3.53	0.93	3.80	411.78
10	165.90	754.89	167.99	4.55	1.01	4.50	457.53
11	180.98	722.99	185.00	3.99	1.02	3.91	503.29
12	202.53	680.46	206.26	3.36	1.02	3.29	549.04
14	249.93	627.30	248.79	2.51	0.99	2.53	640.55
16	349.04	574.14	348.74	1.65	0.99	1.67	732.05

Mobility reduction was calculated by the ratio of pressure drop during polymer injection and before polymer injection. Permeability reduction is calculated by the ratio of pressure drop after and before polymer injection. The apparent viscosity of polymer in situ is a ratio of mobility reduction to permeability reduction multiplied by brine viscosity that is considered 1 cp (Stavland 2013).

Apparent viscosity and shear rate for polymer solution in porous media was calculated by using equations 2.23 and 2.24, respectively. Porous media is

considered as a bundle of capillary tubes and the polymer solution velocity (u) in the tubes is calculated by the flow rates divided by cross section area.

Figure 4.24 shows the apparent viscosity versus shear rate and flow rate in sand pack. As it can be seen a constant viscosity is observed at low shear rate (<100 1/s) however, by increasing the shear rate above 100 1/s the apparent viscosity reaches a maximum of about 4.5 cp at shear rate around 457 1/s (flow rate of 10 ml/min) which is a result of polymer realignment that occurred when the macromolecules elongated with increasing injection rates. Increasing further the flow rate causes the molecule to stretch fully and finally rupture the molecule structure and cause mechanical degradation that reduces the apparent viscosity (Hatzignatiou 2011). Measuring mechanical shear degradation for polymer is essential as it faces different shear rates in its application for EOR.

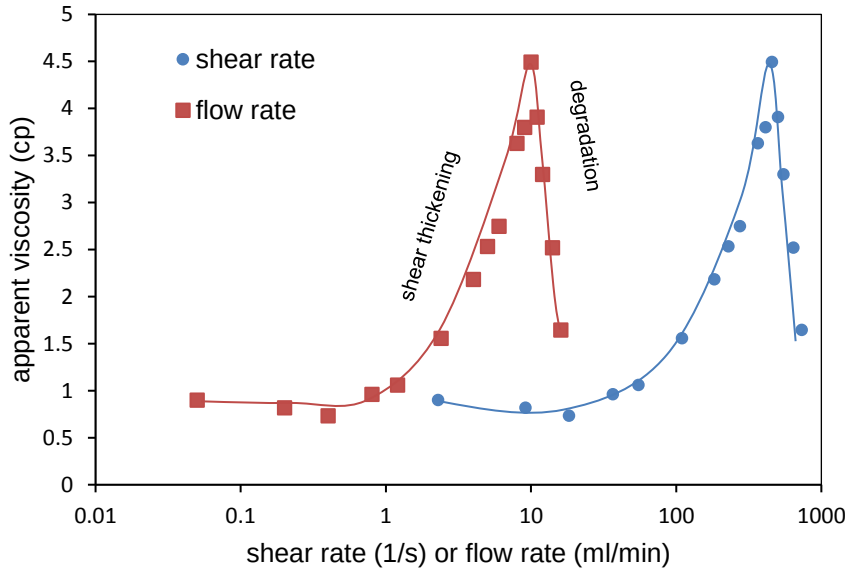

Figure 4. 24: Apparent viscosity of PPAM versus shear rate and flow rate in sand pack**.**

4.2.1.3 Polymer retention experiments in porous media

4.2.1.3.1 Effect of PPAM polymer concentration on retention

A standard curve of the concentration of effluent polymer solutions for all retention tests in this section was created by UV spectrophotometry, Figure 4.2. To achieve this, five polymer solutions with different concentration (ppm)

were tested and the area under curve at each particular wavelength is plotted against polymer concentration. Therefore, the effluent polymer concentration can be calculated by corresponding value of area in calibration curve. Please see Appendix (7.1) for UV data.

Three experiments were carried out to study polymer retention on sand pack as a function of the polymer concentration.

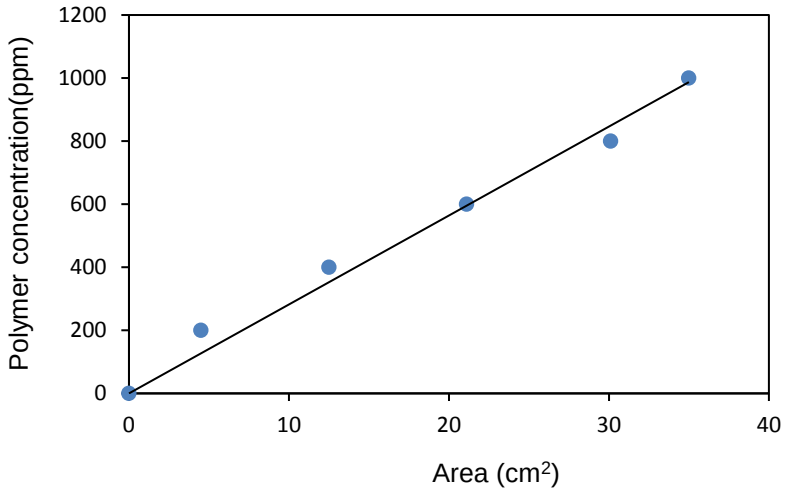

Figure 4. 25: UV-vis standard curve for PPAM at different concentration.

The normalized concentration, the effluent concentration of each sample divided by the injected polymer concentration (C/C_0), is plotted versus volume of injected polymer in Figure 4.26. Initially, the concentration of the polymer in effluent sample was close to zero up to around injection of 1 pore volume (≈30 ml) of the polymer solution and then a sharp increase in polymer concentration at roughly 35 ml of polymer solution was observed. Injecting more polymer solution did not change the effluent polymer concentration significantly as no more polymer retention occurs in the sand pack and it eventually reached a plateau.

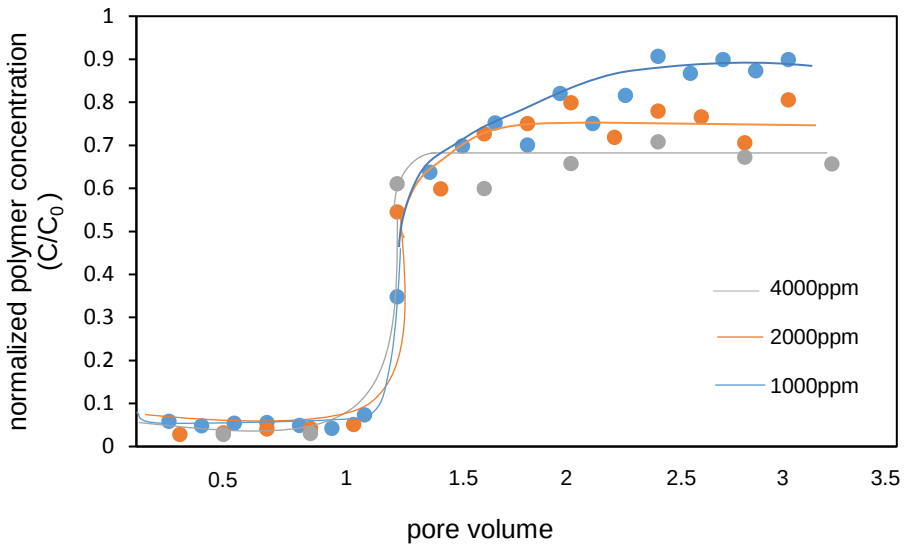

Figure 4. 26: PPAM retention at different polymer concentration.

The retention of each polymer solution in sand pack was calculated by using equation 3.5 in mass of polymer per mass of sand and the result are shown in Table 4.6. UV data is attached in Appendix (7.1) as reference.

Table 4. 6: Polymer retention in sand pack

Initial Polymer concentration (C_0) ppm	C/Co	Pore volume (ml) (PV)	Sand mass (g)	Retention (µg/g)
1000	0.86	31.3	116	37
2000	0.75	30.5	115	134
4000	0.67	30.8	116.7	348

As it can be seen from the results, an increase in polymer retention is observed by increasing the polymer concentration which was shown at higher PPAM concentration, molecules were adsorbed on more vacant sites on the sand surface. Findings of Saavedra (2002), Mezzomo (2002) and Zhang (2013) also showed quite similar retention behaviour for other HMPs.

4.2.1.3.2 Effect of sand grain size on PPAM polymer retention

Figure 4.27 shows the effect of sand size distribution on rate of polymer retention. 1000 ppm polymer solution was injected through sand pack with different sand size distribution, and as it can be seen the smaller sand size the higher polymer retention due to the smaller pore size which is resulted in pore blocking. The retention in smaller sand size occurs mainly due to the

polymer molecule size which is larger than pore size (hydrodynamic retention).

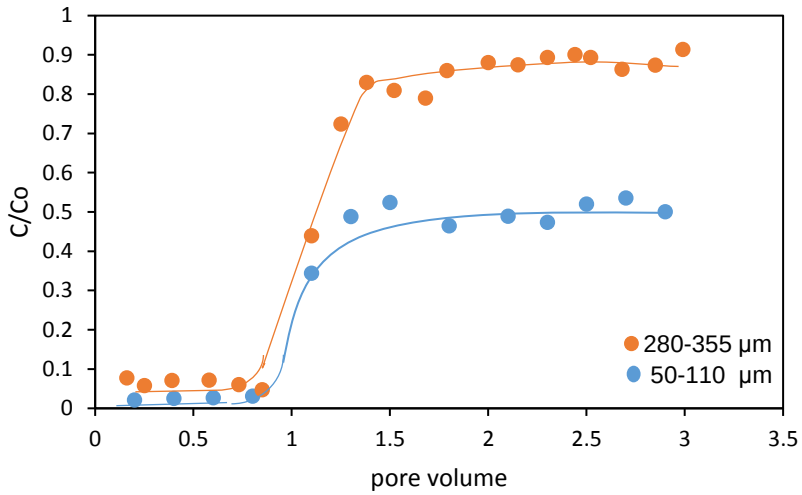

Figure 4. 27: Retention of PPAM in sand packs with different grain size.

4.2.1.3.3 Effect of salinity on polymer retention

Figure 4.28 shows the results of PPAM and HPAM injection in sand pack (280-355 µm) with soft brine (Table 3.1). As it can be seen, slightly higher retention for PPAM than HPAM is observed. This could be due to the slight larger polymer size of PPAM compare to HPAM. The inter-molecular associations at high concentration of polymer become dominant and increase the hydrodynamic volume of the polymer network (Maia 2013).

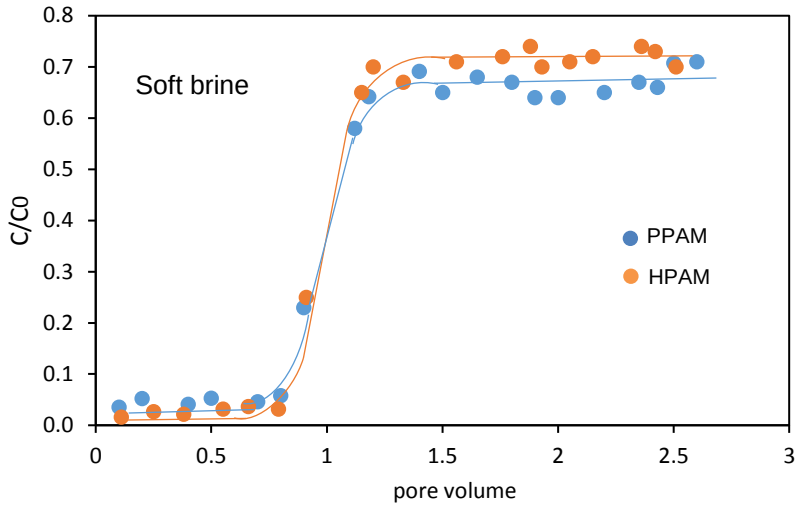

Figure 4. 28: Polymer retention in presence of soft brine in sand pack (280-355 µm).

The same polymer solutions of 4000 ppm were prepared in brine with high salinity (hard brine), the brine composition is in Table 3.2. The concentration of divalent ion (Ca^{2+}) in hard brine is much greater than soft brine (Table 3.1).

Figure 4.29 shows the results for the injection of PPAM and HPAM in hard brine. As it can be seen, no noticeable changes were observed for PPAM retention in sand pack when comparing the soft and hard brine injection, however, HPAM shows an increase in retention into sand pack in high salinity brine. This maybe due to the presence of divalent ions, e.g. Ca^{2+} or Mg^{2+}. It proves that HPAM molecules are more sensitives to divalent ions than monovalent ions. This is because of the strong binding between divalent ions and carboxylate group (COO^-) in HPAM (Calgon 1995). After a certain divalent ions concentration, HPAM will precipitate and this make HPAM unfavourable for EOR process at high salinity condition. Similar results for other HM polymers have been reported by authors such as Rodriguez (2014) and Zhang (2013).

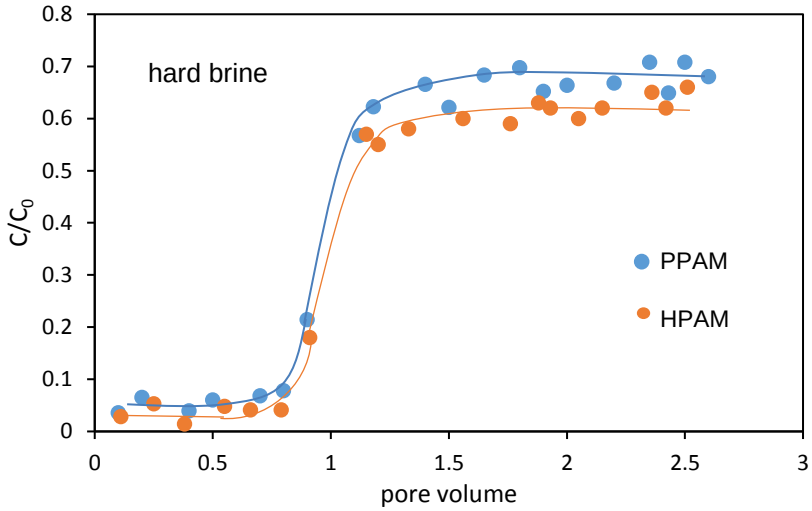

Figure 4. 29: Polymer retention in presence of hard brine in sand pack (280-355 µm).

PPAM retention experiments in Benthemier sandstone (500mD absolute permeability) are also conducted in presence of soft and hard brine. A pore volume of 7.43ml was calculated by saturation method for the core and a porosity of 14.5%. The test was carried out in core flooding set-up (Figure 3.14). The results for injection of 4000 ppm of PPAM and HPAM in soft brine and hard brine are shown in Figure 4.30 and 4.31, respectively.

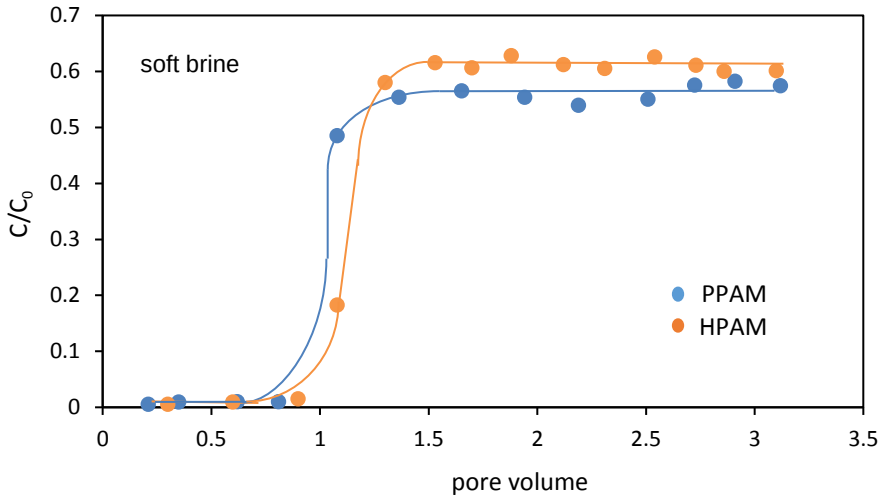

Figure 4. 30 : Polymer retention in presence of soft brine in core sample.

A similar trend for the polymer retention in soft brine analysed in sand pack (Figure 4.28) was observed in the core sample (Figure 4.30) with slightly larger value of the polymer retentions for both the polymer solutions. The increase in polymer retention found in core sample can be attributed to the much lower permeability value of the core sample compared to the sand pack.

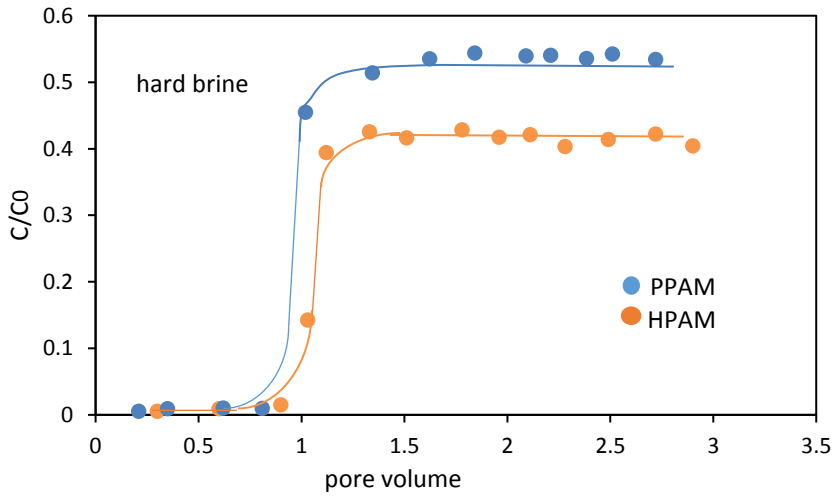

Figure 4. 31: Polymer retention in presence of hard brine in core sample.

Figure 4.31 also shows the polymer retention in core sample in presence of hard brine. A greater retention of HPAM in hard brine in core sample was found compared to the polymer retention in sand pack in hard brine (Figure 4.29). This could be due to smaller pore connectivity of core sample besides a lower permeability of the core sample compare to the sand pack.

Both polymers, PPAM and HPAM, were dissolved in brine with high concentration of divalent ions (very hard brine) and the results are shown in Figure 4.32. PPAM at the right side of the picture and HPAM at the left. As it is clear from image HPAM precipitates in presence of very hard brine (Ca^{2+} and Mg^{2+}), however, PPAM was dissolved without any trace of precipitation or polymer agglomeration. This precipitation is due to the strong binding of carboxylate groups (coo^-) in HPAM molecule structure with divalent ions in brine, however, no active functional groups exist in PPAM structure to react with brine ions.

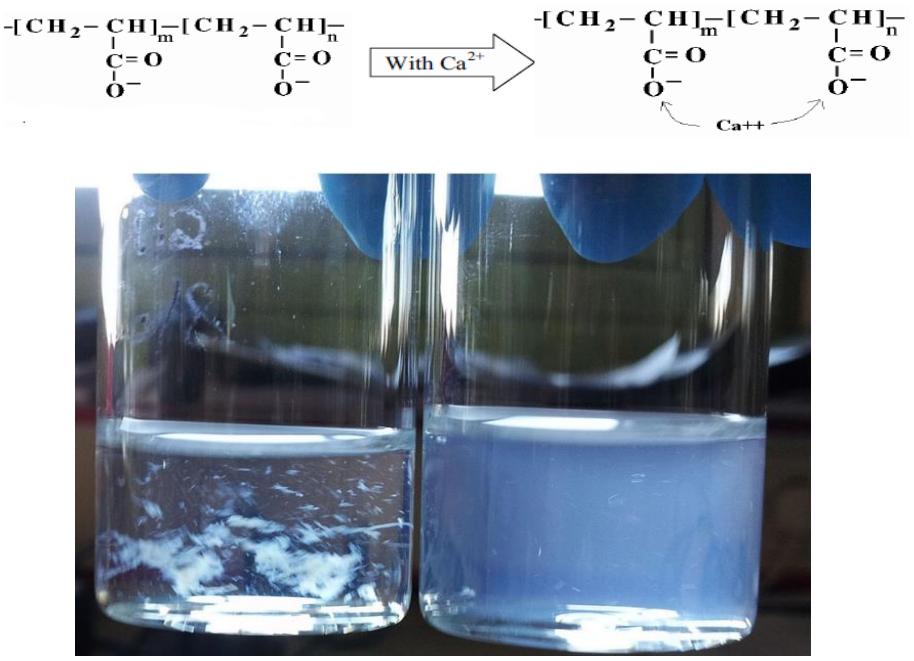

(a) HPAM (b) PPAM

Figure 4. 32: PPAM (b) and HPAM (a) polymer solubility in hard brine.

4.2.1.3.4 *Inaccessible pore volume (IPV) test in sand pack*

Two experiments were carried out to measure inaccessible pore volume (IPV) for PPAM and HPAM solutions in soft brine with 1000 ppm concentration, During the experiments, potassium nitrate (KNO_3) was used as a tracer. The tracer tests were performed with the injection of polymer solutions. The UV spectrophotometer was used to measure the absorbance of the tracer solution in the effluent line of the sand pack. A calibration curve developed between the tracer concentration and absorbance was used to calculate the concentration of tracer in the effluent samples. A solution of 0.1 M KNO3 (potassium nitrate) in brine gives an absorbance at a wavelength of 302 nm.

Finally, the inaccessible pore volume (IPV) of polymer solutions is estimated by calculating the difference in break-through time between the polymer and the salt. Figure 4.33 and 4.34 show the effluent profiles for PPAM and HPAM injection. It is shown that the two miscible flood fronts flow through the porous

media with different velocities. The velocity of polymer that propagates in the sand pack is greater than that of the water.

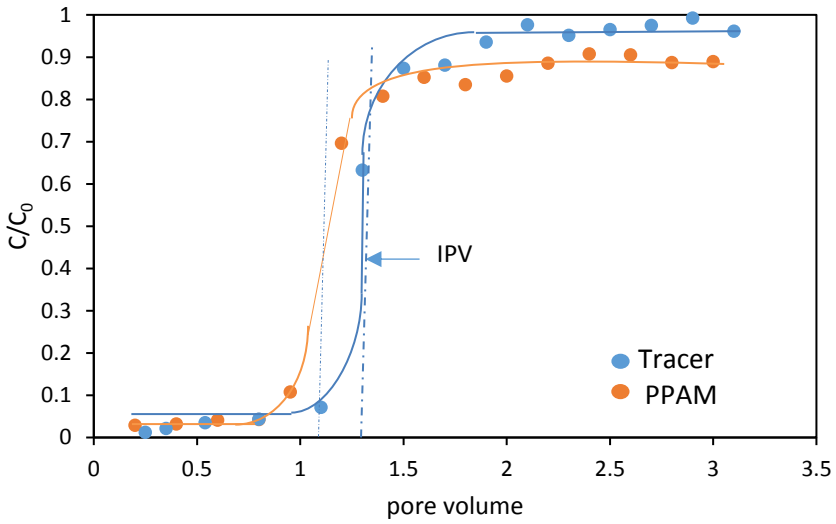

Figure 4. 33: IPV test for PPAM in sand pack.

The gap between polymer breakthrough and tracer shows inaccessible pore volume (IPV). This gap is slightly bigger for the PPAM injection (Fig 4.33) than for the HPAM (Figure 4.34). It shows PPAM breakthrough occurs slightly quicker than HPAM which means that the PPAM molecules have less access to vacant sites of porous media due to its larger molecule structure. Presence of hydrophobic monomers in PPAM cause a greater 3-dimensional structure network, whereas, HPAM has a linear molecular structure. Many authors such as, Aparecida (2002), Pancharoen (2010) and Manichand (2014) have reported larger polymer molecules shows earlier breakthrough and greater IPV for different HM polymers.

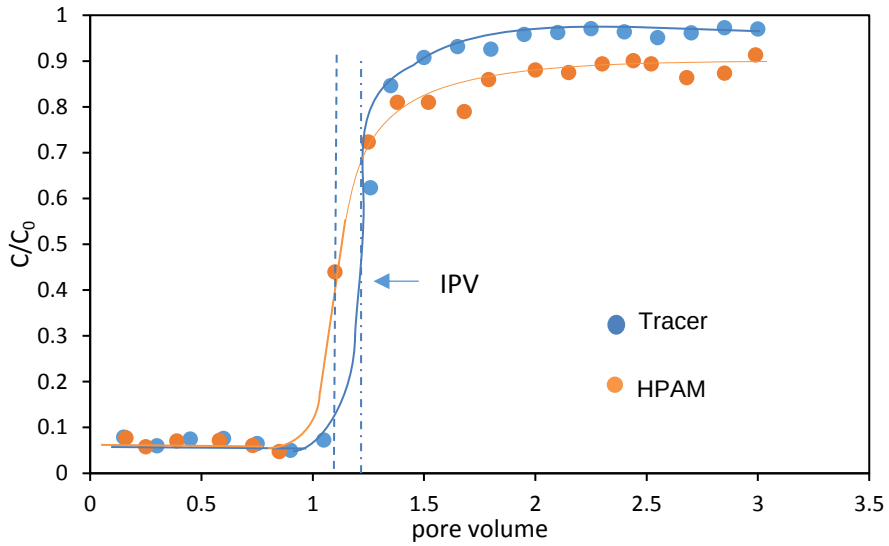

Figure 4. 34: IPV test for HPAM in sand pack.

4.2.2 Oil displacement tests using PPAM and HPAM

The following sections describe a series of coreflood tests to displace heavy oil. The properties of heavy oil is in Table 3.3. Generally, the main purpose of this part of the study was to observe the effect of polymer viscosity on heavy oil recovery performance. The experiments utilized both HPAM and PPAM at concentrations of 2000 ppm and 4000 ppm in soft brine. The comparative analysis included the pressure differential and oil recovery data with respect to injection throughput, as well as tables of resistance and residual resistance data and saturation profiles. The main core sample properties are given in Table 4.7. The absolute permeabilities of the cores were provided by supplier but the rest of the properties were measured in the lab. Fresh core samples were used for each test to ensure the repeatability and precision of the experiments.

The pore volume of the cores was measured by saturation method. The cores were saturated in distilled water for 24 hours. The difference between dry wet and wet weight of the core sample is total mass of water in pore space of the core divided by density of distilled water (1g/ml) give the volume of water in the core sample (pore volume).

Table 4. 7 : Core samples (Benthemier sandstone)

	Test							
Core sample	1	2	3	4	5	6	7	8
Absolute permeability (mD)	500				100			
Length (cm)	10.10	10.02	10.16	9.91	9.96	10.12	9.89	9.95
Diameter (cm)	2.52	2.54	2.50	2.55	2.54	2.57	2.48	2.51
Area (cm^2)	4.98	5.06	4.91	5.10	5.06	5.18	4.83	4.95
Pore volume (cm^3)	7.43	7.38	7.51	7.32	8.75	8.70	8.63	8.66
Porosity (%)	14.8 (±0.3)	14.6 (±0.3)	15.1 (±0.3)	14.5 (±0.3)	17.4 (±0.3)	16.6 (±0.3)	18.1 (±0.3)	17.6 (±0.3)

4.8.1 Oil Injection (drainage)

Table 4.8 shows the results from flooding the core samples with crude oil which is already saturated with brine and measure the oil saturation.

Table 4. 8: Crude oil injection

	Crude oil injection (drainage process)							
Absolute Permeability (mD)	500				100			
Core sample	1	2	3	4	5	6	7	8
Initial oil volume (cm^3)	6.5	6.4	6.4	6.3	7.5	7.2	7.3	7.3
Initial oil saturation (S_{oi})	0.88	0.87	0.85	0.86	0.86	0.83	0.85	0.84

To achieve this, Initial oil saturation (So_i) in core samples was measured by recording the volume of the brine that was pushed out of the core during the injection period. Initial oil saturation was calculated by ratio of initial oil volume to pore volume. The saturation of crude oil in each core slightly varied due to differences in each of the cores, such as the permeability or connectivity between the pore spaces. The oil flow within the cores would have also differed in each core. This would potentially alter the volume of the core sample that would have come in contact with the oil. However, the

levels of saturation were sufficient for the use of studying the oil volumes recovered in the steps that followed.

4.8.2 Brine injection (imbibition)

Brine injection was performed after establishing the initial reservoir condition (drainage) for the cores. Each core varied slightly in the amount of crude oil recovered from the initial oil volumes, varying from 51.7 % to 58.9%.

A low flow rate of 0.2 ml/min was applied in order to keep the pressure constant across the core and make sure a homogenous propagation of brine solution in the cores. The amount of oil recovered during the brine injection is higher than the average oil recovered in a typical reservoir, which is around 35%. The high percent of oil recovery by water flooding in core testing may be due the experimental conditions. Additionally, the small dimensions of the core samples, may result in higher recovery levels in the core. The recovery of the oil with the brine injection was carried out up to the point where only brine was exiting the core for about 20 minutes and pressure drop across the core is constant. This represents the primary oil recovery.

The injection represented a water flooding process that was completed past the point of being economically feasible. Residual oil saturation (Sor) and water saturation in core samples can be measured by remaining volume of oil and water in core sample divided by pore volume as shown in Tables 4.9 and 4.10 as initial water flooding (IWF) process. At this point, pressure drop across the core was getting constant and the brine solution bypasses the crude oil (fingering), following a path of least resistance towards the end of the core. This is demonstrating the need for a new recovery approach to be implemented in order to keep producing oil more economically.

4.8.3 Polymer injection

Polymer injection process was conducted after the initial water flooding (IWF) in which the pressure drop became constant across the core sample and no more oil was produced.

4.8.3.1 Oil displacement experiment using PPAM (2000 ppm) in 500 mD core.

The pressure drop data and the oil recovery is shown in Figure 4.35. The first pressure build-up is an indication of initial water flooding (IWF) until it reaches water breakthrough. At this point of displacement, the pressure starts dropping down until it reaches a stabilised value and no more oil is produced. Polymer flooding (PF) was conducted immediately after that point and a second pressure build-up can be observed until polymer breakthrough is reached. Extended water flooding (EWF) was conducted after the polymer flooding for two purposes; Firstly, to observe more oil recovery and secondly, to calculate permeability reduction after the polymer flooding.

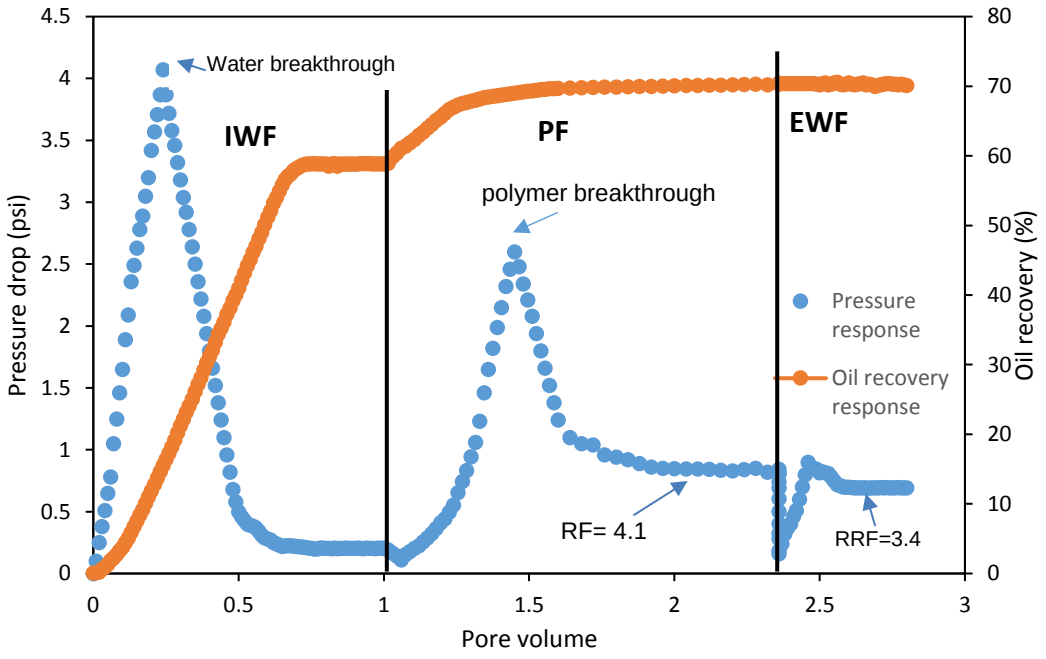

Figure 4. 35: Pressure drop and oil recovery in core 500mD using PPAM (2000 ppm).

It is noticeable from the graph of oil recovery and pressure response, that the polymer flood initial pressure response demonstrated a slight delay. This could be attributed to specifications of experimental set-up. It is believed that the transfer vessel's piston required some time for pressure to be build-up and to move it towards the outlet side.

Almost 1 PV of brine was injected until pressure difference was stabilised at 0.2 psi and oil recovery reached 58.9 % of initial oil volume. Oil saturation in core sample decreased from 0.88 to 0.4 of residual oil saturation (So_r).

The injected polymer viscosity of PPAM was determined to be 32cp at a theoretical shear rate of 14.8 s^{-1} .The subsequent injection of 1.3 pore volumes of polymer solution resulted in a well-stabilized pressure drop of 0.84 Psi, corresponding to a mobility reduction (Resistance factor) of 4.1. After polymer injection oil recovery increased by 11.6% of initial oil volume to 70.4%.

Extended water flooding (EWF) was carried out after the polymer flooding. The final residual oil saturation stayed the same since only a less than 1% more oil recovered after the EWF. The corresponding pressure differential was stabilised at a value of 0.69 psi. This resulted in a residual resistance factor (permeability reduction) of 3.4. The viscosity of produced polymer solution was measured 30.4 cp at 15 s^{-1} theoretical shear rate. There was a slight reduction in the polymer solution viscosity which shows a shear thinning behaviour of the polymer in situ.

4.8.3.2 Oil displacement experiment using HPAM (2000 ppm) in 500 mD core.

The initial waterflood of the core was conducted to approximately 1 pore volume of injection at a rate of 0.2 ml/min until it reached a stabilised pressure drop of 0.19 psi (Figure 4.36). The oil saturation was reduced from 0.87 to 0.38 (Table 4.9). The injected polymer (HPAM) viscosity was 26 cp at shear rate of 15 s^{-1}. Upon switching to polymer injection, an immediate response was observed in the oil recovery followed by an increase in the differential pressure across the core sample. The stable pressure drop was indicated at 0.53 psi that gives a mobility reduction (RF) value of 2.9 at which oil recovery increased by 8.43% of initial oil volume to 67.31%. The extended water flood was carried out until 2.8 pore volume but the final residual oil saturation stayed the same and the differential pressure stabilized at 0.21 Psi, corresponding a permeability reduction (RRF) value of 1.1. The viscosity

of HPAM solution in production was measured 24.1 cp at shear rate of 15.2 s^{-1}. The polymer solution viscosity dropped slightly which proves the shear thinning behaviour of polymer in situ.

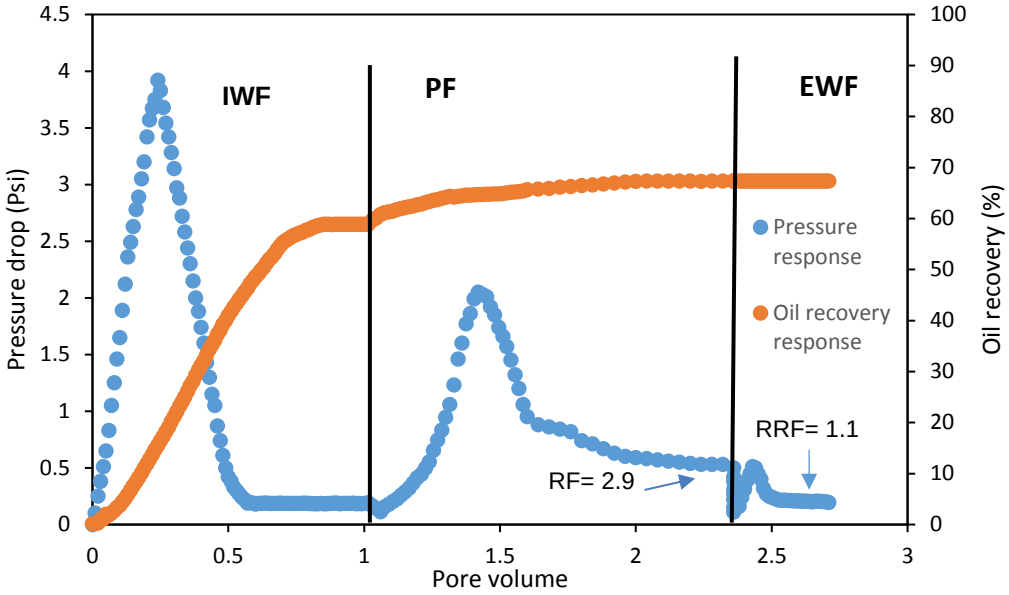

Figure 4. 36: Pressure drop and oil recovery in core 500mD using HPAM (2000ppm).

This experiment shows a slightly lower oil recovery than by PPAM injection, however, permeability reduction to brine for PPAM was greater than HPAM. This could be due to microblocky structure network of PPAM caused by inter-molecular hydrophobic association which give a significant rise to the dimension of the polymer and increase the chance of retention.

4.8.3.3 Oil displacement experiment using PPAM (4000 ppm) in 500 mD core.

The initial waterflood of the core was conducted by almost 1 PV of brine injected (Figure 4.37). The subsequent polymer injection of 1.4 PV was then commenced utilizing PPAM in brine solution. The performance of the initial waterflooding demonstrated 57.9 % of initial oil volume recovered with the corresponding stabilised core differential pressure of 0.19 psi. This resulted in oil saturation decrease from 0.85 to 0.39 (Table 4.9).

The viscosity of injected polymer solution was measured to be roughly 72.1 cp at a calculated theoretical shear rate of 15.17 s^{-1}. The oil recovery

increased by almost 23.2 % to 81.1% OOIP with corresponding pressure drop was stabilised at 1.13 psi. This gives a mobility reduction value of 6.1. The final oil saturation after the polymer injection was determined to be 0.19.

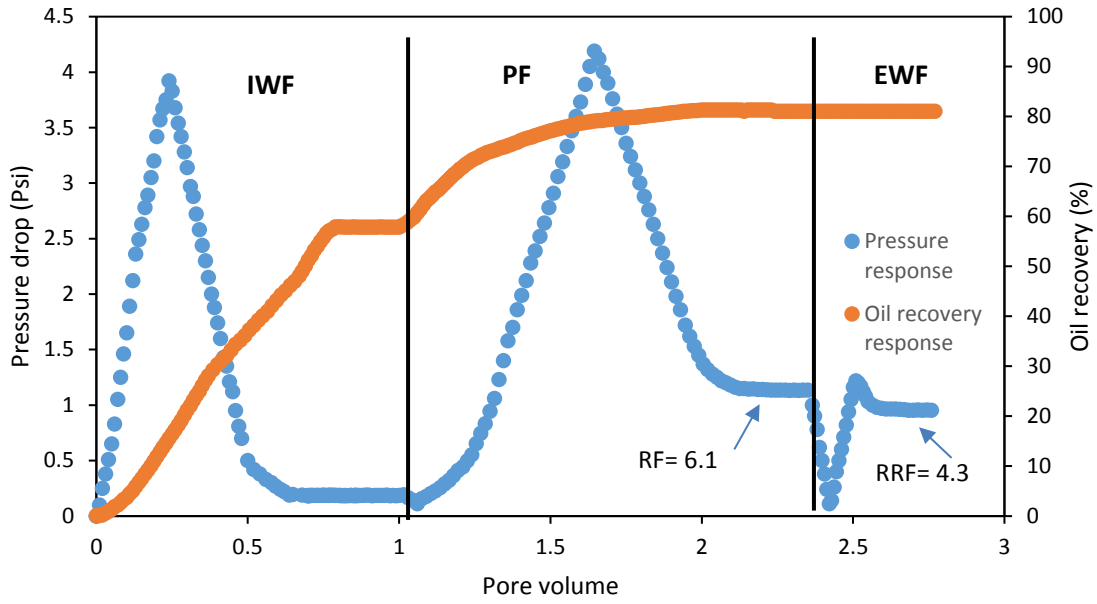

Figure 4. 37: Pressure drop and oil recovery in core 500mD using PPAM (4000ppm).

Extended waterflood (EWF) performance showed the same trend as for the previous scenario with no additional oil recovered (Figure 4.37). The pressure differential was stabilised at 0.95 psi, corresponding to a permeability reduction (RRF) value of 4.3. Final viscosity of the polymer solution at 15 s^{-1} was 70.1 cp which reduces by 2 cp demonstrate a shear thinning behaviour of the polymer.

4.8.3.4 Oil displacement experiment using HPAM (4000 ppm) in 500 mD core.

0.95 pore volume of brine was injected and subsequently switched to polymer injection of HPAM solution. Initial waterflood (IWF) performance reached 57.8 % of initial oil volume in core sample (Figure 4.38), resulting in reduction of oil saturation from 0.86 to residual oil saturation of 0.42 (Table 4.9). The corresponding pressure differential reached a plateau of 0.27 psi.

The viscosity of the injected polymer solution was ~59.4 cp at a calculated theoretical shear rate of 15.71 s^{-1}. The differential pressure was stabilised at 1 psi after polymer injection and incremental oil recovery reached 74.6 % OOIP by 16.6% increase. Ultimately, the stable pressure differential gives a corresponding mobility reduction (RF) value of 3.6.

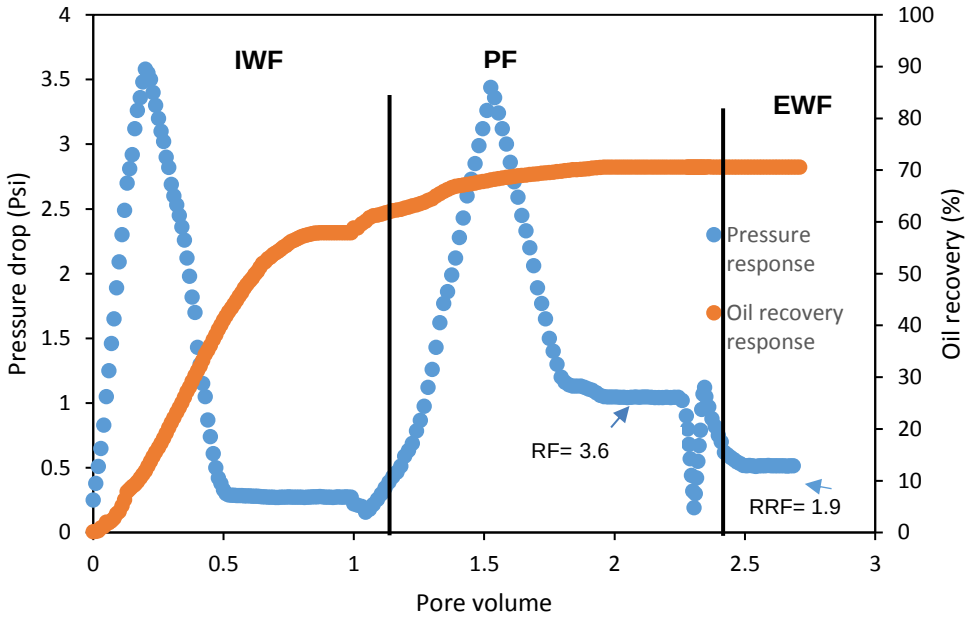

Figure 4. 38: Pressure drop and oil recovery in core 500mD using HPAM (4000ppm).

The extended waterflood (EWF) demonstrated absolutely no additional oil recovery with a corresponding pressure differential of 0.51 psi. This resulted in a permeability reduction (RRF) value of 1.9 to brine. Polymer solution viscosity in production was measured at shear rate 14.9 s^{-1} to 59.4 cp that shows a slight decrease in viscosity the same as previous scenarios.

A summary of the oil saturation after water flooding, polymer injection and extended water flooding for sandstone cores 500mD, is shown in Table 4.9.

Table 4. 9: Summary of oil saturation in core 500 mD

	Tests for core 500mD							
	PPAM (2000 ppm)		HPAM (2000 ppm)		PPAM (4000 ppm)		HPAM (4000 ppm)	
Parameter	S_o	S_w	S_o	S_w	S_o	S_w	S_o	S_w
Oil saturation	0.88	0.12	0.87	0.13	0.85	0.15	0.86	0.14
IWF	0.4	0.6	0.38	0.62	0.39	0.61	0.42	0.59
PF	0.26	0.74	0.29	0.71	0.18	0.82	0.27	0.73
EWF	0.26	0.74	0.29	0.71	0.18	0.82	0.27	0.73

The residual oil saturation (So_r) after initial water flooding remains almost constant (~ 0.4) for all tests (Table 4.9). It proves the high level of similarity between the core samples in terms of rock properties such as porosity, permeability and connected pore spaces. After the polymer flooding, the lowest Sor value (0.18) and the highest value (0.29) were observed by using PPAM (4000 ppm) and HPAM (2000ppm), respectively. These values show that a maximum oil recovery occurred when PPAM (4000 ppm) was used and the lowest oil recovery values by HPAM (2000ppm). These tests show that PPAM at high concentration and high permeability of core sample can have a great impact on oil recovery. Similar results were observed by Wang (2007) for other hydrophobically modified polymers.

4.8.3.5 Oil displacement experiment using PPAM (2000 ppm) in 100 mD core.

An initial waterflood was carried out by approximately 1 PV of injection, then switched to injection of PPAM in brine solution. Oil recovery from IWF reached 53.9% OOIP (Figure 4.39), indicating a lower oil production of at least 10% less compared to other tests due to the difference in core sample permeability. The estimated oil saturation changed from initial oil saturation of

0.86 to 0.46 of So_r. The corresponding pressure differential was stabilised at 0.36 psi.

The viscosity of the injected polymer was ~31.2 cp at a shear rate of 15.6 s^{-1}. The tested polymer system demonstrated the same behaviour in terms of quick oil recovery response as previous tests and oil recovery increased by 13% to 66.9% of initial oil volume with a corresponding stabilised pressure differential of 2.47 psi. This translated to a mobility reduction (RF) value of 6.7. The oil recovery in this case is slightly lower than previous cases which can be attributed to lower permeability value of the core sample.

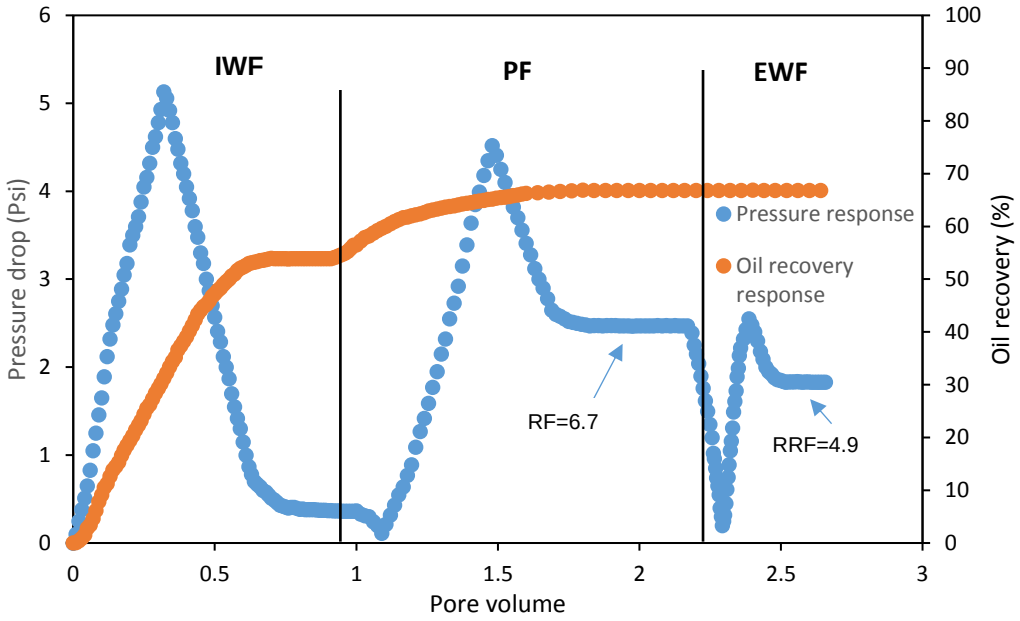

Figure 4. 39 : Pressure drop and oil recovery in core 100Md using PPAM (2000 ppm).

Finally, the extended water flood (EWF) was performed and no further recovery response was observed like in previous cases. The pressure difference response was stabilised at 1.83 psi, corresponding a permeability reduction (RRF) value of 4.9 to water. Viscosity of final polymer solution was measured at 15.1 s^{-1} to be 29.4 cp which shows a shear thinning behaviour in situ.

4.8.3.6 Oil displacement experiment using HPAM (2000 ppm) in 100 mD core.

Nearly 1 PV of brine was injected during the initial waterflooding (IWF) sequence when the flood was changed to injection of HPAM in brine solution (Figure 4.40). Water injection resulted in an oil recovery of 52.9% of initial oil volume with a corresponding differential pressure of 0.45 psi. Oil saturation profile reduced from 0.83 to 0.43 of So_r (Table 4.10).

The viscosity of the tested polymer solution was 24.8 cp as measured in the viscometer at a calculated theoretical shear rate of 15.82 s^{-1}. The incremental oil recovery from polymer flooding increased by 12.4 % to 65.3 % of the initial oil volume with a corresponding final residual oil saturation of 0.34. During the polymer injection, a stabilized differential pressure of 1.98 psi was obtained, corresponding to a mobility reduction (RF) value of 4.4.

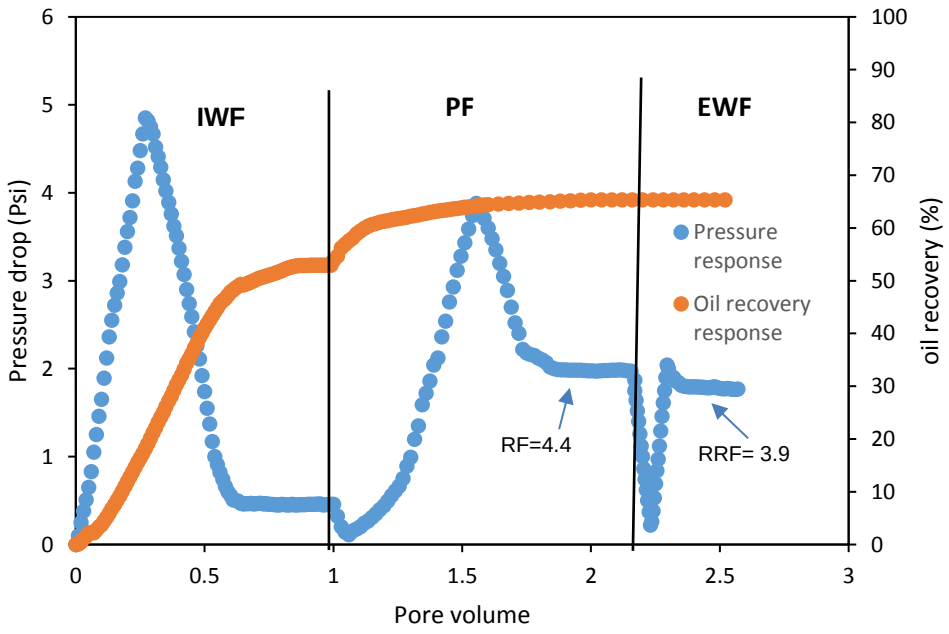

Figure 4. 40: Pressure drop and oil recovery for core 100mD using HPAM (2000 ppm).

No additional oil recovery was observed during EWF with the corresponding stabilized pressure of 1.76 psi, corresponding a permeability reduction (RRF) value of 3.9 to brine. From the results obtained it is clear that PPAM provides a greater permeability reduction to water than HPAM which can be due to

greater polymer retention for PPAM compared to HPAM as discussed earlier in the polymer retention experiments. The viscosity of the produced polymer solution was measured by viscometer at 14.7 s^{-1} to be 22.7 cp.

4.8.3.7 Oil displacement experiment using PPAM (4000 ppm) in 100 mD core.

1 PV of brine was injected during the initial waterflood (IWF) sequence. The IWF was then immediately switched to polymer injection of PPAM in brine solution. The oil recovery from waterflooding was 52.5% OOIP. Residual oil saturation reached from 0.85 to 0.39 of so_r with a corresponding stabilized pressure differential of 0.26 psi.

As measured in the viscometer, the viscosity of polymer solution was 73.2 cp at a shear rate of 15.2 s^{-1}. A fast oil recovery response occurred after approximately 5-6 cm^3 of produced fluid. The initial 0.5 PV of polymer injected resulted in much faster production compared to the HPAM polymer system; however, the final incremental recovery increased by 18.9% to 71.6 % of initial oil volume. The differential pressure was stabilised at 2.72 psi, corresponding to a mobility reduction (RF) value of 10.3 (Figure 4.41). The pressure build-up for polymer injection in this case has a higher peak than previous cases.

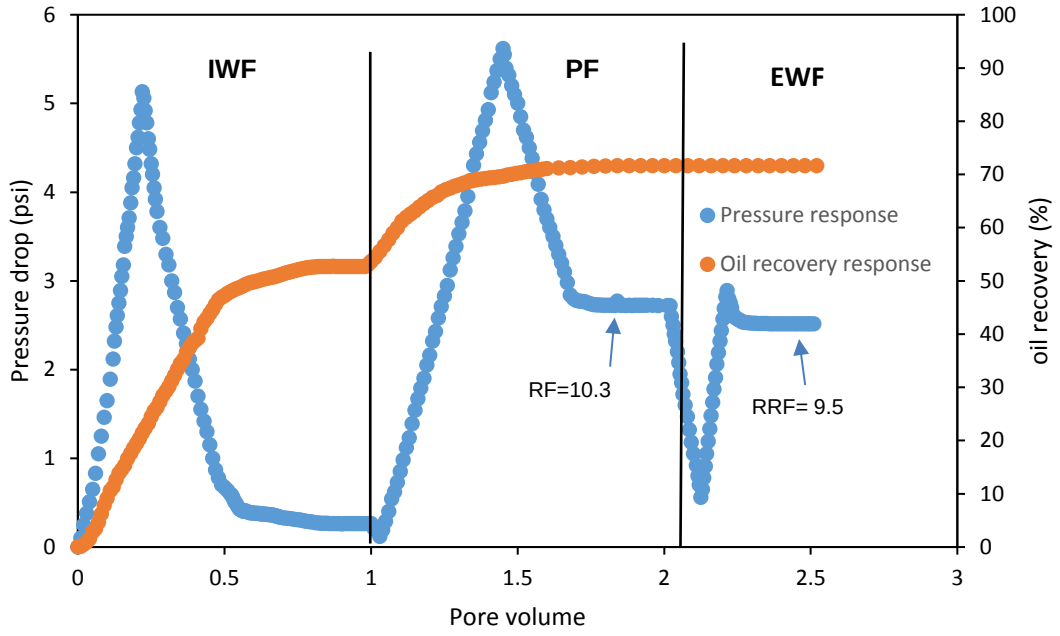

Figure 4. 41: Pressure drop and oil recovery for core 100mD using PPAM (4000ppm).

No more oil was recovered after extended water flooding (EWF) and pressure differential was stabilised at 2.51 psi, corresponding to a permeability reduction (RRF) value of 9.5. Permeability reduction to water in this case increased significantly compared to the previous case; however, oil recovery did not change considerably. The final produced polymer showed a viscosity of 68.9 cp at a shear rate of 15.1 s^{-1}.

4.8.3.8 Oil displacement experiment using HPAM (4000 ppm) in 100 mD core.

An initial waterflood (IWF) was carried out to approximately 1 PV of injection when the test was switched to injection of HPAM in brine solution. Oil recovery from IWF reached 51.6% (Figure 4.42), indicating the lowest oil production compared to other tests. The estimated oil saturation profile changed from initial oil saturation of 0.84 to 0.41 of So_r. The corresponding stable pressure differential reached 0.2 psi.

The viscosity of the injected polymer as measured to be ~60.4 cp at a calculated theoretical shear rate of 15.9 s^{-1}. The incremental oil recovery after polymer injection increased by 17% to 68.6% OOIP with a

corresponding stabilised pressure differential of 2.18 psi. Mobility reduction (RF) was estimated to be 11.2.

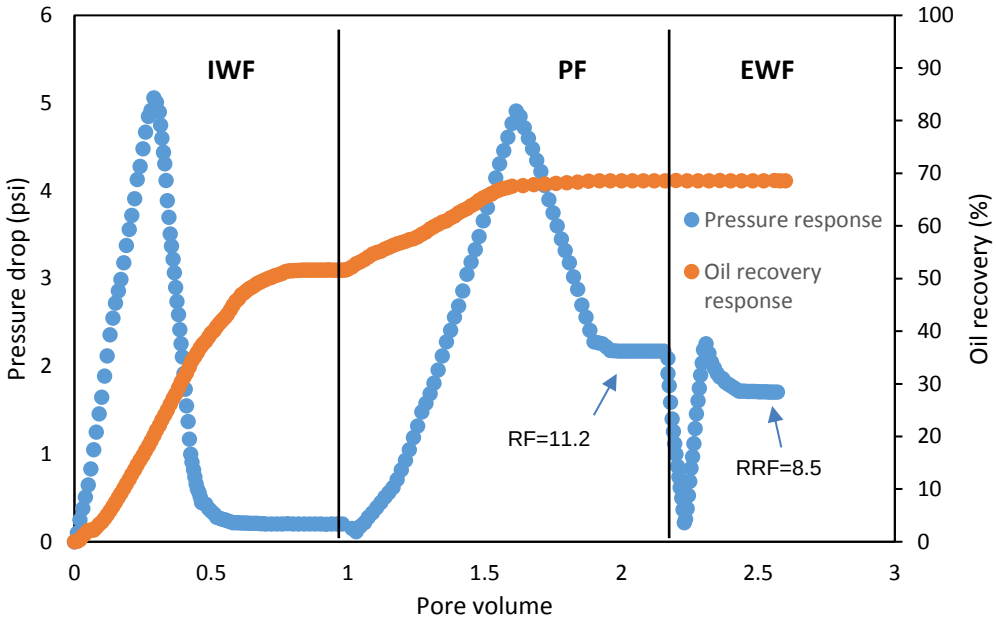

Figure 4. 42 : Pressure drop and oil recovery for core 100mD using HPAM (4000 ppm)

The extended water flood (EWF) was conducted immediately after polymer injection and no more oil was recovered. Pressure differential reached a plateau at 1.71 psi after almost 0.5 PV of brine injection. Permeability reduction (RRF) in this case was estimated to be 8.5. From the results, a high rise in permeability reduction to water was observed as polymer concentration increased. Viscosity of final polymer solution was measured 54.8 cp by viscometer at shear rate of 15.4 s^{-1}.

Summary of oil saturation after water flooding and polymer injection is shown in Table 4.10.

Table 4. 10 : Summary of oil saturation in core 100mD

	Tests for core 100mD							
	PPAM (2000ppm)		HPAM (2000ppm)		PPAM (4000 ppm)		HPAM (4000 ppm)	
Parameter	S_o	S_w	S_o	S_w	S_o	S_w	S_o	S_w
Oil saturation	0.86	0.14	0.83	0.17	0.85	0.15	0.84	0.16
IWF	0.46	0.54	0.43	0.57	0.39	0.61	0.41	0.59
PF	0.28	0.72	0.3	0.7	0.24	0.76	0.27	0.73
EWF	0.28	0.72	0.3	0.7	0.24	0.76	0.27	0.73

The lowest value of Sor (0.24) and the highest value (0.3) after polymer flooding (PF) was observed by using PPAM (4000 ppm) and HPAM (2000 ppm), respectively. This means highest oil recovery occurred by using PPAM (4000ppm) and the lowest oil recovery was obtained by using HPAM (2000 ppm). In these tests, the gap between the highest and the lowest oil saturation values is smaller than for the PF tests in Table 4.9. These results show that PPAM at higher permeability of core sample have a greater effect on the oil recovery than the low permeability core samples. Alexis (2016) and BASF (2016) have reported quite similar results for different hydrophobically modified polymers in sandstone cores with different permeabilities.

The results from the core flood tests indicate an early breakthrough of water which is suggesting that viscous fingering mechanisms of displacement appear to be predominant in heavy oil waterflooding. That is why it is critical to investigate the disadvantage of fingering effect, especially when the addition of water-soluble polymers can reduce the susceptibility of this displacement. A summary of the core flood results are given in Table 4.11

Table 4. 11: Summary of core flood tests

	Test							
Parameter	1	2	3	4	5	6	7	8
Core permeability (mD)	500				100			
Oil viscosity (cp)	115							
Polymer Concentration (ppm)	2000		4000		2000		4000	
Polymer type	PPAM	HPAM	PPAM	HPAM	PPAM	HPAM	PPAM	HPAM
Mobility reduction (RF)	4.1	2.9	6.1	3.6	6.7	4.4	10.3	11.2
Permeability reduction (RRF)	3.4	1.1	4.3	1.9	4.9	3.9	9.5	8.5
Theoretical Shear rate (s^{-1})	14.8	15	15.17	15.7	15.6	15.8	15.2	15.9
Injected polymer viscosity (cp)	32	26	72.1	59.4	31.2	24.8	73.2	60.4
Produced polymer viscosity (cp)	30.4	24.1	70.1	56.3	29.4	22.7	68.9	54.8

As it can be seen from table 4.11, eight tests were performed by using PPAM and HPAM in two core samples with different absolute permeability (500 mD and 100 mD). The concentration of both polymers were 2000 ppm and 4000 ppm in both tests. The total volume of brine and polymer solution injected in to each experiment was less than 3 pore volume. In the 500mD cores, PPAM demonstrate a higher mobility reduction (RF) than the HPAM as well as a higher residual resistance factor (RRF) to water indicating a higher permeability reduction. This could be due to the larger size of the PPAM molecule which is the result of hydrophobic aggregation in the copolymer (Panthi 2014). In the 100mD cores, a higher value in mobility reduction was observed as well as a permeability reduction compare to the 500mD ones. This could be attributed to lower absolute permeability of 100mD cores (BASF 2016).

Low flow rate of 0.2 ml/min was applied to inject polymer solutions for all tests and therefore the effect of the shear rate on the polymer solution

viscosity is negligible. The viscosity of injected PPAM solution is higher than HPAM at the same shear rate (Table 4.11). The viscosity of the produced polymers reduced slightly in all tests; however, HPAM exhibited a slightly larger reduction in viscosity than PPAM in all tests. This could be due to the effect of brine salinity. The presence of monovalent ions (Na^+, K^+) and divalent ions ($Ca^{2+,}$ Mg^{2+}) in the brine forms a shield preventing the repulsion between the negative charges on the HPAM molecule, which in turn the HPAM polymer less stretched. The PPAM molecule structure is in contrary neutral and therefore it shows a higher salinity resistance and therefore a less viscosity reduction in high salinity brine.

The results of oil recovery are shown in Figure 4.43 and Figure 4.44. It is noticeable that the oil recovery value after the initial water injection (IWF) are very similar, with a initial oil volume of 58-59% for the 500mD core samples (Figure 4.43) and a initial oil volume of 52-54% for the 100mD core samples (Figure 4.44). The slightly higher value of oil recovery for the 500mD cores can be attributed to the higher absolute permeability. As results show, oil recovery for tests 1(PPAM 2000ppm) and 2 (HPAM 2000ppm) are quite similar after the polymer flooding. A greater oil recovery was observed in both tests 3 (PPAM 4000ppm) and 4 (HPAM 4000ppm) where a maximum oil recovery was observed in test 3 (81% of initial oil volume). The lowest oil recovery was found in test 2 (67.3% of initial oil volume). Comparison of the oil recovery with different hydrophobically modified polymers and HPAM has been reported by other authors such as Panthi (2014) and Wassmuth (2012) and similar results to this thesis were found.

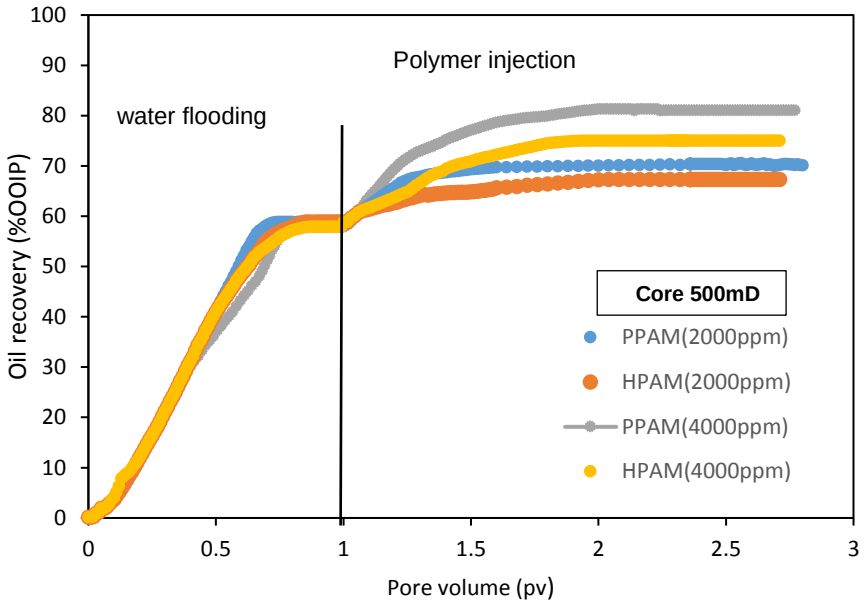

Figure 4. 43 : Oil recovery for core 500mD

As Figure 4.44 shows, polymer concentration did not play predominant role in oil recovery efficiency if tested in the same viscosity oil system for tests 5 to 8. These results coincided with the study of Levitt et al (2011).Thus, significant viscosity or concentration differences of polymer solutions did not alter oil recovery significantly, demonstrating a difference of 12-19% of initial oil volume recovered maximum between the highest and lowest polymer concentrations for 100mD cores. The highest oil recovery, 71.6% was for test 7 (PPAM, 4000ppm) and the lowest oil recovery, 65.3% for test 6 (HPAM, 2000ppm). This shows low permeability cores are not good candidates for polymer injection tests as the final oil recovery values are quite close and comparison is difficult. These results have been reported by authors such as Wassmuth (2012) and San Blas (2014).

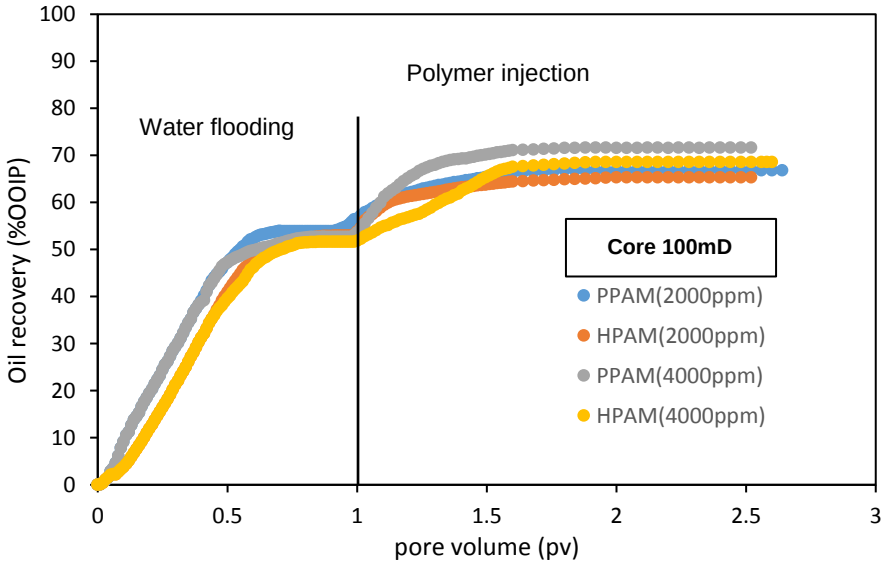

Figure 4. 44 : Oil recovery for core 100mD

In this research, the core samples are used for the experimental investigation on enhanced oil recovery are homogeneous sand stone with small dimensions as a representative of reservoir rocks, however, actual reservoir conditions needs to be studied more in details to have a better understanding of polymer injection. Factors such as heterogeneity of reservoir, long duration of polymer injection from injection wells until producer wells and type of reservoir rock (e.g. carbonate, limestone, etc) are key elements that reduce the viscoelasticity of polymers significantly.

Chapter 5

Conclusions and Recommendations

5. Conclusions and recommendations for future work

5.1 Conclusions

The following conclusions can be drawn from this research

•Micellar copolymerisation of acrylamide and phenyl-acrylamide to synthesis phenyl-polyacrylamide (PPAM) has been studied. The properties of aqueous solution of PPAM depend on the synthesis condition.

•Effect of surfactant concentration on the rate of monomer conversion was investigated. The experimental data shows a reduction in monomer conversion rate to polymer by increasing surfactant concentration in the solution. This might occur due to reaction of active monomers with impurities in the solution by increasing surfactant or the excess surfactant provides free micelles which interrupt the chain propagation.

•Effect of initiator concentration on the rate of monomer conversion was studied and a good fit of the experimental results with Shawik-Hamielec theory (1999) was observed. Increasing the initiator concentration speed up the rate of monomer conversion to polymer. However, it might reduce the average molecular weight of the final PPAM.

•The average viscosity molecular weight (M_w) was also calculated and a reduction in its values was observed by increasing surfactant concentration which might be due to acrylamide reaction with other impurities rather than active monomers in the solution particularly alcohol in the surfactant.

•Viscosity of phenyl-polyacrylamide (PPAM) solution was measured at different concentrations and the results were compared with hydrolyzed polyacrylamide (HPAM). The viscosity for both polymer solutions are almost the same up to the concentration around 180 ppm; however, a higher viscosity for PPAM solution was observed compared to HPAM at the concentration above 180 ppm which is a result of phenyl-acrylamide monomer aggregation.

•PPAM showed a newtonian behaviour at low shear rate (around 1 s^{-1}), however, as the shear rate increases the viscosity reduces significantly and polymer shows a shear thinning behaviour. Viscosity behaviour of polymer at different shear are in EOR application is crucial to understand to design a better polymer flooding process.

•Viscosity reduction for HPAM was greater than PPAM in presence of NaCl. The greater viscosity reduction in HPAM is a result of interaction of carboxylate group in polymer with monovalent and divalent ions in brine. Investigating the polymer behaviour in brine provides a more realistic effect of considering in EOR.

•Polymer retention experiments were carried out in sand pack, effluent concentration was measured and the retention of polymer solutions were calculated. Increasing polymer concentration causes more polymer retention in sand pack which reduces the permeability to water.

•Sand grain size distribution effect on polymer retention was measured and a greater polymer retention was observed as sand size was smaller. This effect can be attributed to pore size of porous media and polymer size. Pore blockage occur due to large dimension of polymer (hydrodynamic retention).

•Effect of brine salinity on retention of both PPAM and HPAM polymer solution in sand pack was measured. Both polymers showed quite close retention value in soft brine; however, an increase in HPAM retention was observed once hard brine was injected in sand pack. No significant changes were observed for PPAM retention. This occurs due to presence of positive ions in brine that bind with negative charges (carboxylic group) of HPAM molecule and cause precipitation of polymer.

•Inaccessible pore volume test was carried out for PPAM and HPAM in sand pack. A quicker polymer breakthrough was achieved for PPAM compared to

HPAM in the same conditions. This means PPAM has less access to small pores. One possible explanation could be the larger dimension of PPAM molecular structure due to aggregation of phenyl-acrylamide monomer. However, HPAM has a linear molecular structure.

•PPAM at high concentration (4000 ppm) gives a better oil recovery than HPAM at the same condition. This could be due to higher viscosity achieved by PPAM compared to HPAM. Sandstone cores with absolute permeabilities of 100mD were also tested for oil recovery, however, data collected were so close to each other that make oil recovery difficult to compare. This can be due to lower permeability of core which affect the ease movement of fluid.

•Permeability reduction (RRF) and mobility reduction (RF) tests were also carried out for both PPAM and HPAM in core samples. Greater permeability and mobility reduction was observed for PPAM. This can be due to its larger molecular structure in solution which increases polymer retention.

•Viscosity reduction for HPAM in core flood tests was slightly greater than PPAM in core sample at the same shear rate. This could be due to presence of monovalent and divalent cations in brine which affect the viscosity of HPAM more than PPAM.

In summary, the synthesised PPAM shows a better viscosity enhancement and more salinity resistance at the same experimental condition with HPAM; however, a greater permeability reduction was also observed for PPAM. Viscosity reduction of PPAM in core flood test for sand stone was lower than HPAM at the same conditions. Therefore, it can be considered as a good candidate for EOR at reservoir condition. However, more experimental work such as heterogeneity of reservoir rock, mechanical and microbial degradation of polymers need to be done to ensure the capability of PPAM usage for oilfield application. Polymer, brine and oil interaction was considered to some extent in this research. Oil with different properties can be tested for further investigation.

5.2 Recommendations for future work

• Study oil recovery in sandstone with larger core to obtain more accurate results. In this research, core with low permeability showed close results for oil recovery.

• Study the effect of heterogeneity of reservoir rock on polymer flow and measure parameters such as polymer retention, inaccessible pore volume, oil recovery, and also investigate the interaction of rock, polymer, oil and brine.

• Cores used for oil recovery tests in this research have low pore volume, so it is important to ensure the saturation of them during each test. It is recommended to use x-ray to assure fully saturation of core samples during injection.

• Compare PPAM with other extensively used polymers in oilfiled such as xanthan and investigates parameters such as polymer retention, viscosity of polymer solution in porous media and oil displacement efficiency.

• Synthesising hydrophobically modified polyacrylamides with new hydrophobic monomers or combination of three monomers (Terpolymers) and compare the rheological behaviour of them with PPAM and HPAM.

• Study the economical aspect of hydrphobically modified polymers in oil filed applications and compare the results with current conventional polymers.

• History matching of the experimental data with the simulators such as CMG or Eclipse.

Chapter 6

References

6. References

Ahmed A.Abdala, 2002 Solution Rheology and Microstructure of Associative Polymers, Department of chemical engineering &Fiber of polymer science program, North Carolina state university, December

Alexis D, 2016, Evaluation of innovative associative polymers for low concentration polymer flooding, SPE-179696-MS.

Almgren M, 2000, Mixed micelles and other structures in the solubilization of bilayer lipid membranes by surfactants, Biochimica et Biophysica Acta Biomembranes, vol. 1508, pp 146–163.

Alvarado, V.; Manrique, 2010, Enhanced oil Recovery, An update review. Energies, 3(9), 1529-1575.

Aparecida M, 2002, Polymer Injection Projects in Brazil: Dimensioning, Field Application and Evaluation, SPE-75194-MS.

Baojiao G, 2008, Preparation of hydrophobic association polyacrylamide in a new Micellar copolymerization system and its hydrophobically associative property, Macromolecules, 41, 2890-2897.

BASF, 2016, Can associative polymers reduce the residual oil saturation, SPE-179801-MS.

Biggs S, SelbJ,Candau F.1991 “Copolymerization of acrylamide and a hydrophobic monomer in an aqueous micellar medium” Journal of Physical Chemistry, 96, 1505-1511

Blagodatskikh I.V., Vasil eva O.V, Ivanova E.M., Bykov S.V. 2004 New approach to the molecular characterization of hydrophobically modified polyacrylamide, Polymer 45, 5897–5904.

Brian C Cook 2003 “Characterization of Comb Polymer Kypam for Enhanced oil recovery” Kansas University.

Broseta, D., et al., *Polymer Adsorption/Retention in porous media: Effects of core wettability on residual oil.* SPE Advanced Technology Series, 1995. **3**(01): p. 103-112.

Buchgraber et al, 2009, The displacement of viscous oil by associative polymer solutions, SPE-122400.

Calgon, 1995, Anionic polymers for reduction of viscosity of a magnesium hydroxide filter cake paste, US patent 4375526 A.

Candau F, Biggs S, Hill A, 1994, “Synthesis, Structure and Properties of hydrophobically associating polymers”polymer, 24, 11-19

Caram et al, 2006, On the rheological modelling of associative polymers, Article in Rheological Act 46(1):45-57.

Chauveteau G, 1984, Propagation of polymer slugs through porous media, SPE 13034, 17-19.

Delshad M, 2008, Mechanistic Interpretation and Utilization of Viscoelastic Behavior of Polymer Solutions for Improved Polymer-Flood Efficiency, SPE-113620-MS.

Denys k, 2003, flow of polymer solutions through porous systems, PhD thesis, Delft.

Dominguez, j.G and Willhite, G.P. 1977 “Retention and flow characteristics of polymer solutions in porous media”, university of Kansas.

Dossier, Oil & Gas Science and Technology - Rev. IFP, Volume 63, No **1**, January-February 2008.

Du Y, Guan L, (2004) Field-scale polymer flooding: lessons learnt and experiences gained during past 40 years. In: SPE 91787 presented at SPE international petroleum conference, Mexico, 7–9 Nov 2004.

Dupuis G, Rousseau D, 2010 “How to get the best out of hydrophobically associative polymers for IOR”, SPE 129884

Egbogah E, 1980, Microvisual Studies of Size Distribution of Oil Droplets in Porous Media, Bulletin of Canadian Petroleum Geology, Vol. 28 (1980), No. 2. Pages 200-210.

Fei-peng W, 2008, Properties and influence of hydrophobically associating polyacrylamide modified with 2-phenoxylethylacrylate, Front.Mate.Sci, 2,113-118.

Gouveia M, 2009, Sythesis and rheological properties of hydrophobically modified polyacrylamides with lateral chains of poly(propylene oxide) oligomers, Journal of Colloid and Interface Science,333, 152-163.

Gramain P, 1981, Elongational deformation by shear flow of flexible polymers adsorbed in porous media, Macromolecules, 14 (1), pp 180–184.

Grant M. Effect of Water Pre-Flush Volumes on Polymer Flooding Oil Recovery from Sandstone Core Samples, Dalhousie University,

Guillaume. D, Rousseau. D, 2010 “How to get the best out of Hydrophobically associative polymers for IOR? New experimental insights” SPE 129884

Hatzignatiou, D. G., Norris, U. L. and Stavland, A. (2013) Core-scale simulation of polymer flow through porous media, *Journal of Petroleum Science and Engineering,* 108, pp. 137-150.

Hill Alain, Candau Francoise, 1993 “Properties of hydrophobically Associating polyacrylamides: Influence of the method of synthesis” Macromolecules 26, 4521-4532

Hirasaki, G.J, Pope. G.A, 1974 “Analysis of factors influencing mobility and adsorption in the flow of polymer solution through porous media” SPE 4026

Homsy, G. M. Annu. 1987 Viscous fingering in porous media. Annul Rev. of fluid mechanics, volume 19, 271-311.

Huang G, 1995, Formation and coexistence of the micelles and vesicles in mixed solution of cationic and anionic surfactant, Colloid and Polymer Science, Vol 273, pp 156–164.

Huang R, 2004, Synthesis and rheological behaviour of poly[acrylamide-acrylic acid-N-(4-butyl)phenylacrylamide] hydrophobically modified polyelectrolytes, Colloid polymer science, 282, 305-313.

"IEA - Statistics Search". *Iea.org*. N.p., 2015. Web. 19 Dec. 2016.

(https://www.iea.org/statistics/statisticssearch/)

Jimenez-Regalado, Gregorio Cadenas-Pliego, 2004 Characterization and Rheological Properties of Dilute solutions of Three Different Families of Water-soluble Copolymers Prepared by Solution Polymerization, Macromolecular Research,.12, 5, 451 – 458.

Karlson, Leif, 2002 Hydrophobically Modified Polymers Rheology and Molecular Associations, Centre for Chemistry & Chemical Engineering.

Kasimbazi G, 2014. Polymer flooding, Norwegian university of Science and Technology.

Krishna Panthi, Kishore K. Mohanty, 2014 “A triblock copolymer flood in porous media” *Journal of Petroleum Science and Engineering,* 114, pp 52-60.

Lara-Ceniceros et al, 2007, Synthesis and characterization of telechelic polymers obtained by micellar polymerization, Polymer Bulletin, 59, 499–508,México.

Lake, L. W. Enhanced Oil Recovery*;* Prentice-Hall Inc.: Englewood Cliffs, NJ, 1989; Vol. 1, pp 550.

Lindley. J, 2001, Chemical flooding (polymer). http://www.netl.doe.gov.

Littmann W, 1988. Polymer flooding, Development in petroleum science, ELSEVIER.

Liu jenny, Harvest operations corp, 2012 “Suffield Area, Alberta, Canada-Caen polymer flood pilot project” SPE 157796.

Li, Kewen, Wenjie sun, Fen Li, 2014 “ Novel method for characterizing single-phase polymer flooding” China university of Geosciences.

Lopez x, 2004, Pore-Scale Modelling of Non-Newtonian Flow. Department of Earth Science & Petroleum Engineering, Imperial College London.

Maia M, 2009, Comparison between a polyacrylamide and a hydrophobically modified polyacrylamide flood in a sandstone core, Materials Science and Engineering, 29, 505-509.

Maia M, 2013, Interplay between rheological and structural evolution of benzoxazine resins during polymerization, polymer, vol 54, pp 1880–188.

Manichand R.N, 2014, Filed vs Laboratory Polymerr Retention Values for a Polymer Flood in the Tambaredjo Field, SPE-169027-MS.

Mansri A, Tennouga L, Desbrieres J, 2007 “Viscometric behaviour of hydrolyzed polyacrylamide-poly (4-vinylapridine) mixture in aqueous solution”, European Polymer Journal, 43, 540-549.

Mark J. 1999, Polymer Data Handbook, Oxford University press.

Maugeri, L. 2012, Belfer Center for Science and International Affairs, Harvard Kennedy School.

Mezzomo R, 2002, A New Approach to the Determination of Polymer Concentration in Reservoir Rock Adsorption Tests, SPE-75204-MS.

Morel, D.C., et al. 2008. Polymer injection in deep offshore field: the Dalia Angola case. SPE 129899.

Needham, R.B. and P.H. Doe, 1987 Polymer flooding review. Journal of Petroleum Technology. 39(12): p. 1,503-1,507.

Nodar et al, 2009, Preparation and Characterization of Cross-Linked Polymeric Nanoparticles for Enhanced Oil Recovery Applications, Oslo.

Odian George, 1970 “Principle of polymerization” New York; Maidenhead: McGraw-Hill.

Omar, A.E. King saud U, 1983 “Effect of polymer Adsorption on mobility ratio” SPE 11530.

Pancharoen, M, Thiele, M.R and Kovscek, A.R, 2010 “Inaccessible pore volume of Associative polymer floods”, SPE 129910.

Pancharoen M, 2009 “Physical properties of associative polymer solutions” Stanford university.

Pandey, A. Beliveau and M. Suresh Kumar, 2008 “ Evaluation of Chemical flood potential for Mangala Field, Rajasthan, India-Laboratory Experiment Design and results” IPTC 12636.

Panthi K, 2014, A triblock copolymer for polymer flood in porous media, Journal of Petroleum Science and Engineering, 114, pp 52-60.

Pantus, 2012. Experimental investigation of viscosity ratio effect on displacement performance of polymer systems during heavy oil recovery, Regina University.

Pope G, et al, 2014. Fundamentals of Enhanced Oil Recovery. PP 496, ISBN: 978-1-61399-328-6, SPE.

Porwal S, 2012, C-NMR and Raman Studies of Fullerene-Based Poly (Acrylamides), International journal of organic chemistry, Vol. 2 No. 4, Article ID: 25892.

Rassenfoss S, 2014, Aging offshore fields demand new thinking, Journal of petroleum technology.

Rodriguez F, 2014, Polymer Flooding for Extra-heavy oil: New insights on the key polymer transport properties in porous media, SPE 172850-MS.

Romero Z, 2014, Oil displacement mechanisms of viscoelastic polymers in enhanced oil recovery (EOR): a review, Vol 4, pp 113–121.

San blas, P and Vittoratos. E, 2014 “The polymer in polymer flooding: is its value overestimated” SPE 170104-MS.

Saaverda, N.F, Ecopetrol, Gaviria, W. 2002 “Laboratory testing of polymer flood candidates: San Francisco Field” SPE 75182.

Shaohua G, Yang H, 2015, An anti-biodegradable hydrophobic sulfonate-based acrylamide copolymer containing 2,4-dichlorophenoxy for enhanced oil recovery. New J. Chem, 39, 9265-9274.

Sheng, J., 2010. Modern chemical enhanced oil recovery: theory and practice: Gulf Professional Publishing.

Shushui wu, 2006, Properties of hydrophobically modified polyacrylamide with low molecular weight and interaction with surfactant in aqueous solution, Journal of Applied Polymer Science 100(6):4348 – 4360.

Smith, F.W, 1970, The behavior of partially hydrolyzed polyacrylamide solutions in porous media. Journal of Petroleum Technology. 22(02): p. 148-156.

Sochi T, 2010, Flow of non-newtonian fluids in porous media, journal of polymer science, Volume 48, 2437–2767.

Sorbie, K. S. 1991, Polymer-improved oil recovery*;* CRC Press: Boca Raton, FL. p.341-354.

Stahl and D. N. Schulz, 1986 “Water-soluble polymers for petroleum recovery” California, American chemical society.

Stavland, A. Jonsbraten, H.C and Lohne, A. 2010 “Polyemr flooding-Flow properties in porous media versus rheological parameters” SPE 131103.

Stavland Arne, BASF Construction polymers GmbH,, 2013 “New insight into the mechanism of mobility reduction by associative type copolymers” SPE 165225.

Sun et al, 2007, Well-Defined Vinyl Ketone-Based Polymers by Reversible Addition−Fragmentation Chain Transfer Polymerization, J. Am. Chem. Soc, 129 (33), pp 10086–10087.

Szabo, M.T. Calgon Corp, 1973 “Laboratory investigations of factors influencing polymer flood performance” SPE 4669.

Taber J et al, 1997, EOR Screening Criteria Revisited. vol 12, SPE-35385-PA.

Taylor Kevin C, Hisham A. Nasr-El-Din, 1998, Water-soluble hydrophobically associating polymers for improved oil recovery: A literature review, Journal of Petroleum Science and Engineering, 19, 265–280.

Terry C, 1977, Recovery of petroleum from tar and heavy oil sands**,** US patent No. 4019578 A**.**

Volpert E, 1997, Associating behaviour of polyacrylamides hydrophobically modified with dihexylacrylamide, Polymer, vol 39, No 5, pp 1025-1033.

Wang et al, 2003, Polymer-Encapsulated Carbon Nanotubes Prepared through ultrasonically Initiated in Situ Emulsion Polymerization, Chem. Mater, 15 (20), pp 3879–3886.

Washington. Dc, Annual Energy Review 2011, US Energy Information Administration.

Wassmuth F, 2012, Associative polymers outperform regular polymers displacing heavy oil heterogenous systems, SPE-157916.

Wever D.A.Z, F.Picchioni,A.A. Broekhuis, 2011 “ Polymer for enhanced oil recovery: A paradigm for structure-property relationship in aqueous solution”, Progress in polymer science Journal, 36, 1558-1628.

Wiley j, 1994 “Encyclopedia of polymer science &Technology” vol 1, pp 41-79.

Xue w, IanW,Hamley, 2004 “Synthesis and characterization of hydrophobically modified polyacrylmides”, European Polymer Journal,24,47-56.

Yabin Niu, Ouyang jian and et al, 2001 “Research on Hydrophobically associating water-soluble polymer used for EOR” SPE 65378.

Yilmaz, N. Akshin S. Bakhtiyarov, 2009 “Experimental investigation of Newtonian and non-Newtonian fluid flows in porous media” *Mechanics Research Communications* 36, pp 638-641.

Zaitoun, A., P. Makakou, et al. (2011). Shear Stability of EOR Polymers. SPE International Symposium on Oilfield Chemistry. The Woodlands, Texas, USA.

Zekri Y, 2004, The effect of fracture characteristics on reduction of permeability by asphaltene precipitation in carbonate formation, Journal of Petroleum Science and Engineering, Vol 42, Pages 171–182.

Zhang, G. and Seright, R. S. (2013) Effect of Concentration on HPAM Retention in Porous Media, SPE 166265.

Chapter 7

Appendix

7.1 UV data for injection of PPAM at different concentration into sand pack

• Injection of 1000 ppm of PPAM in sand pack

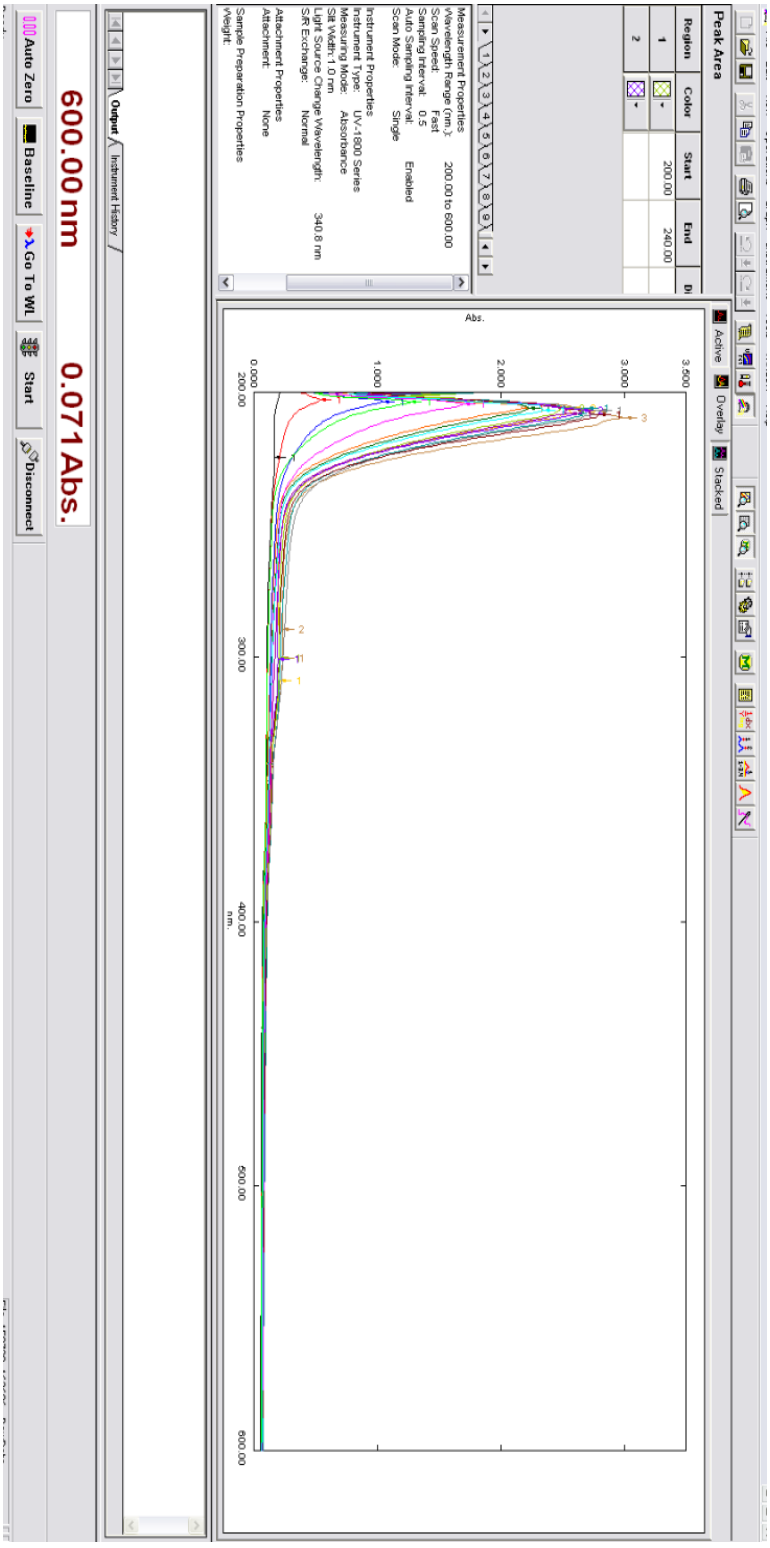

• Injection of 2000 ppm of PPAM in sand pack

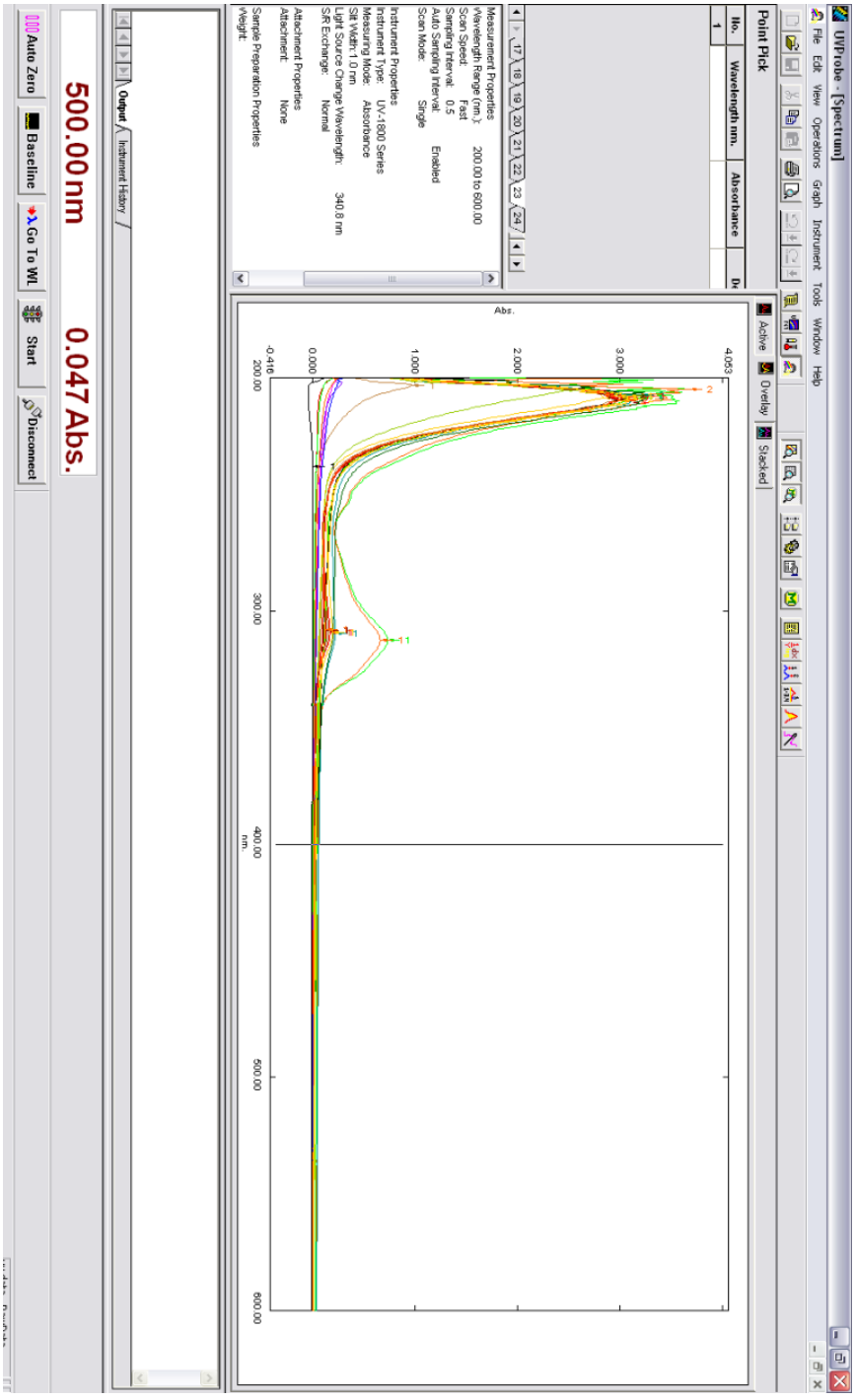

• Injection of 4000 ppm of PPAM in sand pack

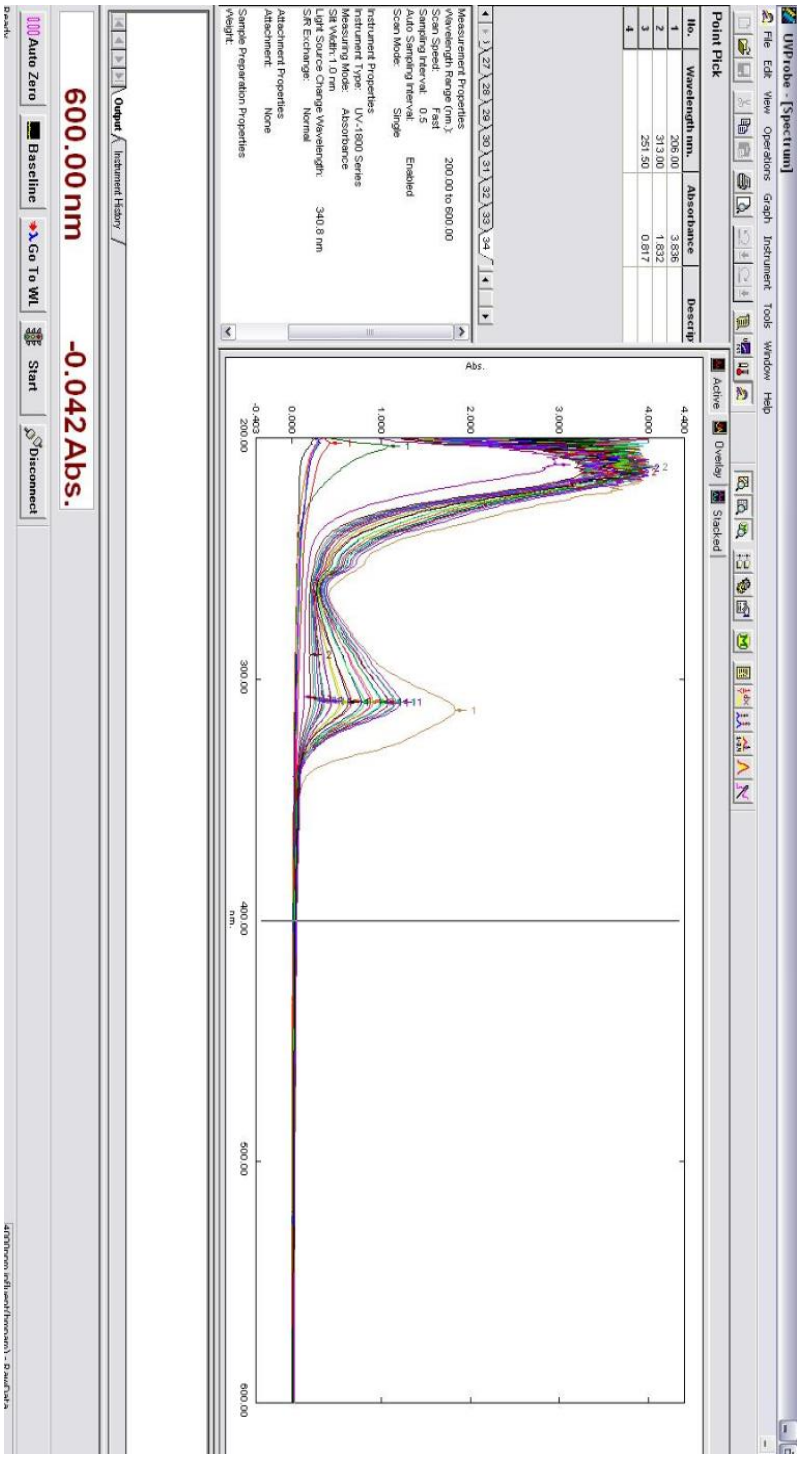

7.2 Research publications

7.2.1 Journal papers

• **Zabihi .H**, Jahanzad. F, Diaz. P (2017) "*Synthesis, Characterization and Rheological Behavior of Hydrophobically Modified Copolymers of Acrylamide and N- phenylacrylamide".* Materials Science and Engineering B. Manuscript submitted.

• **Zabihi. H**, Diaz. P, Jahanzad. F (2017) "*Comparison between a polyacrylamide and a hydrophobically modified polyacrylamide flood in a sandstone core*". Materials Science and Engineering C. Manuscript in preparation.

7.2.2 Conference papers

• **Zabihi. H**. Shahri. P.M, (2012) "*A New Model for Determining the Radius of Mud Loss during Drilling Operation in a Radial Fractured Network*" 36th Annual SPE International Technical Conference and Exhibition in Abuja, Nigeria.

• **Zabihi. H**, Jahanzad. F, Diaz. P (2015) "Copolymerisation of Acrylamide and a hydrophobic monomer in an aqueous micellar medium" IchemE Conference (ChemEngDayUK) and Exhibition in Sheffiled, UK.

• **Zabihi. H**, Jahanzad. F, Diaz. P (2015) "*Synthesis of hydrophobically modified polyacrylamide and its application in EOR*" London South Bank University seminar, London, UK.

• **Zabihi. H**, Diaz. P, Vajihi. F (2017) "Effect of low salinity water on wettability and capillary pressure in carbonate" Society of Core Analysis, Viena, Austria. Abstract accepted.

7.3 Training sessions

7.3.1. Postgraduate Certificate in Research Skills Key Skills Development Programme Training

Attended the following courses. The certificates of attendance are attached to the thesis.

• Conference Presentation -24 June 2013.
• Thesis Submission and Viva – 26 June 2013.
• Key Skills in the Research Environment – 6 November 2013.
• The Student-Supervisor Relationship – 02 March 2016.

• Insight into Personal Effectiveness- 3 March 2016.
• Academic Publication – 08 March 2016.
• Career Development – 10 March 2016.

7.3.2 Additional training sessions

• Health and Safety Induction – 12 June 2013.
• Career Management – 25 May 2014.
• Development Plan and Portfolio – June 2014.
• After your research degree-Looking ahead – 30 September 2015.